Dissertation zur Erlangung des Doktorgrades
Der Fakultät für Chemie und Pharmazie
Der Ludwig-Maximilians-Universität München

New Analytical Methods for the Assessment of the Physical Stability of Therapeutical Proteins

Veronika Maria Spalthoff
aus
Meppen

2013

Erklärung

Diese Dissertation wurde im Sinne von § 7 der Promotionsordnung vom 28. November 2011 von Herrn Prof. Dr. Gerhard Winter betreut.

Eidesstattliche Versicherung

Diese Dissertation wurde eigenständig und ohne unerlaubte Hilfe erarbeitet.

München, den 17.12.2012

……
(Veronika Spalthoff)

Dissertation eingereicht am:

1. Gutachter:	Prof. Dr. Gerhard Winter
2. Gutachter:	Prof. Dr. Wolfgang Frieß

Mündliche Prüfung am: 07.02.2013

Acknowledgements

The presented thesis was written at the Department of Pharmacy, Pharmaceutical Technology and Biopharmaceutics at the Ludwig-Maximilians-University in Munich and at Sanofi-Aventis in Frankfurt under supervision of Prof. Dr. Gerhard Winter.

First of all, I would like to express my deepest gratitude to my supervisor Prof. Dr. Gerhard Winter for giving me the opportunity to work in his research group. Especially, I want to thank him for his professional guidance and scientific support. I would like to thank him for the opportunity to present my work at national and international conferences. Thank you for the possibilities you opened me. Thank you for your help and your guidance.

I would like to thank Prof. Dr. Wolfgang Frieß for kindly being co-referee of this thesis as well as for his interest in my work. Thank you for the scientific input and advice over the last years.

Sanofi-Aventis is gratefully acknowledged for scientific an d financial support.
I am deeply grateful to Dr. Thomas Gehrmann, Dr. Gerrit Hauck and Dr. Norbert Lill from Sanofi-Aventis. They opened me the great opportunity to write this thesis in an industrial cooperation. Thank you for your support and scientific advises.
Especially, I want to thank my supervisor from Sanofi-Aventis, Dr. Thomas Gehrmann. Thank you, for the discussions and advises.

I am very thankful for the great working climate at Sanofi-Aventis. I want to thank my colleagues for the support and the fun time. Thank you Annika, Beate, Bettina, Christiane, Christine, Katrin, Tanja, Ahmed, Jens, and Oliver for the good times and all your help.

Many thanks are expressed to all the colleagues from the research groups of Prof. Winter and Prof. Friess. The times in Munich are characterized with an outstanding working climate and lots of fun. Thank you for all the inspiring discussions and your support. Particularly, I want to thank Angelika, Elsa, Kerstin,

Miriam, Gerd, Markus, Raimund, Sebastian, and Thomas. Thank you for the enjoyable time during tours to congresses and further activities.

I thank my friends Dr. Angelika Freitag, Dr. Katrin Kinkel and Dr. Lars Schiefelbein for proof-reading this work. Thank you for the quick responses and the scientific input.
My very special thanks go to Lars: thank you for all the scientific and non-scientific discussions. Thank you for being my best friend.

I am deeply thankful to my parents, my sister Brigitte, my brother Stephan and my grandfather: thank you for your support, your encouragement, and your love.

Finally I want to thank Markus for his encouragement and his love. Thank you for always being there for me.

For my parents

Table of Content

1. General Introduction and Objective of the Thesis 1

1.1 Introduction 1

1.2 Protein instability 2

1.2.1 Chemical instability 2

1.2.2 Physical instability 3

1.2.3 Factors that affect protein stability 5

1.3 Analytical methods for stability assessment of therapeutical protein formulations 7

1.3.1 Light scattering 8

1.3.2 Chromatography 9

1.3.3 Analytical ulatracentrifugation (AUC) 10

1.3.4 Asymmetrical flow field-flow fractionation (AF4) 11

1.3.5 Particle counting 12

1.3.5.1 Light obscuration 13

1.3.5.2 Microscopic particle counting 13

1.3.5.3 Microflow Imaging (MFI) 14

1.3.5.4 AccuSizer FY nano 15

1.3.5.5 Electrical sensing zone 16

1.4 The compendial and analytical gap 16

1.5 Objective of the thesis 20

1.6 Reference List 22

2. Material and Methods 33

2.1 Materials 33

2.1.1 Therapeutic proteins 33

2.1.1.1 IgG_1-α and IgG_1-ß 33

2.1.1.2 GCSF 33

2.1.1.3 rPA 33

2.1.2 Chemicals and reagents 34

2.2 Methods 35

2.2.1 Protein sample processing 35
2.2.1.1 Shaking stress 35
2.2.1.2 Stirring stress 35
2.2.1.3 Thermal stress 36
2.2.1.4 Freeze-thawing 36
2.2.1.5 Lyophilization 37
2.2.2 Protein aggregate characterization methods 38
2.2.2.1 Particle counting 38
2.2.2.1.1 Particle Counting with AccuSizer FY nano (AS) 38
2.2.2.1.2 Classical light obscuration (LO) particle couting 39
2.2.2.1.3 Microflow imaging (MFI) particle counting 39
2.2.2.1.4 Evaluation of particle counting measurements 40
2.2.2.2 Microscopic examination 40
2.2.2.3 Dynamic light scattering (DLS) 41
2.2.2.4 Size-exclusion chromatography (SEC) 41
2.2.2.5 Optical density at 550 nm (OD) 42
2.2.3 Other methods 44
2.2.3.1 Quantification of protein adsorption to glass vials 44
2.2.3.2 Differential scanning calorimetry (DSC) 44
2.2.3.3 Karl-Fischer titration 44
2.2.3.4 Zeta potential titration 45
2.2.3.5 Stress simulations 45
2.3 Reference List 47

3. Relevance of Submicron Particle Counting for Development and Quality Assurance of Protein Pharmaceuticals 49
3.1 Introduction 49
3.2 Experimental setup 53
3.3 Results and discussion 55
3.3.1 Light obscuration measurements with USP-qualified LO instruments in comparison to AS 55
3.3.2 Focused extinction and autodilution of AS 57
3.3.3 Is the very early onset of aggregation detectable with AS? 57

3.3.3.1 Lower detection limit of AS 57
3.3.3.2 Onset of aggregation and particle formation 58
3.3.4 Aggregation theory 60
3.3.5 Comparison of AS with DLS 63
3.3.6 Comparison of AS with turbidity measurements 66
3.3.7 Comparison of AS with SEC 68
3.3.8 Does MFI deliver earlier information? 70
3.4 Conclusion 73
3.5 Reference List 75

4. Dilution of Stressed Protein Solutions into Serum: Effects on Particle counting 79
4.1 Introduction 79
4.2 Experimental setup 80
4.3 Results and discussion 82
4.3.1 Mechanical stress and dilution of IgG_1 82
4.3.2 Freeze-thawing and dilution of IgG_1 83
4.3.3 Mechanical stress and dilution of GCSF 83
4.3.4 Freeze-thawing and dilution of GCSF 85
4.3.5 Mechanical stress and dilution of rPA 86
4.3.6 Freeze-thawing and dilution of rPA 88
4.3.7 Thermal stress 90
4.3.8 Kinetics 92
4.4 Conclusion 93
4.5 Reference List 95

5. Buffer-Screening: Effects of Dilution, pH and Standing Time on Particulate Matter in IgG_1-Solution 99
5.1 Introduction 99
5.2 Experimental setup 100
5.3 Results and discussion 101
5.3.1 Experiment 1 101

5.3.1.1 Results of particle counting: LO and MFI 101
5.3.1.2 Effect of dilution on pH 103
5.3.1.3 Dilution effect on particulate matter 103
5.3.1.4 Zeta potential measurements 104
5.3.1.5 Microscopic results 107
5.3.2 Experiment 2 109
5.3.2.1 Results of particle counting: LO and MFI 109
5.4 Conclusion 111
5.5 Reference List 113

6. Comparison of TopLyo® (Schott) Vials with Standard Glass Type I Vials concerning repression or enhancement of particle formation 115
6.1 Introduction 115
6.2 Sample preparation and experimental setup 117
6.3 Results and discussion 118
6.3.1 Physicochemical properties of lyophilizates 118
6.3.2 Particle counting after freeze-drying IgG_1-α 118
6.3.3 Zeta potential 120
6.3.4 Desorption of protein 120
6.4 Conclusion 123
6.5 Reference List 124

7. Simulation of Stir Stress and Prediction of Resulting Particle Formation in IgG_1-Solutions 127
7.1 Introduction 127
7.2 Experimental setup 128
7.3 Results and discussion 129
7.3.1 Situation for particles ≥1 µm 129
7.3.2 Situation for particles ≥10 µm 132
7.3.3 Upscaling experiment 133
7.4 Conclusion 135
7.5 Reference List 136

8. Final summary of the thesis **139**

8.1.1 Relevance of submicron particle counting 139

8.1.2 Particulate matter in serum solutions 141

8.1.3 Effects of dilution, pH and standing time on particulate matter 142

8.1.4 Comparison of TopLyo® vials (Schott) with standard glass type I vials 142

8.1.5 Stress simulations 143

8.2 Conclusion 143

9. Appendix **145**

9.1 Overview tables of time points of first detection after stressing IgG_1-α 146

9.2 Overview tables of time points of first detection after stressing IgG_1-ß 147

9.3 Overview tables of time points of first detection after stressing GCSF 149

9.4 Overview tables of time points of first detection after stressing rPA 150

1. General Introduction and Objectives of the Thesis

1.1 Introduction

During the last 35 years protein pharmaceuticals have become more and more important. Protein pharmaceuticals belong to the group of biotechnologically produced pharmaceuticals; biotechnology uses living systems and organisms to generate pharmaceutical products. Biopharmaceuticals, such as proteins or peptides, offered millions of people hope to cure diseases like diabetes, cancer or immune mediated diseases. About 30 years ago, the first biosynthetically produced human protein was approved by Eli Lilly and company: recombinant human insulin (Humulin). During the following years, the manufacturing processes were substantially improved and other recombinant therapeutic proteins such as antibodies were developed. In 2008, 633 biotechnological molecules were in development and today, numerous biopharmaceuticals have already gained approval.

The outstanding advantage of biopharmaceutical therapeutics is the specific effect of the proteins on a certain target. Side effects, often occurring during therapies with small molecules, are minimized.

Biopharmaceuticals are usually administered parenterally due to their poor bioavailability after application by most other administration routes. Proteins are not resistant against enzymatic and hydrolytic degradation in the gastrointestinal tract, further the protein molecules are too large to be resorbed during gastrointestinal passage. Protein pharmaceuticals have physical and chemical properties that imply difficulties in development, formulation, storage and shipping e.g. denaturation or aggregation. Maintaining stability is most crucial during the life-cycle of a therapeutic protein drug. This includes numerous steps, such as purification, formulation, storage and handling of protein drugs. Special care has to be taken during handling to avoid stress on the proteins and subsequent aggregation.

1.2 Protein instability

Protein instability can result in loss of native molecules and thus efficacy of the drug. Especially aggregation is a well-known instability that occurs and might lead to immunogenic side effects or blood vessel occlusions [Rosenberg, 2006; Schellekens, 2003]. Therefore, such instabilities have to be prevented to the utmost possible extent, which is a challenging task for drug development and manufacturing since the protein is exposed to numerous stress factors and changes in the environmental conditions that might destabilize the weak structure. In literature, proteins instability is subdivided into physical and chemical instabilities [Frokjaer et al., 2005; Lai et al., 1999; Manning et al., 1989]. However, a protein can also undergo both classes of instability at the same time during purification, separation, manufacturing or storage.

1.2.1 Chemical instability

Proteins can be affected by different chemical reactions like deamidation, oxidation, proteolysis or hydrolysis. Chemical reactions result in strong structural changes of the protein e.g. the formation of new or release of existing covalent or non-covalent bonds or other decomposition reactions.

Hydrolysis and oxidation of protein's amino acids can lead to deamidation [Brange et al., 1992; Li et al., 1995; Reubsaet et al., 1998a] of side-chain amides (asparagine, glutamine) or degradation of asparagine and proline.

Oxidation is a second pathway for chemical degradation, which results in modification of the protein by bond formation. Most susceptible amino acids are those that contain a sulphur or an aromatic ring such as cysteine or tyrosine [Stadtman, 1992]. Oxidation can be triggered by metals, oxygen, light and oxidizing-agents. Well-known is the oxidation in the presence of Fe(III) or Cu(II) [Tleugabulova et al., 1999; Wu et al., 2008]. Photooxidation may occur during processing or storage, protein pharmaceuticals are susceptible to light. Autoxidation is the reaction between molecular oxygen and the compound in absence of any catalytic process [Donbrow et al., 1978].

To prevent oxidation reactions in therapeutic protein formulations either physical or chemical procedures can be conducted.

Lyophilization can be used to prevent oxidation by physical means. The reduced mobility and the lack of solvent have been shown to prevent oxidation in a freeze-dried cake [Jennings et al., 1995]. To chemically prevent oxidation, additives like chelating agents and antioxidants can be added to the formulation [Wang, 2000].
Further chemical degradation pathways that have been shown to occur in therapeutic proteins are for example ß-elimination reactions, disulphide exchange reactions and racemisation. Wang *et al.* provided summarizing literature on chemical stability of proteins [Wang et al., 2007; Wang et al., 2010].

1.2.2 Physical instability

Proteins possess higher order structures (primary, secondary, tertiary) and a three-dimensional conformation, required for biological activity. The primary structure describes the sequences of amino acids; the structure resulting from hydrogen bonds is defined as secondary structure. Such intermolecular bonding leads, for example, to α-helices and ß-sheet folding. The tertiary structure refers to the three-dimensional structure of a single protein molecule, driven by non-specific hydrophobic interactions (burial of hydrophobic residues in the protein core) and specific interactions like salt bridges and disulfide bonds.
Physical instability refers to unfolding of protein's native structure. In general, native and normally folded structures of proteins bury the hydrophobic groups. The native protein formation is preserved by many forces, such as hydrophobic and electrostatic interactions, hydrogen bonding and van der Waals forces [Dill, 1990]. The loss of the native structure is referred to as protein denaturation, which often leads to the formation of aggregates. Once unfolded, hydrophobic groups are exposed to the usually hydrophilic environment. In order to minimize free energy, the proteins tend to associate to hydrophobic surfaces and/or interact with other hydrophobic protein surfaces forming aggregates [Manning et al., 1989; Manning et al., 2010].

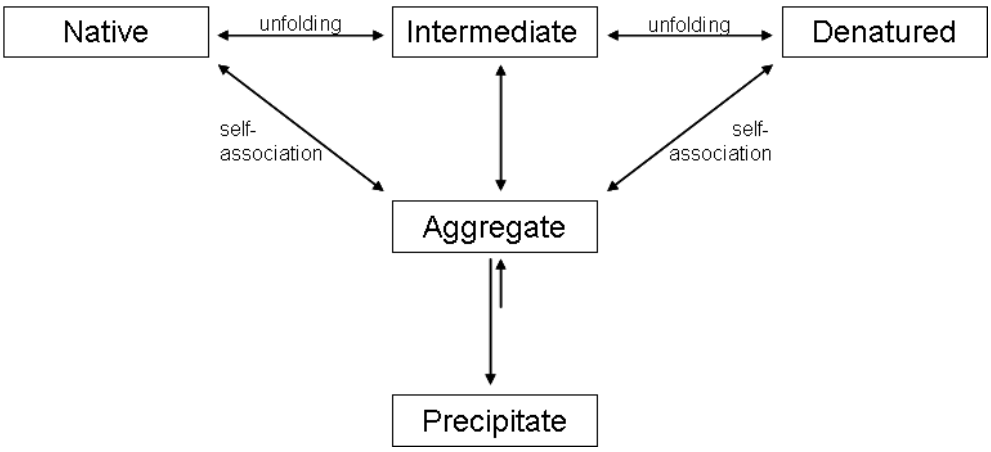

Fig. 1: Simplified model of protein aggregation and association [Wang et al., 2010]

The native protein can reversibly unfold to an intermediate state [Reubsaet et al., 1998b], that is also often referred as molten globule [Bam et al., 1996; Brange, 2000; Goolcharran et al., 2000]. Most protein aggregates are built from such partially unfolded intermediates [Andrews et al., 2007; Liu et al., 2008], which exist in equilibrium with the native state [Frokjaer et al., 2005]. A minor change in the environmental conditions, such as pH or temperature alterations, can shift the equilibrium toward the unfolding intermediates. The intermediate state is usually thermodynamically unstable and thus can either enhance the protein's tendency to aggregate [Krishnan et al., 2002] or lead to complete unfolding of the protein, resulting in denaturation. Protein molecules of each conformational state (native [Roberts, 2007], molten globule, and modified or denatured [Krishnan et al., 2002]) can be involved in self-association leading to aggregation and precipitation (figure 1). The refolding of the intermediate to the native state exists in an equilibrium state; hence refolding in a certain percentage is given. However, in some cases, such as high pressure, the equilibrium can be shifted preferring the native state [Zhang et al., 1995].

Aggregation can result from many protein destabilizing factors, such as mechanical or thermal stress. Aggregates can be classified in numerous ways, such as soluble/insoluble, non-covalent/covalent, reversible/irreversible or native/denatured [Cromwell et al., 2006].

Insoluble aggregates are removable by filtration through 0.22 µm filters. Insoluble aggregates can be further subdivided into visible and subvisible aggregates. Aggregates ≤1 µm often are referred to as subvisibles, whereas aggregates ≥1 µm are referred to as visible aggregates [Carpenter et al., 2008; Narhi et al., 2011].

Soluble aggregates can be defined as aggregates not removable by a 0.22 µm filter [Cromwell et al., 2006].

Covalent aggregates between two monomers can be formed via disulfide bridges between sulphur-residues of amino acids such as cysteine. Non-covalent aggregates have weak interactions, such as hydrogen bonding or electrostatic forces [Demeule et al., 2007].

Non-covalent weak interactions often result in reversible aggregates. The formation of reversible aggregates is considered to be caused by self-association as a result of pH-shift or changes in ionic strengths [Kendrick et al., 1998]. In case of reversible aggregation an equilibrium between aggregates and native protein exists, whereas irreversible aggregates do not have the equilibrium with monomer.

Native aggregates are referred to as aggregates with remaining native protein structure. Structural changes within proteins lead to denatured aggregates [Chi et al., 2003].

1.2.3 Factors that affect protein stability

Chemical and physical protein instability and subsequent aggregation can be caused by various stress factors, such as elevated temperatures, exposure to light [Kerwin et al., 2007] and interfaces [Bee et al., 2009a; Bee et al., 2010], agitation [Eppler et al., 2010; Maa et al., 1996], freeze-thawing [Bhatnagar et al., 2007] or impurities [Chi et al., 2005; Jones et al., 2005; Thirumangalathu et al., 2009; Tyagi et al., 2008; Van Beers et al., 2012]. The most important and further elaborated factors are thermal and mechanical stress, as well as freeze-thawing.

Temperature is a critical parameter for storage and use of protein therapeutics since the stability of proteins is even at physiological temperature weak [Brange, 2000]. Elevated temperatures can cause unfolding of the protein. Such conditions can induce unfolding which leads to reduction of ß-sheet and ß-turn conformations in protein structure and simultaneously increase the amount of α-helices [Vermeer et al., 1998]. These changes can subsequently even cause protein denaturation [Chen et al., 1994; Hawe et al., 2009]. In general protein stability is increasingly reduced with higher temperatures. Formation of aggregates due to thermal stress has been investigated for many proteins, such as antibodies [Harn et al., 2007; Hawe et al., 2009], human serum albumin [Lin et al., 2009] and insulin [Singh et al., 1991].

Several studies have investigated the thermal stability of proteins with regards to concomitant stress factors. Treuheit *et al.* showed that heat induced unfolding and

the resulting aggregation of e.g. GCSF increased at high protein concentrations [Treuheit et al., 2002]. For Interferon-τ it was reported that the composition of formulation buffer can have a profound effect on the thermal stability [Katayama et al., 2006].

Another factor that can impact protein stability is agitation. Mechanical stresses a protein can be exposed to during production and handling are shaking and stirring. Agitation of protein solutions can lead to the creation of new air-water interfaces. These interfaces can lead to protein unfolding and aggregation. Proteins are surface active substances and thus able to adsorb to the new formed air-water-interfaces [Burke et al., 1992]. The protein tends to unfold its hydrophobic cores and interact with or attach to hydrophobic air surfaces. Hydrophobic interactions between proteins are likely [Privalov et al., 1988]. Therefore the headspace in primary packaging materials is an important parameter. A large headspace usually increases the protein's tendency to form aggregates [Kiese et al., 2008]. Aggregation caused by mechanical stress has been reported for many proteins, such as monoclonal antibodies [Bee et al., 2009b] and haemoglobin [Kerwin et al., 1999].

Freeze-thawing is the last factor that should be mentioned in this context. Freeze-thawing exerts different stresses on the protein. It has been reported that freezing rate and control of thawing influences the rate of protein aggregation [Cao et al., 2003]. Aggregation upon freeze-thawing is reported of antibodies [Hawe et al., 2009] or human growth hormone [Eckhardt et al., 1991]. Privalov *et al.* reported that low temperature can cause unfolding due to favourable hydration of non-polar groups within the protein [Privalov, 1990]. The exposure of non-polar groups to water is thermodynamically unstable and thus aggregation or adsorption to hydrophobic surfaces or interfaces [Kreilgaard et al., 1998; Strambini et al., 1996] can occur. During freezing, crystallisation of the solvent molecules occurs resulting in increasing concentrations of protein and excipients in the remaining solution. Hence, aggregation can for example be caused by high protein concentration, imbalance of stabilizing and destabilizing agents and/or pH-shifts due to water removal. Proteins, such as antibodies, have been shown to be instable at low pH [Ejima et al., 2007], that can be generated during freezing of a phosphate buffer formulation [Pikal-Cleland et al., 2000].

1.3 Analytical methods for stability assessment of therapeutical protein formulations

To date, many analytical techniques have been developed to assess the stability of proteins. These analytical techniques are dedicated to give information on protein denaturation and aggregation or conformational and structural changes.

As mentioned above aggregates can strongly differ in size. Unfortunately, one single method covering the whole size spectrum in aggregate detection does not exist [Philo, 2006]. Hence, scientists and pharmaceutical companies have to use orthogonal techniques to characterize protein aggregates. Numerous different methods for aggregate detection are already well-established.

For our studies, mainly methods to quantify protein aggregates were used. To give a broad overview and for the sake of completeness, not only applied methods are described within this chapter but also those quantification methods that are found to be important. A comprehensive collection of literature regarding analytical methods is summarized [Zoells et al., 2011].

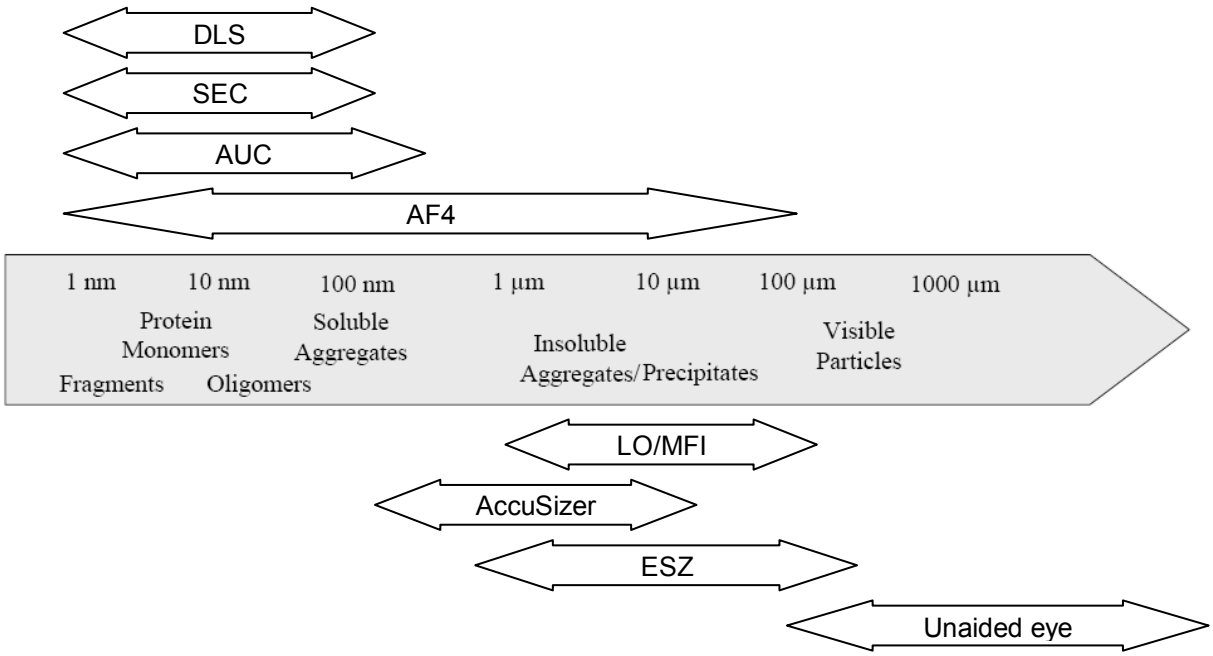

Fig. 2: Aggregate quantifying and sizing methods and their detection limits; DLS (Dynamic Light Scattering), SEC (Size Exclusion Chromatography), AUC (Analytical Ultra Centrifugation), AF4 (Asymmetrical flow field-flow fractionation), LO (Light obscuration), MFI (Microflow Imaging), ESZ (Electrical Sensing Zone). Figure adapted from presentation Klaus Zwiorek, Sanofi, July 11th 2007.

Figure 2 gives an overview which methods can be applied to determine the amount and size of protein aggregates. The detection sizes reflected in this figure show the ranges where a reliable quantification of aggregates can be obtained by each method.

1.3.1 Light scattering

Dynamic Light Scattering (DLS)

In DLS, which is also referred to as photon correlation spectroscopy (PCS) or quasi elastic light scattering (QELS), intensity fluctuations of scattered light are measured. Depending on their size, particles in suspension undergo Brownian motion [Malvern, 2007]. The intensity of scattered light is size dependent, smaller particles move more rapidly [Ahrer et al., 2003]. Therefore, the time dependent fluctuations are a rate of the diffusion constant of the molecules and are related to the hydrodynamic diameter of a molecule [Jachimska et al., 2008]. Possibly existing protein aggregates within the protein solutions can be considered as suspensions. For non-interacting rigid spheres (ideal solutions) the hydrodynamic radius is defined by the Stokes-Einstein equation [Demeester et al., 2005] as:

$$r_h = \frac{k_B T}{6\pi\eta D_\tau}$$

Where k_B is the Boltzmann's constant, T is the absolute temperature, η is the solvent viscosity and D_τ is the diffusion coefficient [Jiskoot et al., 1990]. Only extremely diluted solutions without interactions can be accounted as ideal, and are in general not existent in the field of protein formulations. Instead, proteins form non-ideal solutions.

Non ideal solutions are defined as solutions where protein interactions occur. In non ideal solutions, which occur practically, DLS measures the mutual diffusion coefficient D_m, which varies with protein concentration:

$$D_m = D_\tau (1 + k_D c_p)$$

Where k_D is a factor of interparticle action and c_p is the protein concentration.

DLS measurements provide information about the molecules respective the protein aggregates hydrodynamic radius, which is the radius of the molecule and its hydration layer.

DLS analytics need low effort in sample preparation, since proteins in solution can theoretically be analyzed without dilution. Furthermore, DLS platereaders enable high-throughput measurements of many samples in several minutes. However, a

drawback of the method is its susceptibility to interfering scattering effects deriving from air bubbles, dust and large aggregates or turbidity [Mahler et al., 2008].

Static Light Scattering (SLS)

In SLS, the scattered light intensity is measured as a function of the angle between detector and the incident laser beam direction. SLS measurements give information concerning molar mass, molecular root mean square radius, conformation, and intermolecular interactions [Minton, 2007]. However, small changes in molecular weight (e.g. protein deamidation) can not be detected [Demeester et al., 2005]. Static light scattering measurement at various angles is called multi-angle light scattering (MALS) [Andersson et al., 2003]. MALS determines the angular dependence of scattered light and thus enables the direct calculation of molecular sizes. It is very common to connect a MALS-detector to a separation technique to supplement the detection with UV detector. Using the combination SEC-MALS [Philo, 2006; Wen et al., 1996; Ye, 2006], molecular mass and small aggregate concentrations can be determined [Mahler et al., 2008].

1.3.2 Chromatography

Chromatographic methods are used for separating molecules. Separation is based on interactions of molecules with a mobile and a stationary phase. Molecules in the mobile phase travel with a constant speed down the chromatographic column or carrier material. The speed molecules travel with depends on their affinity for the stationary phase.

A common chromatographic method in the field of protein analysis is Size Exclusion Chromatography (SEC), often referred to as gel filtration. The separation principle relies on the different sizes respectively hydrodynamic volumes of proteins relative to a given pore diameter of the stationary phase [Gabrielson et al., 2007]. Ideally, there should be no interaction between the proteins and the stationary phase [Bischoff et al., 2005], but usually this is not the case.

In protein analytics Size Exclusion Chromatography (SEC) can give useful information about fragments, monomer- and small oligomer content. Protein aggregates, fragments and monomer are eluted depending on their sizes; the larger the protein aggregates the earlier they are diluted as they can not penetrate into the pores of the gel. The size of protein particles that can be determined by SEC is restricted to ~200 nm diameter, as usually a 0.2 µm filter prevent larger particles from

entering and clogging the column. If aggregates are too large, they are directly eluted with the mobile phase without penetrating into pores of the gel [Mahler et al., 2008]. Therefore, the relevant detection range of SEC was defined as 1-200 nm (see figure 2).

By recalculating the recovery in a given sample assumptions on the amount of aggregates >200 nm can be made. Aggregates >200 nm are given as a percentage of total protein. However, conclusions regarding size of those aggregates are not possible.

Separation can be coupled with detectors such as UV-Vis (ultraviolet-visible) or fluorescence spectroscopy detectors, which offer information about the aggregate concentrations. Further, separation can also be coupled with light scattering detectors to determine the molar mass [Philo, 2006; Ye, 2006]. Further, an additional refractive index detector delivers useful information on the aggregates' sizes [Wen et al., 1996].

Disadvantageously, samples analyzed by SEC are highly diluted by the mobile phase and can also interact with the stationary phase. In both cases the result might be adulterated due to conformational changes of the protein molecules [Wen et al., 1996] or dissolution of aggregates [Liu et al., 2006; Philo, 2006].

1.3.3 Analytical ultracentrifugation (AUC)

AUC is one of the eldest methods for characterization of protein's solution structure and conformation [Liu et al., 2006; Wandrey et al., 2011]. The instrument is composed of a high-speed centrifuge with an added optical system for measuring the distribution of different sized protein aggregates. Optical systems, that measure differences between protein sample and buffer, can be either absorbance systems (190-800 nm) or Raleigh interference systems measuring refractive index gradients [Philo, 2005]. Concentration distributions can be estimated based on physical properties [Chou et al., 2011]. AUC experiments can be further subdivided in 2 methods determining different parameter of a sedimentation process:

During a sedimentation velocity (SV) experiment the centrifuge is rotating at a very high speed (up to 60.000 rpm) implying that all protein molecules to be driven completely to the wall within a few hours. Different protein species, such as the monomer and aggregates, sediment at their own rate and thus are separated, sediment can be distinguished from each other based on their varying sedimentation velocities. These rates for example depend on the one hand side on properties of the

protein to be analyzed like concentration, the sedimentation coefficient of the protein species, their molecular mass and conformation, and on the other hand side on solvent properties like viscosity and solvent density. Monitoring the sedimentation process of single molecules and agglomerates allows the determination of their hydrodynamic and thermodynamic characteristics in solution, without interaction with any matrix or surface [Lebowitz et al., 2002].

A second option of performing AUC measurements is to monitor the sedimentation equilibrium of proteins which provides information about the respective molar mass and self-association of protein species as well as heterogeneous interactions as soon as an the equilibrium of protein species in solution upon centrifugation is reached [Mahler et al., 2008]. At a low rotor speed the macromolecules diffuse to the outside of the rotor until a steady-state is reached [Philo, 2009]. Smaller particles move and diffuse more rapidly to the outside than larger particles.

Both AUC methods do not rely on protein standards and can be performed in formulation buffers [Philo, 2005]. However, experienced staff is needed due to complex and tedious validation, instrumentation, and data analysis [Liu et al., 2006]. Disadvantageously, both methods have a very low throughput rate of maximum seven samples per day.

1.3.4 Asymmetrical flow field-flow fractionation (AF4)

Asymmetrical flow field-flow fractionation is another widely used technique to detect and quantify protein aggregates [Mahler et al., 2008]. Instead of separation in a column packed with solid material like in SEC, AF4 relies on separation in a channel of defined height. The channel is made of an upper impermeable wall, a spacer defining channel height and shape, and a lower permeable channel wall [Fraunhofer et al., 2004]. The latter is permeable for the mobile phase and composed of an ultrafiltration membrane with a certain molecular weight cut-off to retain the analytes of interest placed on a frit. After injection to the channel and subsequent focussing or relaxation of the sample, the protein species are forced by a laminar forward flow of the mobile phase to pass the channel towards the detection outlet. The laminar flow profile entails a high velocity in the channel center and a low velocity at the channel walls. A perpendicular field of force (also called cross flow) is applied, that forces the protein species towards the accumulation wall. The cross flow is made of mobile phase as well and is able to permeate the ultrafiltration membrane and frit that form the lower channel wall. The antagonist of the cross flow is the size dependent

diffusion of the particles directed back to the channel interior. For small species diffusion predominates over cross flow and thus smaller particles are able to reach the center of the channel, whereas larger particles stay near the accumulation wall. Hence, smaller particles travel faster than larger particles and are therefore eluted earlier.

Compared to SEC, the key benefits of AF4 are a more gentle fractionation at lower pressure. AF4 has a narrow flow channel which potentially reduces interactions of [Demeule et al., 2007; Liu et al., 2006]; SEC has a packed column posing interaction possibilities with the analytes. For AF4 separations, the fractionation force can be adjusted during one measurement and less sample preparation is required. SEC separations require sample preparation and online adjustment of fractionation is not possible [Philo, 2006]. Advantageously, AF4 detects protein particles up to 100 µm, whereas particles of such size would already be hindered by the frit to enter the SEC column. However, the resolution is not as sensitive as it is known for SEC.

1.3.5 Particle counting

Particle counting is a compendial requirement for parenteral solutions. Formation of particles is a major concern during development and manufacturing of protein pharmaceuticals. Particles can be differentiated into visible (>100 µm) and subvisible particles (0.1-100 µm) [Carpenter et al., 2008]. Detection and quantification of subvisible particles has to be performed with particle counters or microscopic methods, whereas visible particles can be seen with the unaided eye.

Pharmacopoeias require the monitoring of particulate matter for particles ≥10 µm and ≥25 µm in parenteral solutions. Preparations supplied in containers with a volume of more than 100 ml must not obtain more than 25 particles/ml ≥10 µm and 3 particles ≥25 µm. The requirements for preparations supplied in containers with a volume of 25 – 100 ml are as follows: particle counts for particles ≥10 µm must not exceed 6000 per container; particle counts for particles ≥25 µm must not exceed 600 per container [European Directorate For The Quality of Medicine (EDQM), 2011; United States Pharmacopeia, 2009]. The relevance of those numbers and the need to determine particulate matter <10 µm is currently discussed in the scientific community [Cao et al., 2009; Carpenter et al., 2008; Singh et al., 2010].

1.3.5.1 Light obscuration

Light obscuration (LO, also called light blockage) instruments with a detection range from 1 µm to 100 µm or more are the most commonly used instruments for quantification of subvisible particles and are described in the pharmacopoeias as method of choice for determination of particulate matter. The particle size is deduced from the amount of light blocked as the particles pass the detector in a single file fashion [Mahler et al., 2008].

Artificial and even irreproducible [Cao et al., 2010] results may occur at high protein particle concentrations, when detection limit is reached and the particles can not be counted anymore in single file fashion [Zoells et al., 2011]. If two or more particles pass the laser beam simultaneously, coincidence occurs. Particles could either be not detected, because particles are covering each other, or instead of detecting single small particles one large particle is detected. The pharmacopoeias require additional microscopic particle counting for preparations with particle counts exceeding the instruments limits, since dilution of samples can lead to redissolving of particles.

Light obscuration instruments are calibrated with polystyrene standards of defined circular diameters and defined contrast in refractive index to the liquid. However, protein particles do not have defined shapes, refractive indices (RI) and sizes [Sharma et al., 2010a; Sharma et al., 2010b]. Protein particles can have a RI close to the solvent solution RI. Such low RI differences can lead to oversight of protein particles and subsequently false (too low) particle counts.

False results can also be caused by particles of high transparency that cannot be detected by light obscuration [Demeule et al., 2010; Huang et al., 2008], since a sufficient contrast of particle and liquid is necessary. Thus, particle number and size can be underestimated.

A further drawback is that LO instruments can not differentiate between proteinaceous and non-proteinaceous particles or air bubbles.

The advantage of the LO principle is the fast and simple measurement and evaluation handling.

1.3.5.2 Microscopic particle counting

Microscopic particle counting on filters is described within the pharmacopoeias as an alternative method for particulate matter determination [European Directorate For

The Quality of Medicine (EDQM), 2011; United States Pharmacopeia, 2009]. The total particle numbers obtained from microscopic particle counting can not be compared with the results from compendial light obscuration due to different sensibilities [Demeule et al., 2010]. The acceptance criteria for microscoping particle counting by microscopy differ from those of light obscuration: Preparations supplied in containers with a volume of more than 100 ml should not obtain more than 12 particles/ml ≥10 µm and 2 particles ≥25 µm. The requirements for preparations supplied in containers with a volume of 25 – 100 ml are as follows: particle counts for particles ≥10 µm must not exceed 3000 per container; particle counts for particles ≥25 µm must not exceed 300 per container.

Particle counting tests with a binocular microscope at 100 ± 10 magnifications are performed using an ocular micrometer. The ocular micrometer is equipped with a graticule and reference circles of 10 µm and 25 µm. The graticule is devided into quadrants by crosshairs [United States Pharmacopeia, 2009].

According to light obscuration method described above samples have to be pooled. The sample to be tested is transferred to a filtration funnel, and then a vacuum is applied until the membrane filter is free from liquid. The dried membrane filter is scanned under reflected light and particles ≥10 µm and ≥25 µm are counted.

A clear drawback of microscopic particle counting is the manual operation. Sample preparation and particle counting is not automated, implicating the influence of the operator and human mistakes. Furthermore, microscopic particle counting is very time-consuming and not feasible for routine production or development processes.

An advantage of this method is the possibility to determine particulate matter in highly contaminated solutions. As mentioned above it is even compendially required to test samples of particle counts exceeding the limits of light obscuration instruments with the microscopic particle counting test.

1.3.5.3 Microflow Imaging (MFI)

The Microflow Imaging technique to detect and count subvisible particles in the µm - range has been developed during the last 10 years. It combines digital microscopy, micro-fluidics and image processing. Images from samples are captured when passing a laser beam in a flow cell. Microflow imaging analyzes each particle detected with regards to its size, transparency and shape. For each measurement a database is created, from which the particle properties can be recalled at any time. The databases can be used to attribute particles with defined properties to respective

origins. For example, circular particles in protein solution usually are silicone oil or air bubbles.

The range of particle detection is dependent on the equipment from 750 nm or 1 µm to 200 µm.

An outstanding advantage is the possibility to get information about shape and transparency of particles [Narhi et al., 2011; Sharma et al., 2007; Sharma et al., 2010b; Sharma et al., 2010a]. With experience, detected particles can be attributed to respective origins, such as protein-related, air bubble, silicone oil or glass particles [Demeule et al., 2010; Sharma et al., 2009].

A drawback of MFI is, similar to light obscuration, that highly contaminated protein solutions can not be measured without dilution of the sample due to the appearance of coincidences. Further MFI depends on differences in the refractive index difference of particles and liquids. This implicates that highly concentrated solutions or very transparent particles provide insufficient contrast from particle to liquid. However, the minimal difference in refractive required for successful MFI analysis is smaller than for classical light obscuration.

1.3.5.4 AccuSizer FY nano

The AccuSizer FY nano is also a new particle counting method developed by PSS Nicomp (Santa Barbara, CA, US) and emerged on the market about four years ago. The AccuSizer nominally counts particles in the range of 150 nm to 10 µm using two detectors [Nicomp, 2008]. When a particle passes the sensing zone, light is absorbed, reflected or scattered in an angle, dependent from particle size. A light scattering detector is counting particles in the nanometer range by sensing different intensities of scattered light which are related to defined sizes. Larger particles are counted by a light obscuration detector.

Advantageously, the instrument dilutes the samples automatically with filtered water, until an eligible particle count is reached. Measuring sufficiently diluted samples ensures that the particles pass one at a time the illuminated region. Coincidences can be avoided. However, as mentioned before, dilution can also have an impact on protein aggregates and hence on the results. A focused extinction is used during measurements. Only a few particles flowing through the focus within the flow cell are counted. As for MFI, the particle count is recalculated to obtain the count per milliliter. Disadvantageously, particle counts can e.g. be underestimated [Demeule et al.,

2010], if samples with very low particle counts are measured and randomly a fraction without particles is counted. The recalculation would lead to a biased particle count.
The detection limit of the AccuSizer FY nano is very promising, as it closes the gap of quantitative particle detection in the nanometer size range. A rigorous assessment of the new AccuSizer FY nano has been performed throughout this thesis and is extensively discussed in chapter 3.

1.3.5.5 Electrical sensing zone method

This method is based on an electrical field for counting and sizing particles in solutions and is most commonly known as Coulter Counter® or Coulter principle. Particles moving in the electrical field cause an increase of the electrical resistance. Therefore, sufficiently diluted particles should be suspended in a conducting liquid to ensure an electrical current. The electrical current is changed by each particle proportional to the particles size as soon as a particle pass the electrical sensing zone.
The electrical sensing zone principle can be compared to classic light obscuration as required within pharmacopoeia. Both methods deliver the information about particle size and particle count.
The benefit of the Coulter principle is the detection of particles independent on their refractive index. As the Coulter principle is not relying on refractive index differences between particles and liquids, even less compact proteinaceous particles with low contrast to the liquid can be detected without any problems [Barnard et al., 2012; Rhyner, 2011]. Further, particulate matter in highly concentrated solutions with a high refractive index and respective low contrast between particle and liquid can be determined [Demeule et al., 2010]. A drawback of the electrical sensing zone is the requirement to dilute the particles into conducting liquids if the formulation buffer possesses sufficient conductivity.

1.4 The compendial and analytical gap

Strategies for stability assessment for protein formulations become more and more important [den Engelsman et al., 2011] for development and manufacturing of protein pharmaceutics. The authorities require increasingly more detailed investigations and

understanding of a protein's quality (with special focus on particles) prior to approval. Regulatory frameworks regarding absence of particles and aggregates have to be very strict to assure protein safety, efficacy and stability [ICH Q8, 2009]. Quality by design is required to maximize protein quality. Therefore, predefined specifications "should focus on those molecular characteristics found to be useful in ensuring the safety and efficacy of the product" [ICH Q6B, 1999].

During the last years, the scientific community has been discussing the need of implementing new pharmacopoeial methods, such as Microflow Imaging [Mire-Sluis et al., 2011], for counting protein particles. The bones of contention were guidelines regarding particulate matter in parenteral solutions. USP <788> stated that "Particulate matter consists of *extraneous*, mobile, undissolved substances, other than gas bubbles, unintentionally present in parenteral solutions". Similarly, Ph.Eur. 2.9.20 defined "Particulate contamination of injections and parenteral infusions consists of *extraneous*, mobile undissolved particles, other than gas bubbles, unintentionally present in the solutions".

Those guidelines have originally been set for small molecules and are not appropriate anymore in times when biologicals with high molecular weights play an important role on the market. Proteins themselves can contribute to significant colloidal particle counts, they tend to form aggregates; those can impact safety and efficacy. In 2007, USP, European Pharmacopoeia and Japanese Pharmacopoeia defined that "Particulate matter in injections and parenteral infusions consist of mobile undissolved particles, other than bubbles, unintentionally present in solutions" [United States Pharmacopeia, 2009]. This harmonization of definition for particulate matter includes protein aggregates as well as unintentionally extraneous present particles.

After harmonization a new discussion was raised regarding the monitored particle size classes. Currently, monitoring of particles ≥10 µm and ≥25 µm is required and limits are defined. These size ranges are still leftovers from ancient guidelines and inadequate for protein pharmaceuticals nowadays. The limitation was defined because of the risk for blood vessel occlusions that can be triggered by particles >10 µm, whereas aggregates >10 µm and also <10 µm are discussed to cause immunogenic side effects [Barnard et al., 2010; Fradkin et al., 2009; Jiskoot et al., 2009; Rosenberg, 2006; Schellekens, 2003]. Recently, it was reported in literature

that large insoluble aggregates of murine growth hormone generated by freeze-thawing or agitating can induce immune responses [Fradkin et al., 2011].
In theory, protein aggregation starts with very small aggregates, called precursors or nuclei [Golub et al., 2007; Mahler et al., 2005], which can grow further forming larger aggregates. Therefore, it is discussed, whether the requirements to monitor only particles ≥10 µm and ≥25 µm are sensitive enough for protein pharmaceuticals. Protein particles might be in the subvisible range during release and to small to be detected. During storage growth of particles has to be considered, large protein particles might harm the patients after parenteral application of aggregated solutions. Many authors postulate a new pharmacopoeial method to monitor also subvisible particles in the range from 1 µm till 10 µm or even below.
Besides the monitoring also an “equipment gap” for particle detection is discussed. One single method covering all possible instabilities and aggregate sizes does not exist [Das et al., 2008; Narhi et al., 2009; Philo, 2006]. As mentioned before, subvisible particles ≥10 µm are monitored and counted using classical light obscuration. This technique is not capable of counting particles smaller than 1 µm (figure 1). Aggregates <1 µm can be determined semi-quantitatively using light scattering or chromatographic methods. Each method comes with advantages and disadvantages and none can provide a complete overview on a product by its own. Thus, usually a variety of analytical methods complementing or being orthogonal to each other are used to characterize protein formulations. For each product it is important to close existing gaps in analytical equipment [Carpenter et al., 2008] to improve safety and efficacy. These gaps can include a certain size range, or for example can be caused by high translucency of the particles impacting detection by light based methods. Lately, a method independent on optical properties has been assessed regarding its ability to provide more information on protein aggregation in the subvisible size range [Barnard et al., 2012]. As the Coulter method does not depend on optical properties of particles, detection of translucent protein particles was unproblematic.

Recently, new particle counters with additional beneficial read-out parameters emerged on the market. Microflow Imaging (MFI) possesses the add-on to visualize detected and counted particles. Information about shape or transparency of particles is provided, which allows differentiation between proteinaceous and non-

proteinaceous particles [Sharma et al., 2009]. It has already been addressed in literature that MFI is more sensitive to translucent particles than classical light obscuration [Huang et al., 2008; Sharma et al., 2010b].

AccuSizer nano FY is also a new particle counter with promising detection limit for particles from 150 nm to 10 µm, which would perfectly close the equipment gap for particle counting.

Only recently brand-new technologies, such as Archimedes [Mire-Sluis et al., 2011] and nanoparticle tracking analysis (NTA) [Zoells et al., 2011], were discussed. Archimedes technology determines the mass of the submicron aggregates. NTA records the scattered light of individual moving protein particles and a software visualizes microscopic images.

1.5 Objective of the thesis

The most important objective of the thesis was to evaluate new analytical instruments and techniques for counting particles within protein pharmaceuticals. AccuSizer FY nano® and Micro-Flow Imaging™ DPA 4200 were rigorously assessed regarding their abilities to deliver more information about protein aggregation and to close the gap in analytical techniques for determination of subvisible particles as described in literature [Carpenter et al., 2008]. For this purpose four different proteins were stressed mechanically, thermally and by freeze-thawing to generate aggregates. Sampling was performed at defined time points during stressing. Stressed samples were analyzed using the new particle counters and "standard" instruments, such as light obscuration, dynamic light scattering and size exclusion chromatography. Results of the measurements were evaluated to find the point of detection for each instrument, which is the time point, where stress results in measurable aggregation or e.g. decrease of monomer amount. To compare the new instruments with the classically used methods, time points of detection were compared. These comparisons deliver valuable information about the sensitivity of the instruments, the usefulness to implement such methods within the pharmacopoeia and the relevance of submicron particle counting.

Further, this thesis is intended to elucidate the fate of protein particles after administration into serum solution. Much research has been done in the field of protein aggregation, however, most of it *in vitro*. The thesis aims to contribute to the raising discussion about the fate of proteins and their aggregates when administrated into human serum. Three different proteins were stressed mechanically, thermally and by freeze-thawing to generate aggregates. The aggregates were administered in a 1:50 dilution into serum solution and particle counts were taken after defined time points. It was of great interest, whether particles accumulate and grow or whether particles redissolve after administration. Further, the ability of particle counters to detect particles in yellowish serum solution was to be checked.
Evaluating the effects of dilution, pH and standing time on particulate matter was defined as a sub-goal. An antibody was stressed mechanically and diluted into

phosphate buffers with different pH values and molarities. Particle counts were taken and assessed. Particles generated after lab stress might redissolve over time and if so, they are to be considered differently compared to those that do not redissolve.

In the field of protein formulation development the discussion was raised, whether aggregation prediction during upscaling is possible. Protein formulators perform their experiments in the small lab scale. As soon as those experiments have to be scaled up, questions regarding e.g. stirring speed in the technical scale are posed. What correlations can be found between particle formation and stirring speed and is particle formation in a larger scale predictable? As aggregation prediction is not a common process, upscaling means to experimentally test the optimal stirring speed. The possibility of aggregation prediction would be an improvement and save time, money and active pharmaceutical ingredient (API). One objective of this thesis was to study and simulate the possibility of aggregation prediction with use of Computational fluid dynamics.

1.6 Reference List

1. Ahrer,K., Buchacher,A., Iberer,G., Josic,D., Jungbauer,A., 2003. Analysis of aggregates of human immunoglobulin G using size-exclusion chromatography, static and dynamic light scattering. Journal of Chromatography A, 1009, 89-96.

2. Andersson,M., Wittgren,B., Wahlund,K.G., 2003. Accuracy in Multiangle Light Scattering Measurements for Molar Mass and Radius Estimations. Model Calculations and Experiments. Anal. Chem., 75, 4279-4291.

3. Andrews,J.M., Roberts,C.J., 2007. A Lumry-Eyring nucleated polymerization model of protein aggregation kinetics: 1. Aggregation with pre-equilibrated unfolding. J Phys. Chem. B, 111, 7897-7913.

4. Bam,N.B., Cleland,J.L., Randolph,T.W., 1996. Molten globule intermediate of recombinant human growth hormone: stabilization with surfactants. Biotechnol. Prog., 12, 801-809.

5. Barnard,J.G., Rhyner,M.N., Carpenter,J.F., 2012. Critical evaluation and guidance for using the coulter method for counting subvisible particles in protein solutions. J Pharm. Sci., 101, 140-153.

6. Barnard,J.G., Singh,S., Randolph,T.W., Carpenter,J.F., 2010. Subvisible particle counting provides a sensitive method of detecting and quantifying aggregation of monoclonal antibody caused by freeze-thawing: Insights into the roles of particles in the protein aggregation pathway. J Pharm. Sci., 100, 492-503.

7. Bee,J.S., Chiu,D., Sawicki,S., Stevenson,J.L., Chatterjee,K., Freund,E., Carpenter,J.F., Randolph,T.W., 2009a. Monoclonal antibody interactions with micro- and nanoparticles: adsorption, aggregation, and accelerated stress studies. J Pharm. Sci., 98, 3218-3238.

8. Bee,J.S., Davis,M., Freund,E., Carpenter,J.F., Randolph,T.W., 2010. Aggregation of a monoclonal antibody induced by adsorption to stainless steel. Biotechnol. Bioeng., 105, 121-129.

9. Bee,J.S., Stevenson,J.L., Mehta,B., Svitel,J., Pollastrini,J., Platz,R., Freund,E., Carpenter,J.F., Randolph,T.W., 2009b. Response of a concentrated

monoclonal antibody formulation to high shear. Biotechnol. Bioeng., 103, 936-943.

10. Bhatnagar,B.S., Bogner,R.H., Pikal,M.J., 2007. Protein stability during freezing: separation of stresses and mechanisms of protein stabilization. Pharm. Dev. Technol., 12, 505-523.

11. Bischoff,R., Barroso,B., 2005. Liquid Chromatography. In: Jiskoot,W., Crommelin,D.J. (Eds.), AAPS, Arlington, 277-329.

12. Brange,J., 2000. Physical Stability of Proteins. In: Frokjaer,S., Hovgaard,L. (Eds.), Taylor & Francis, London, 89-112.

13. Brange,J., Langkjaer,L., Havelund,S., Volund,A., 1992. Chemical stability of insulin. 1. Hydrolytic degradation during storage of pharmaceutical preparations. Pharm. Res., 9, 715-726.

14. Burke,C.J., Steadman,B.L., Volkin,D.B., Tsai,P.K., Bruner,M.W., Middaugh,C.R., 1992. The adsorption of proteins to pharmaceutical container surfaces. International Journal of Pharmaceutics, 86, 89-93.

15. Cao,E., Chen,Y., Cui,Z., Foster,P.R., 2003. Effect of freezing and thawing rates on denaturation of proteins in aqueous solutions. Biotechnol. Bioeng., 82, 684-690.

16. Cao, S., Jiang, Y., and Narhi, L., 2010, A Light-Obscuration Method Specific for Quantifying Subvisible Particles in Protein Therapeutics. Pharmacopeial Forum 36[3], 824-834.

17. Cao,S., Jiao,N., Jiang,Y., Mire-Sluis,A., Narhi,L.O., 2009. Sub-visible particle quantitation in protein therapeutics. Pharmeur. Bio Sci. Notes, 2009, 73-79.

18. Carpenter,J.F., Randolph,T.W., Jiskoot,W., Crommelin,D.J., Middaugh,C.R., Winter,G., Fan,Y.X., Kirshner,S., Verthelyi,D., Kozlowski,S., Clouse,K.A., Swann,P.G., Rosenberg,A., Cherney,B., 2008. Overlooking subvisible particles in therapeutic protein products: Gaps that may compromise product quality. J Pharm. Sci., 98, 1-5.

19. Chen,B.L., Arakawa,T., Hsu,E., Narhi,L.O., Tressel,T.J., Chien,S.L., 1994. Strategies to suppress aggregation of recombinant keratinocyte growth factor during liquid formulation development. J Pharm. Sci., 83, 1657-1661.

20. Chi,E.Y., Krishnan,S., Randolph,T.W., Carpenter,J.F., 2003. Physical stability of proteins in aqueous solution: mechanism and driving forces in nonnative protein aggregation. Pharm. Res., 20, 1325-1336.

21. Chi,E.Y., Weickmann,J., Carpenter,J.F., Manning,M.C., Randolph,T.W., 2005. Heterogeneous nucleation-controlled particulate formation of recombinant human platelet-activating factor acetylhydrolase in pharmaceutical formulation. J Pharm. Sci., 94, 256-274.

22. Chou,C.Y., Hsieh,Y.H., Chang,G.G., 2011. Applications of analytical ultracentrifugation to protein size-and-shape distribution and structure-and-function analyses. Methods, 54, 76-82.

23. Cromwell,M.E., Hilario,E., Jacobson,F., 2006. Protein aggregation and bioprocessing. AAPSJ, 8, E572-E579.

24. Das,T., Nema,S., 2008. Protein particulate issues in biologics development. Am. Pharm. Rev., 11, 52, 54-52, 57.

25. Demeester,J., de Smedt,S.S., Sanders,N.N., Haustraete,J., 2005. Light scattering. In: Jiskoot,W., Crommelin,D.J. (Eds.), AAPS, Arlington, 245-275.

26. Demeule,B., Lawrence,M.J., Drake,A.F., Gurny,R., Arvinte,T., 2007. Characterization of protein aggregation: the case of a therapeutic immunoglobulin. Biochim. Biophys. Acta, 1774, 146-153.

27. Demeule,B., Messick,S., Shire,S.J., Liu,J., 2010. Characterization of particles in protein solutions: reaching the limits of current technologies. AAPSJ, 12, 708-715.

28. den Engelsman,J., Garidel,P., Smulders,R., Koll,H., Smith,B., Bassarab,S., Seidl,A., Hainzl,O., Jiskoot,W., 2011. Strategies for the assessment of protein aggregates in pharmaceutical biotech product development. Pharm. Res., 28, 920-933.

29. Dill,K.A., 1990. Dominant forces in protein folding. Biochemistry, 29, 7133-7155.

30. Donbrow,M., Azaz,E., Pillersdorf,A., 1978. Autoxidation of polysorbates. J. Pharm. Sci., 67, 1676-1681.

31. Eckhardt,B.M., Oeswein,J.Q., Bewley,T.A., 1991. Effect of freezing on aggregation of human growth hormone. Pharm. Res., 8, 1360-1364.

32. Ejima,D., Tsumoto,K., Fukada,H., Yumioka,R., Nagase,K., Arakawa,T., Philo,J.S., 2007. Effects of acid exposure on the conformation, stability, and aggregation of monoclonal antibodies. Proteins, 66, 954-962.

33. Eppler,A., Weigandt,M., Hanefeld,A., Bunjes,H., 2010. Relevant shaking stress conditions for antibody preformulation development. Eur. J Pharm. Biopharm., 74, 139-147.

34. European Directorate For The Quality of Medicine (EDQM), 2011. Ph.Eur.2.9.19 Particulate contamination: subvisible particles.

35. Fradkin,A.H., Carpenter,J.F., Randolph,T.W., 2009. Immunogenicity of aggregates of recombinant human growth hormone in mouse models. J Pharm. Sci., 98, 3247-3264.

36. Fradkin,A.H., Carpenter,J.F., Randolph,T.W., 2011. Glass particles as an adjuvant: a model for adverse immunogenicity of therapeutic proteins. J Pharm. Sci., 100, 4953-4964.

37. Fraunhofer,W., Winter,G., 2004. The use of asymmetrical flow field-flow fractionation in pharmaceutics and biopharmaceutics. Eur. J Pharm. Biopharm., 58, 369-383.

38. Frokjaer,S., Otzen,D.E., 2005. Protein drug stability: a formulation challenge. Nat. Rev Drug Discov., 4, 298-306.

39. Gabrielson,J.P., Brader,M.L., Pekar,A.H., Mathis,K.B., Winter,G., Carpenter,J.F., Randolph,T.W., 2007. Quantitation of aggregate levels in a recombinant humanized monoclonal antibody formulation by size-exclusion chromatography, asymmetrical flow field flow fractionation, and sedimentation velocity. J Pharm. Sci., 96, 268-279.

40. Golub,N., Meremyanin,A., Markossian,K., Eronina,T., Chebotareva,N., Asryants,R., Muronets,V., Kurganov,B., 2007. Evidence for the formation of start aggregates as an initial stage of protein aggregation. FEBS Lett., 581, 4223-4227.

41. Goolcharran,C., Khossravi,M., Borchardt,R.T., 2000. Chemical Pathways of Peptide and Protein Degradation. In: Frokjaer,S., Hovgaard,L. (Eds.), Taylor & Francis, London, 70-88.

42. Harn,N., Allan,C., Oliver,C., Middaugh,C.R., 2007. Highly concentrated monoclonal antibody solutions: direct analysis of physical structure and thermal stability. J Pharm. Sci., 96, 532-546.

43. Hawe,A., Kasper,J.C., Friess,W., Jiskoot,W., 2009. Structural properties of monoclonal antibody aggregates induced by freeze-thawing and thermal stress. Eur. J Pharm. Sci., 38, 79-87.

44. Huang,C.T., Sharma,D., Oma,P., Krishnamurthy,R., 2008. Quantitation of protein particles in parenteral solutions using micro-flow imaging. J Pharm. Sci., 98, 3058-3071.

45. ICH Q6B, 1999. Specifications: Test procedures and acceptance criteria for Biotechnological/Biological Products. In: International Conference on Harmonization (Ed.).

46. ICH Q8, 2009. Pharmaceutical Development. In: International Conference on Harmonization (Ed.).

47. Jachimska,B., Wasilewska,M., Adamczyk,Z., 2008. Characterization of globular protein solutions by dynamic light scattering, electrophoretic mobility, and viscosity measurements. Langmuir, 24, 6866-6872.

48. Jennings,T.A., Duan,H., 1995. Calorimetric monitoring of lyophilization. PDA. J. Pharm. Sci. Technol., 49, 272-282.

49. Jiskoot,W., Beuvery,E.C., de Koning,A.A., Herron,J.N., Crommelin,D.J., 1990. Analytical approaches to the study of monoclonal antibody stability. Pharm. Res., 7, 1234-1241.

50. Jiskoot,W., van Schie,R.M., Carstens,M.G., Schellekens,H., 2009. Immunological risk of injectable drug delivery systems. Pharm. Res., 26, 1303-1314.

51. Jones,L.S., Kaufmann,A., Middaugh,C.R., 2005. Silicone oil induced aggregation of proteins. J. Pharm. Sci., 94, 918-927.

52. Katayama,D.S., Nayar,R., Chou,D.K., Valente,J.J., Cooper,J., Henry,C.S., Vander Velde,D.G., Villarete,L., Liu,C.P., Manning,M.C., 2006. Effect of buffer species on the thermally induced aggregation of interferon-tau. J Pharm. Sci., 95, 1212-1226.

53. Kendrick,B.S., Cleland,J.L., Lam,X., Nguyen,T., Randolph,T.W., Manning,M.C., Carpenter,J.F., 1998. Aggregation of recombinant human interferon gamma: kinetics and structural transitions. J Pharm. Sci., 87, 1069-1076.

54. Kerwin,B.A., Akers,M.J., Apostol,I., Moore-Einsel,C., Etter,J.E., Hess,E., Lippincott,J., Levine,J., Mathews,A.J., Revilla-Sharp,P., Schubert,R., Looker,D.L., 1999. Acute and long-term stability studies of deoxy hemoglobin and characterization of ascorbate-induced modifications. J. Pharm. Sci., 88, 79-88.

55. Kerwin,B.A., Remmele,R.L., Jr., 2007. Protect from light: photodegradation and protein biologics. J Pharm. Sci., 96, 1468-1479.

56. Kiese,S., Papppenberger,A., Friess,W., Mahler,H.C., 2008. Shaken, not stirred: mechanical stress testing of an IgG1 antibody. J Pharm. Sci., 97, 4347-4366.

57. Kreilgaard,L., Jones,L.S., Randolph,T.W., Frokjaer,S., Flink,J.M., Manning,M.C., Carpenter,J.F., 1998. Effect of Tween 20 on freeze-thawing- and agitation-induced aggregation of recombinant human factor XIII. J Pharm. Sci., 87, 1597-1603.

58. Krishnan,S., Chi,E.Y., Webb,J.N., Chang,B.S., Shan,D., Goldenberg,M., Manning,M.C., Randolph,T.W., Carpenter,J.F., 2002. Aggregation of Granulocyte Colony Stimulating Factor under Physiological Conditions: Characterization and Thermodynamic InhibitionΓÇá. Biochemistry, 41, 6422-6431.

59. Lai,M.C., Topp,E.M., 1999. Solid-state chemical stability of proteins and peptides. J Pharm. Sci., 88, 489-500.

60. Lebowitz,J., Lewis,M.S., Schuck,P., 2002. Modern analytical ultracentrifugation in protein science: a tutorial review. Protein Sci., 11, 2067-2079.

61. Li, S., Schoeneich, C., and Borchardt, R.T., 1995, Chemical instability of proteins. Pharm.News 2[5], 12-16.

62. Lin,J.J., Meyer,J.D., Carpenter,J.F., Manning,M.C., 2009. Aggregation of human serum albumin during a thermal viral inactivation step. International Journal of Biological Macromolecules, 45, 91-96.

63. Liu,D., Ren,D., Huang,H., Dankberg,J., Rosenfeld,R., Cocco,M.J., Li,L., Brems,D.N., Remmele,R.L., Jr., 2008. Structure and stability changes of human IgG1 Fc as a consequence of methionine oxidation. Biochemistry, 47, 5088-5100.

64. Liu,J., Andya,J.D., Shire,S.J., 2006. A critical review of analytical ultracentrifugation and field flow fractionation methods for measuring protein aggregation. AAPSJ, 8, E580-E589.

65. Maa,Y.F., Hsu,C.C., 1996. Effect of high shear on proteins. Biotechnol. Bioeng., 51, 458-465.

66. Mahler,H.C., Friess,W., Grauschopf,U., Kiese,S., 2008. Protein aggregation: Pathways, induction factors and analysis. J Pharm. Sci., 98, 2909-2934.

67. Mahler,H.C., Muller,R., Friess,W., Delille,A., Matheus,S., 2005. Induction and analysis of aggregates in a liquid IgG1-antibody formulation. Eur. J Pharm. Biopharm., 59, 407-417.

68. Malvern., 2007, Dynamic light scattering; technical note. http://www.malvern.com/labeng/technology/dynamic_light_scattering/dynamic_light_scattering.htm .

69. Manning,M.C., Chou,D.K., Murphy,B.M., Payne,R.W., Katayama,D.S., 2010. Stability of protein pharmaceuticals: an update. Pharm. Res., 27, 544-575.

70. Manning,M.C., Patel,K., Borchardt,R.T., 1989. Stability of protein pharmaceuticals. Pharm. Res., 6, 903-918.

71. Minton,A.P., 2007. Static light scattering from concentrated protein solutions, I: General theory for protein mixtures and application to self-associating proteins. Biophys. J, 93, 1321-1328.

72. Mire-Sluis,A., Cherney,B., Madsen,R., Polozova,A., Rosenberg,A., Smith,H., Arora,T., Narhi,L., 2011. Analysis and Immunogenic Potential of Aggregates and Particles. BioProcess International, 9, 38-54.

73. Narhi,L.O., Schmit,J., Bechtold-Peters,K., Sharma,D., 2011. Classification of protein aggregates. J Pharm. Sci., 101, 493-498.

74. Narhi,L.O., Jiang,Y., Cao,S., Benedek,K., Shnek,D., 2009. A critical review of analytical methods for subvisible and visible particles. Curr. Pharm. Biotechnol., 10, 373-381.

75. Nicomp., 2008, Accusizer Theory. http://www.pssnicomp.com/accutheory.htm .

76. Philo,J.S., 2005. Analytical Ultracentrifugation. In: Jiskoot,W., Crommelin,D.J. (Eds.), AAPS, Arlington, 379-412.

77. Philo,J.S., 2006. Is any measurement method optimal for all aggregate sizes and types? AAPSJ, 8, E564-E571.

78. Philo,J.S., 2009. A critical review of methods for size characterization of non-particulate protein aggregates. Curr. Pharm. Biotechnol., 10, 359-372.

79. Pikal-Cleland,K.A., Rodriguez-Hornedo,N., Amidon,G.L., Carpenter,J.F., 2000. Protein Denaturation during Freezing and Thawing in Phosphate Buffer Systems: Monomeric and Tetrameric b-Galactosidase. Arch. Biochem. Biophys., 384, 398-406.

80. Privalov,P.L., 1990. Cold denaturation of proteins. Crit. Rev. Biochem. Mol. Biol., 25, 281-305.

81. Privalov,P.L., Gill,S.J., 1988. Stability of protein structure and hydrophobic interaction. Adv. Protein Chem., 39, 191-234.

82. Reubsaet,J.L., Beijnen,J.H., Bult,A., van Maanen,R.J., Marchal,J.A., Underberg,W.J., 1998a. Analytical techniques used to study the degradation of proteins and peptides: chemical instability. J Pharm. Biomed. Anal., 17, 955-978.

83. Reubsaet,J.L., Beijnen,J.H., Bult,A., van Maanen,R.J., Marchal,J.A., Underberg,W.J., 1998b. Analytical techniques used to study the degradation of proteins and peptides: physical instability. J Pharm. Biomed. Anal., 17, 979-984.

84. Rhyner,M.N., 2011. The Coulter principle for analysis of subvisible particles in protein formulations. AAPSJ., 13, 54-58.

85. Roberts,C.J., 2007. Non-native protein aggregation kinetics. Biotechnol. Bioeng., 98, 927-938.

86. Rosenberg,A.S., 2006. Effects of protein aggregates: an immunologic perspective. AAPSJ, 8, E501-E507.

87. Schellekens,H., 2003. Immunogenicity of therapeutic proteins. Nephrol. , Dial. , Transplant., 18, 1257-1259.

88. Sharma,D.K., Oma,P., Pollo,M.J., Sukumar,M., 2010a. Quantification and characterization of subvisible proteinaceous particles in opalescent mAb formulations using micro-flow imaging. J Pharm. Sci., 99, 2628-2642.

89. Sharma, D., King, D., Moore, P., Oma, P., and Thomas, D., 2007, Flow microscopy for particulate analysis in parenteral and pharmaceutical fluids. Eur.J.Par.Pharm.Sci 12[4], 97-101.

90. Sharma,D.K., King,D., Oma,P., Merchant,C., 2010b. Micro-flow imaging: flow microscopy applied to sub-visible particulate analysis in protein formulations. AAPSJ, 12, 455-464.

91. Sharma,D.K., Oma,P., Krishnan,S., 2009. Silicone microdroplets in protein formulations. Detection and enumeration. Pharm. Technol., 33, 74-76, 78.

93. Singh,B.P., Bohidar,H.B., Chopra,S., 1991. Heat aggregation studies of phycobilisomes, ferritin, insulin, and immunoglobulin by dynamic light scattering. Biopolymers, 31, 1387-1396.

94. Singh,S.K., Afonina,N., Awwad,M., Bechtold-Peters,K., Blue,J.T., Chou,D., Cromwell,M., Krause,H.J., Mahler,H.C., Meyer,B.K., Narhi,L., Nesta,D.P., Spitznagel,T., 2010. An industry perspective on the monitoring of subvisible particles as a quality attribute for protein therapeutics. J Pharm. Sci., 99, 3302-3321.

95. Stadtman,E.R., 1992. Protein oxidation and aging. Science, 257, 1220-1224.

96. Strambini,G.B., Gabellieri,E., 1996. Proteins in frozen solutions: evidence of ice-induced partial unfolding. Biophys. J, 70, 971-976.

97. Thirumangalathu,R., Krishnan,S., Ricci,M.S., Brems,D.N., Randolph,T.W., Carpenter,J.F., 2009. Silicone oil- and agitation-induced aggregation of a monoclonal antibody in aqueous solution. J Pharm. Sci., 98, 3167-3181.

98. Tleugabulova,D., Falcón,V., Pentón,E., Sewer,M., Fleitas,Y., 1999. Aggregation of recombinant hepatitis B surface antigen induced in vitro by oxidative stress. Journal of Chromatography B: Biomedical Sciences and Applications, 736, 153-166.

99. Treuheit,M.J., Kosky,A.A., Brems,D.N., 2002. Inverse relationship of protein concentration and aggregation. Pharm. Res., 19, 511-516.

100. Tyagi,A.K., Randolph,T.W., Dong,A., Maloney,K.M., Hitscherich,C., Jr., Carpenter,J.F., 2008. IgG particle formation during filling pump operation: A case study of heterogeneous nucleation on stainless steel nanoparticles. J Pharm. Sci., 98, 94-104.

101. United States Pharmacopeia, 2009. Particulate Matter in Injections <788>.

102. Van Beers,M.M., Gilli,F., Schellekens,H., Randolph,T.W., Jiskoot,W., 2012. Immunogenicity of recombinant human interferon beta interacting with particles of glass, metal, and polystyrene. J Pharm. Sci., 101, 187-199.

103. Vermeer,A.W., Bremer,M.G., Norde,W., 1998. Structural changes of IgG induced by heat treatment and by adsorption onto a hydrophobic Teflon surface studied by circular dichroism spectroscopy. Biochim. Biophys. Acta, 1425, 1-12.

104. Wandrey,C., Hasegawa,U., van der Vlies,A.J., O'Neil,C., Angelova,N., Hubbell,J.A., 2011. Analytical ultracentrifugation to support the development of biomaterials and biomedical devices. Methods, 54, 92-100.

105. Wang,W., 2000. Lyophilization and development of solid protein pharmaceuticals. Int. J. Pharm., 203, 1-60.

106. Wang,W., Nema,S., Teagarden,D., 2010. Protein aggregation--pathways and influencing factors. Int. J Pharm., 390, 89-99.

107. Wang,W., Singh,S., Zeng,D.L., King,K., Nema,S., 2007. Antibody structure, instability, and formulation. J Pharm. Sci., 96, 1-26.

108. Wen,J., Arakawa,T., Philo,J.S., 1996. Size-exclusion chromatography with on-line light-scattering, absorbance, and refractive index detectors for studying proteins and their interactions. Anal. Biochem, 240, 155-166.

109. Wu,L.Z., Ma,B.L., Zou,D.W., Tie,Z.X., Wang,J., Wang,W., 2008. Influence of metal ions on folding pathway and conformational stability of bovine serum albumin. Journal of Molecular Structure, 877, 44-49.

110. Ye,H., 2006. Simultaneous determination of protein aggregation, degradation, and absolute molecular weight by size exclusion chromatography-multiangle laser light scattering. Anal. Biochem, 356, 76-85.

111. Zhang,J., Peng,X., Jonas,A., Jonas,J., 1995. NMR study of the cold, heat, and pressure unfolding of ribonuclease A. Biochemistry, 34, 8631-8641.

112. Zoells, S., Tantipolphan, R., Wiggenhorn, M., Winter, G., Jiskoot, W., Friess, W., and Hawe, A., 2011, Particles in therapeutic protein formulations, Part 1: Overview of analytical methods. J.Pharm.Sci. 101[3], 1-22.

2. Material and Methods

2.1 Materials

2.1.1 Therapeutic proteins

2.1.1.1 IgG_1-α and IgG_1-ß

Two humanized monoclonal antibodies (Immunoglobulines) of the IgG_1 class were used as model proteins. In order not to use the names of patented IgG_1 and to distinguish them though, the immunoglobulines were named IgG_1-α and IgG_1-ß.
Monoclonal antibodies are Y shaped and glycoproteins of the immune system [Wang et al., 2007]. There are five isotypes of immunoglobulines (Ig): IgA, IgD, IgE, IgG, IgM. The isotypes can be further differentiated into different subclasses. IgG is the most important group of immunoglobulines. Antibodies consist of two heavy and two light polypeptide chains, which are connected by two disulfide bonds.
IgG_1-α used in this thesis is formulated at 5.0 mg/ml in 10 mM histidine, 65 mM NaCl and 5 % sucrose at pH 6.0.
IgG_1-ß used is formulated at 10.3 mg/ml in 25 mM histidine, 250 mM glycine, 1% sucrose and 0.01 % polysorbate 80 at pH 5.8. For our studies the bulk was diluted to a concentration of 5.0 mg/ml.

2.1.1.2 GCSF

Granulocyte colony stimulating factor (GCSF) was used as the third model protein. GCSF is a glycoprotein that stimulates the bone marrow to produce granulocytes and stem cells [Basu et al., 2002]. Further, GCSF stimulates the proliferation of mature neutrophils.
GCSF was obtained at 4.2 mg/ml in 20 mM phosphate buffer at pH 4.0. For our studies the concentration was set to 0.5 mg/ml.

2.1.1.3 rPA

Reteplase (rPA) is a recombinant non-glycosilated form of human tissue plasminogen activator (alteplase), a thrombolytic drug [Nordt et al., 2003]. It was used as a further

model protein. rPA is formulated at 3.0 mg/ml in 500 mM arginine and 260 mM phosphate at pH 7.2. Concentration for experiments was set to 1.0 mg/ml.

2.1.2 Chemicals and reagents

Table 1: Chemicals and Reagents

Reagent	Description	Supplier
Glycine	Ph.Eur.	Sigma-Aldrich Chemie GmbH, Steinheim, Germany
L-Histidine	Ph.Eur.	Merck KGaA, Darmstadt, Germany
D(+)-Sucrose	Ph.Eur.	VWR International, Darmstadt, Germany
NaCl	p.a.	Merck KGaA, Darmstadt, Germany
L-Arginine	p.a.	Applichem GmbH, Darmstadt, Germany
$NaH_2PO_4 * 2H_2O$	p.a.	Merck KGaA, Darmstadt, Germany
$Na_2HPO_4 * 2H_2O$	min. 98%	Merck KGaA, Darmstadt, Germany
Polysorbate 80	Ph.Eur.	Sigma-Aldrich Chemie GmbH, Steinheim, Germany
BSA	Fraction V	Merck KGaA, Darmstadt, Germany
Sodium dodecyl sulphate (SDS)	>99%, ACS	Sigma-Aldrich Chemie GmbH, Steinheim, Germany
Apura water standard Oven 1%	1% water	Merck KGaA, Darmstadt, Germany
KH_2PO_4	p.a.	Sigma-Aldrich Chemie GmbH, Steinheim, Germany
$K_2HPO_4 * 2H_2O$	p.a.	Sigma-Aldrich Chemie GmbH, Steinheim, Germany
KCl	p.a.	Sigma-Aldrich Chemie GmbH, Steinheim, Germany
2-Propanol	for HPLC	Sigma-Aldrich Chemie GmbH, Steinheim, Germany
Reversible Protein Detection Kit	for membranes and polyacrylamide gels	Sigma-Aldrich Chemie GmbH, Steinheim, Germany
NIST tracable size standard	150nm, 200nm, 220nm, 240nm, 269nm, 300nm, 700nm	Thermo Fisher Scientific (Pao Alto, CA, USA)
Particle counting standard	300nm and 498nm	Thermo Fisher Scientific (Pao Alto, CA, USA)
Hydrazinsulfate	Ph.Eur.	Merck KGaA, Darmstadt, Germany
Hexamethylentetramine	Ph.Eur.	Merck KGaA, Darmstadt, Germany

2.2 Methods

2.2.1 Protein sample processing

2.2.1.1 Shaking stress

Mechanical shaking stress was performed with a Combidancer (Hettlab AG, Bäch, Switzerland) at 1000 rpm. Aliquots of 3.5 ml of each solution were filled into 4 ml Zinsser Analytic glass vials (Zinsser Analytic, Frankfurt, Germany) adequate for the Combidancer and sealed with screw caps with silicone seal disc (Zinsser Analytic, Frankfurt, Germany). Sampling of 3.5 ml glass vials (n = 3) was accomplished at defined time points: to assess the relevance of submicron particle counting (chapter 3), sampling from IgG_1-α, GCSF and rPA formulations was performed every 30 min and for IgG_1-ß every 90 min. The determination of particulate matter of stressed protein solutions after dilution into serum solution (chapter 4) was performed after 2 h (rPA), 3 h (GCSF), 4 h (IgG1-α), and 9 h (IgG1-ß) shaking. Different shaking times were applied in order to generate sufficient concentration of particles. The dilution into different buffers (chapter 5) was performed after 5 hours shaking in order to study the effect of dilution, different pHs and standing time.

2.2.1.2 Stirring stress

For stress simulation experiments (chapter 7) stirring stress was performed in glass bottles at 150 rpm, 200 rpm, 300 rpm, 400 rpm, 500 rpm and 600 rpm using magnetic stirrer bars and magnetic stirrers with different dimensions (table 2). Glass containers were of different sizes and filling volumes: standard 5 ml glass type I vials filled with 5 ml IgG_1-α-formulation and crimped with crimping caps with silicone seal disc (West Pharmaceuticals, Eschweiler, Germany) during stirring, 100 ml glass bottles filled with 40 ml IgG_1-α-solution and 500 ml glass bottles filled with 200 ml IgG_1-solution (n=3). Furthermore, 2000 ml IgG_1-α-solution were stirred at 400 rpm in a 5000 ml glass bottle (n=1). All used glass bottles and glass vials were from glass type I. The Duran® glass bottles (Duran Group GmbH, Mainz, Germany) were sealed with screw caps during stirring to prevent contamination with extraneous particles.

Table 2: Dimensions of stir bars and glass bottles

Dimensions

Stir bar dimensions	Short Side [mm]	Long Side without Curve [mm]	Long Side Total [mm]
Stir bar 5 ml vial	3.00	6.00	4.00
Stir bar 100 ml bottle	5.20	20.69	24.88
Stir bar 500 ml bottle	7.47	33.73	39.90
Stir bar 5000 ml bottle	9.89	74.47	81.70

Bottle dimensions	Total Height [mm]	Height up to shoulder [mm]	Outer Diameter [mm]	Inner Diamter [mm]
5 ml vial	40	25	20	18
100 ml bottle	100	50	56	52
500 ml bottle	176	97	86	82
5000 ml bottle	330	199	182	176

2.2.1.3 Thermal stress

For thermal stress aliquots of 5 ml of each solution and corresponding placebo were filled into standard 5 ml glass type I vials (Schott, St. Gallen, Switzerland) and crimped using crimping caps with silicone sealing discs (West Pharmaceuticals, Eschweiler, Germany). The vials were placed at 65 °C (for both IgG_1 formulations), 60 °C for rPA and 50 °C for GCSF in a Heraeus hot-air cabinet (Haraeus, Hanau, Germany). Temperatures for thermal stresses were set to be at least 5 °C below the respective protein melting temperature T_m. Sampling (three vials of protein formulation and one vial of matching placebo were taken per sampling-point from the hot air cabinet) was accomplished at defined time points: to assess the relevance of submicron particle counting (chapter 3), sampling of both IgG_1 formulations every 20 min over 3 h, for GCSF and rPA formulations every 15 min over 2 h. To assess particulate matter in serum-solution (chapter 4), proteins were heated over 3 h at given temperatures.

2.2.1.4 Freeze-thawing

Freeze-thaw cycles were used in these studies to apply stress on therapeutic proteins. In order to determine the relevance of submicron particle counting (chapter 3) aliquots of 5 ml protein solution and corresponding placebo were filled into standard 5 ml glass type I vials (Schott, St. Gallen, Switzerland) and crimped using crimping caps with silicone sealing discs (West Pharmaceuticals, Eschweiler, Germany). At least five freeze-thaw cycles were performed using a -86 °C ULT

Freezer Thermo Scientific (Thermo Scientific, Karlsruhe, Germany). Sampling was performed after each cycle (3 vials with protein formulation and 1 vial with placebo formulation were sampled).

To generate enough particles for particulate matter determinations after dilution into serum solution and buffers (chapter 4), ten freeze-thaw cycles were applied to rPA and GCSF.

2.2.1.5 Lyophilization

Lyophilization was performed using either a Christ Epsilon 2-12D freeze-dryer (Christ, Osterode am Harz, Germany) or a FTS Systems Durastop freeze-dryer (Stone Ridge, New York, USA). Aliquots of 3 ml were filled into TopLyo® vials (Schott, St. Gallen, Switzerland) and standard glass type I vials (Schott, St. Gallen, Switzerland) and partially stoppered with lyophilization stoppers (West pharmaceuticals, Eschweiler, Germany).

A conventional freeze-drying cycle was applied (see table 3). During the lyophilization process product temperature was controlled using thermocouples. After freeze-drying the lyophilization chamber was vented with dry nitrogen up to a pressure of 1000 mbar and the vials were completely stoppered.

Table 3: Lyophilization parameters

Step	Ramp [K/min]	Shelf temperature [°C]	Hold Time [min]	Vacuum [mbar]
Freezing	1.0	2	20	1000
Freezing	0.8	-50	120	1000
Primary Drying	0.5	-30	390	0,09
	0.5	-35	3600	0,09
	0.2	-20	600	0,09
Secondary Drying	0.3	+20	600	0,013
Venting and Unloading	-	+20	-	1000

The freeze-dried samples were degassed after reconstitution with purified water using ultrasound bath Bandelin Sonorex TK 52 (SCHALLTEC GmbH, Mörfelden-Walldorf, Germany) for 3 min to remove air bubbles.

2.2.2 Protein aggregate characterization methods

In general, from each measuring point 3 vials with stressed protein and 1 vial placebo are taken. From each vial one measurement with each method is performed. The order of measurements in chapter 3 is always kept the same to have comparable results, starting with the most sensitive methods: particle counting with AccuSizer is performed directly after sampling, followed by light obscuration and Micro-Flow Imaging. Dynamic Light Scattering, Size-Exclusion Chromatography and turbidity measurements are performed subsequently.

2.2.2.1 Particle counting

2.2.2.1.1 Particle counting with AccuSizer FY nano (AS)

Particles in the range from 150 nm to 10 µm were counted with an AccuSizer FY nano (PSS Nicomp, California). 1.5 ml sample was extracted from the vials via syringe and needle. For each sampling point 3 vials protein formulation and 1 vial placebo were sampled. The syringe was placed onto the AccuSizer port. After 10 min waiting to discharge micro and nanosized airbubbles the sample was injected into the instrument. In order not to stress the proteins and not to generate particles, the protein formulations were allowed to stand in the syringe for 10 minutes.

Figure 1 shows a schematic representation of the optical system: Larger particles in the range from 0.61 µm are counted via light obscuration. In the range below 0.61 µm the light scattering detector comes into operation.

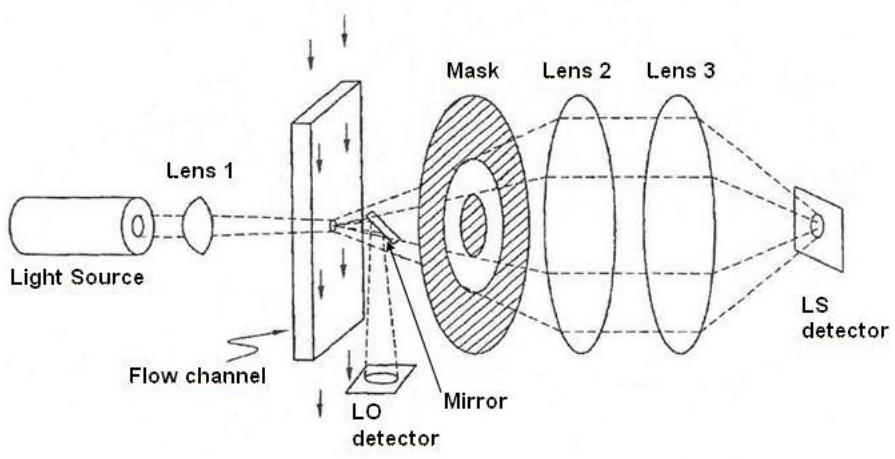

Fig. 1: Two detectors system of AccuSizer

The AccuSizer FYCD Application software (Vers. 4.32) was set to collect data in the range from 0.61 µm to 10 µm over 90 seconds, in the range from 0.31 µm to 0.61 µm and in the range from 0.15 µm to 0.31 µm over 120 seconds. The system automatically conducts three measurements from the stirred, homogeneous sample. The first measurement is for the larger particles, the last measurement for the smallest particles. In parallel the automatic sample dilution takes place with a speed of 15 ml/min until the maximum of 2000 particles/second is counted in the respective measurement. During automatic sample dilution also a rinsing of the measurement system was accomplished.

To better evaluate the results, the data were classified into different particle size classes, plotted cumulatively. The size classes ≥250 nm, ≥500 nm, ≥750 nm, ≥1 µm, ≥2.5 µm, ≥5 µm and ≥7.5 µm were used. Originally, the particle size class >10 µm has also been chosen for evaluation, as its number is limited within pharmacopoeias. However, the AccuSizer was not able to detect any particles of this size class.

2.2.2.1.2 Classical light obscuration (LO) particle counting

Subvisible particles in the range from 1 - 200 µm were either counted with a light obscuration instrument Syringe (Klotz, Bad Liebenzell, Germany) using SW-CA2 software and LDS23/25bs sensor or with a light obscuration instrument PAMAS SVSS-C (PAMAS, Bad Salzuflen, Germany), Sensor HCB-LD-25/25 (PAMAS, Bad Salzuflen, Germany). From each vial (n = 3 vials) one measurement of a volume of 1.0 ml was performed, the instrument takes the defined volume automatically from the vials using a needle. The obtained results were averaged and standard deviations were calculated. The first measurement was always considered as rinsing and eliminated from calculations.

To better evaluate the results, the data were classified into different particle size classes and plotted cumulatively. The size classes ≥1 µm and ≥10 µm were chosen. The pharmacopoeial requirements regarding subvisible particles are related to particles ≥10 µm and ≥25 µm, therefore the size class ≥10 µm is chosen.

2.2.2.1.3 Microflow imaging (MFI) particle counting

A second instrument to assess subvisible particles in the range from 1 - 100 µm is MFI (either DPA 4100 or DPA 4200, Brightwell Technologies, Toronto, Canada, now ProteinSimple, Santa Clara, CA, USA). From each vial (n = 3) one measurement of 0.5 ml was performed. The samples were taken from the vials using an Eppendorf

pipette (Eppendorf AG, Hamburg, Germany) and barrier tips. The barrier tip prevents the samples to be contaminated with extraneous particles. The results were averaged and standard deviations were calculated.

MFI DPA 4100 measurements and analysis was performed using DPA4100 software version 6.9.7.1. Measurements with DPA 4200 were carried out with MVSS software version 2, analysis was done with MVAS1.1.

To better evaluate the results, the data were classified into different particle size classes and plotted cumulatively. The size classes ≥1 µm and ≥10 µm were chosen for comparison.

2.2.2.1.4 Evaluation of particle counting measurements

Observing strict rules is necessary when evaluating particle counting measurements. Otherwise comparison is impossible. We were interested to define the “point of detection”, where applied stress results in a significant increase of particle counts, by statistical analysis.

At each sampling point one measurement is performed from three vials (n = 3), this also applies for the reference samples. From these three results the mean value and standard deviations (SD) are calculated.

Mean values of particle counting measurements with their standard deviations were plotted over stress time to find the point where stress on the proteins results in aggregate formation, the “point of detection”.

We defined the “point of detection” as the first measuring point with no overlap of its SD with the SD of the reference. Only for particle counting measurement this rule is extended due to generally high variability in counts. Especially after mechanical stress outliers are prevalent, increasing the mean of counted particles and the respective SD. An increased mean and SD would lead to a false “point of detection”. Therefore, also the averaged relative SD of all measuring points must not have an overlap at time point of detection. Observing both rules, a consistent evaluation of results was ensured.

2.2.2.2 Microscopic examination

Microscopic examination (chapter 5) was performed using Olympus BX50 microscope (Olympus, Hamburg, Germany) and 10*0.30p U-PLan FI objective. The magnification used was 10-fold. 10 µm protein samples were placed on a microscope slide and pictures were taken.

2.2.2.3 Dynamic light scattering (DLS)

Particle size distributions for IgG_1-α and -ß (chapter 3) were measured with a Zetasizer Nano-ZS (Malvern Instruments, Germany) at 25 °C using ZetaSizer software (Vers. 6.01). The ZetaSizer Nano is performing non-invasive back-scattering technique (NIBS) with a 4 mW He-Ne-Laser at 633 nm.

Each sample was recorded once with 20 subruns of 20 seconds. Z-average was evaluated, calculated from correlation function using ZetaSizer software.

The hydrodynamic diameter of the native antibody was 11 nm. Denaturation of the monomer was assumed when the size of the main peak was ≥13 nm. The occurrence of additional large size peaks was interpreted as existence of protein aggregates.

GCSF and rPA formulations were not assessed by DLS.

2.2.2.4 Size-exclusion chromatography (SEC)

Relative levels of remaining monomer and soluble aggregates were determined by SEC.

An Agilent 1100 system (Agilent Technologies GmbH, Böblingen, Germany) was used for this study. UV-detection at 280 nm (IgG_1-α, IgG_1-ß, GCSF) and 215 nm (rPA) (table 3) was applied for quantification of relative amounts of monomer, dimer/trimer, fragments and soluble high-molecular weight (HMW) aggregates (chapter 3). Calculations were performed using ChemStation software (Vers. A.10.02). Relative amounts of insoluble aggregates were indirectly calculated: if recovery decreases, insoluble aggregates were assumed to form to the same amount.

All samples (n = 3) were centrifuged at 14000 rpm over 10 min to separate from insoluble aggregates before injection.

Areas under the curve were evaluated and the results of performed three measurements were averaged. The amount of monomer, dimer, fragments, oligomer and insoluble aggregates are calculated by percentage relatively to reference chromatogram and plotted in one graph.

Table 4: Size-Exclusion chromatography parameters

Protein	Column	Pre-Column	Injection volume [µl]	Flow rate [ml/min]	Running buffer	UV-Detection [nm]	Fluorescence-Detection [nm]
IgG_1-α	TSK-GEL G3000 SW_{XL} 7.8 mm ID * 30.0 cm[1]	TSK-GEL SWXL[1]	100	0.3	0.25 M KCl, 0.2 M potassium phosphate, pH 7.0, 10% (V/V) isopropanol	280	-
IgG_1-ß	Superose 6[2]	-	100	0.35	0.01 M sodium phosphate, 0.5 M NaCl, pH 7.0	280	-
GCSF	TSK-GEL G3000 SW_{XL} 7.8 mm ID * 30.0 cm[1]	TSK-GEL SWXL[1]	100	0.6	0.1 M phosphate buffer, pH 7.0	215	-
rPA	TSK-GEL G3000 SW 7.5 mm ID * 30.0 cm[1]	-	50	0.45	0.5 M L-Arginin and H_3PO_4, pH 7.2	280	-
any (Protein adsorption)	TSK-GEL G3000 SW_{XL} 7.8 mm ID * 30.0 cm[1]	-	400	0.75	PBS; 0.05 mg/ml SDS	-	Intrinsic Fluorescence: Ext. 280 nm; Em. 334 nm

[1] Tosoh Bioscience GmbH, Stuttgart, Germany

[2] GE Healthcare, Freiburg, Germany

Protein desorption of adsorbed protein was performed in chapter 6. The exact amount of desorbed protein (2.2.3.1) was determined via Size-Exclusion Chromatography (SEC) on an Agilent 1100 system and corresponding Agilent 1200 fluorescence detector. Calculations were performed using ChemStation software (Vers. B.02.01). 6-point calibrations from 0.0001-0.01 mg/ml for each protein were performed to calculate the exact amount of desorbed protein.

2.2.2.5 Optical density at 550 nm (OD)

Measuring optical density at a high wavelength was used to determine turbidity with small sample volumes.

Optical density was determined at 550 nm using a Tecan GENios Plus Microplate reader (Tecan GmbH, Germany) using XFluor4 software. 200 µl sample were measured in a Nunc 96-well-plate.

We were interested to find the “point of detection”, where applied stress resulted in a significant increase of turbidity. OD measurement results (n = 3) are averaged and standard deviations are calculated. The mean values are plotted over time with their relative standard deviations. The first point with no overlap of standard deviations mirrors the time “point of detection”. Additionally, OD values have to be ≥0.0287. Turbidity limits are defined by the pharmacopoeia, relationship to optical density was established (see chapter 3.3.6).

2.2.3 Other methods

2.2.3.1 Quantification of protein adsorption to glass vials

The adsorption behaviour of IgG_1 on inner surfaces of standard 5 ml glass type I vials and 6R TopLyo® vials was studied adapting the standardized desorption method developed by Johannes Mathes [Mathes, 2010].

Samples were prepared and split into different parts. One part of the samples was freeze-dried, reconstituted and degassed (n = 3 for both vials), one part of the samples was freeze-thawed (n = 3 for both vials), one part was kept as reference in the different vials (n = 3 for both vials) over 4 h to incubate the protein.

To quantify the protein adsorption to glass vials via SDS-desorption, vials were quantitatively emptied after incubation of the protein solution. Into the empty vials respective formulation buffer was filled four times for 5 min and vials were quantitatively emptied after each cycle. Vials were centrifuged headfirst over 2 min at 1500 rpm using a Megafuge 1.0R (Heraeus, Hanau, Germany). After the last cycle, 0.05 % SDS in PBS (10 mM phosphate buffer and 145 mM NaCl) at pH 7.2 was filled into the vials and incubated for 24 h at 25 °C.

2.2.3.2 Differential scanning calorimetry (DSC)

Differential scanning calorimetry was used to assess the physicochemical characteristics of the lyophilized cakes. A Netzsch DS Calorimeter 204 Phoenix (Netzsch, Selb, Germany) was applied to determine the glass transition temperature of the maximally freeze-concentrated solution (T_g') and the lyophilizates (T_g).

To determine T_g' 20 µl were transferred into aluminium crucibles and cooled to -90 °C. Samples were then heated up to 10 °C to determine the glass transition.

To determine T_g 5 - 10 mg of the dried lyophlizates were weighed into aluminium crucibles and sealed in a dry nitrogen atmosphere. Two heating scans were performed: cooling down to -20 °C and heating up to 100 °C, cooling down again to -20 °C and heating up to 200 °C. T_g was determined from the heating scans.

2.2.3.3 Karl-Fischer titration

Residual moisture contents of the samples were determined using a Karl Fischer coulometric titrator Aqua 40.00 (Analytik Jena AG, Halle, Germany) with headspace oven. An oven connected to the reaction vessel and flushed with Nitrogen heated the lyophilized cake up to 80 °C. Dry nitrogen transported the evaporated water into the

titration solution and residual water was determined. Before and after measuring the sample batch, a pure water standard was analyzed, as well as at least three blank values.

2.2.3.4 Zeta potential titration

Zeta potential (ZP) and surface charge densities of proteins in solutions were measured using a ZetaSizer (Malvern Instruments, Herrenberg, Germany), operating with a 4 mW He-Ne laser at 633 nm. Measurements were performed in Malvern disposable zeta cells at 25 °C. A starting volume of 8 ml of filtered protein solution was filled into a polypropylene tube and stirred during measurement. The pH adjustment was computer-controlled by a MPT-2 Autotitrator (Malvern Instruments, Herrenberg, Germany); titration was performed using 0.1 M HCl to pH 4.0 (for IgG1) and 0.1 M NaOH to pH 12.0. Device control and final data analysis were performed using Malvern Dispersion Technology Software version 6.12 (Malvern Instruments, Herrenberg, Germany).

2.2.3.5 Stress simulations

Stress simulations were performed at 150 rpm, 200 rpm, 300 rpm, 400 rpm, 500 rpm, and 600 rpm using STAR-CCM+ software (CD Adapco, Nürnberg, Germany) in 5 ml standard glass type I vials, 100 ml, 500 ml, and 5000 ml Duran® glass bottles.
To perform the complex calculations the following information was needed: viscosity and density of formulation, dimension of glass containers and magnetic stirrer bars and stirring speed. Exact bottle dimensions were obtained from Duran Group GmbH, Mainz, Germany. Exact stirrer bar dimensions were determined using a slide-rule.
Stress tensor magnitudes [Pa] as the obtained stress unit were extracted from the simulations.
Stress tensor magnitude is a parameter to quantify stress in Pascal, calculated by STAR-CCM+ software, using a complex three dimensional momentum Navier-Stokes equation, which describes the flow of Newton's liquids:

$$\frac{\partial \rho u_i}{\partial t} + \frac{\partial}{\partial x_j}\left(\rho u_j u_i - \tau_{ij}\right) = -\frac{\partial p}{\partial x_i} + s_i$$

Whereas t is the time, x_i the Cartesian coordinate, u_i the velocity component in direction x_i, p the pressure, ρ the density, τ_{ij} the stress tensor components and s_i the momentum source components.

Simplified, the Navier-Stokes equation describes: change of impulse + change of tensor over distance = change of pressure over distance.

The Stress Tensor Magnitude is defined as $\left\|\underline{\underline{T}}\right\| = \sqrt{\frac{1}{2}\sum_i \sum_j \tau_{ij}}$

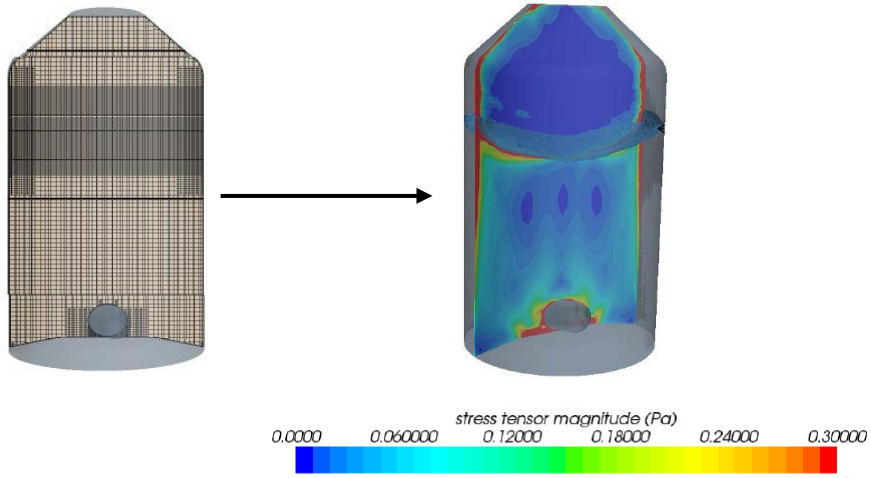

Fig. 2: Mesh refinement to capture the formulation surface and calculation into Stress Tensor Magnitude

For the computational calculations a 3D-virtual mesh is built and the stress tensor is calculated for each cuboid. Mesh refinements are applied to exactly characterize areas where the IgG_1-formulation has contact with glass, air or stir bar surfaces (figure 2). In those areas maximal (red) stress tensor is found, whereas minimal (dark blue) stress tensor is found in areas with no contact of IgG_1-solution to glass, air or stir bar.

For each cuboid stress tensors are calculated using STAR-CCM+ software. From those calculations the minimal and maximal averaged stress tensors are obvious. The averaged stress tensor is calculated by multiplying the stress tensor of each cuboid with the cuboids volume and dividing the result by the total volume of the cuboids.

2.3 Reference List

1. Basu,S., Dunn,A., Ward,A., 2002. G-CSF: function and modes of action (Review). Int. J Mol. Med., 10, 3-10.

2. Mathes, J.M., 2010, Protein Adsorption to Vial Surfaces - Quantification, Structural and Mechanistic Studies. Department of Pharmacy, LMU Munich, [PhD].

3. Nordt,T.K., Bode,C., 2003. Thrombolysis: newer thrombolytic agents and their role in clinical medicine. Heart, 89, 1358-1362.

4. Wang,W., Singh,S., Zeng,D.L., King,K., Nema,S., 2007. Antibody structure, instability, and formulation. J Pharm. Sci., 96, 1-26.

3. Relevance of Submicron Particle Counting for Development and Quality Assurance of Protein Pharmaceuticals

3.1 Introduction

During the last years therapeutic proteins have become a major part of the modern drug portfolio and are the fastest growing group of new pharmaceuticals. Their specifity and efficacy opened new options in the treatment of severe diseases [Singh et al., 2010].

Unfortunately, proteins are typically not very stable molecules, neither chemically nor physically. Denaturation, aggregation and precipitation can occur during manufacture, handling, storage and shipping and may compromise the pharmaceutical quality of protein drug products [Carpenter et al., 2008]. Stress factors inducing aggregation are elevated temperatures, exposure to light and interfaces [Bee et al., 2009; Bee et al., 2010], agitation [Eppler et al., 2010], freeze-thawing [Bhatnagar et al., 2007] or impurities [Chi et al., 2005; Jones et al., 2005; Thirumangalathu et al., 2009; Tyagi et al., 2008]. In extreme cases, loss of declared content and loss of efficacy can be a result of aggregation, but proper formulation and quality control will exclude such products from the patient. Difficulties arise, when small amounts of protein aggregate in otherwise stable formulations. The presence of aggregates and particles is not just a matter of “pharmaceutical quality” but compromises the safety of such products with regard to their immunogenicity [Barnard et al., 2010; Fradkin et al., 2009; Rosenberg, 2006; Schellekens, 2003; Schellekens, 2005].

It has become obvious that a certain correlation between presence of aggregates/particles and unwanted immunogenicity of protein drug products exists [Carpenter et al., 2008; Schellekens, 2003]. On the other hand it is still unclear, what type of aggregates, what sizes and numbers etc. may lead to clinically relevant immune reactions.

In protein aggregates the native structure of the protein can either be retained or unfolded proteins can attach to each other. Furthermore, the aggregation can be irreversible or reversible [Mahler et al., 2008; Philo et al., 2009]. Aggregates can

cover the size range from a few nm (as for protein dimers) up to large precipitates, visible with the unaided eye (i.e. more than about 80 µm in size).

Before any further conclusions can be drawn and measures can be taken about the safety of aggregates and precipitates in protein drug products, the size and numbers of such aggregates have to be measured with reliable methods.

One single method covering the whole range of aggregate sizes and types does not exist [Das et al., 2008; Narhi et al., 2009]. Therefore, complementary methods must be used and existing methods have to be improved or better methods have to be developed.

In general, particulate matter has to be measured in parenteral drug products as set out in the pharmacopoeias [European Directorate For The Quality of Medicine (EDQM), 2011b; United States Pharmacopeia, 2009]. The USP and EP both have set limits for subvisible particles ≥10 µm and ≥25 µm to be counted by light obscuration (LO) or by microscopic methods and in addition ask for the absence of visible particles in parenterals. Originally these limits had been set for “extraneous, mobile and undissolved impurities” of any origin, including those from filters, packaging material, machinery, airborne dust etc. With protein solutions emerging on the market, these specifications have been kept and the same limits for particle sizes and numbers still apply, but the origin of particles has in many cases dramatically shifted towards aggregated and precipitated protein drug. With that background in mind it must be questioned, whether the existing specifications are still appropriate and meaningful, and if not, how they may be adapted to the actual situation. Subvisible particles <10 µm are not considered at all in the actual pharmacopoeial specifications. Of course, smaller particles are often present in protein solutions, their numbers need to be determined and their relevance must then be discussed [Golub et al., 2007; Mahler et al., 2005].

Although we have a large number of particle sizing and counting methods, including light blockage (LO), coulter counter (CC), micro flow imaging (MFI), dynamic light scattering (DLS) etc. we do not routinely use them from 1-10 µm and we have difficulties to reliably count particles below 1 µm , e.g. in the range from 100-1000 nm. Many methods, preferably DLS, detect and size such particles but cannot count, i.e. determine the number per volume [Malvern, 2007].

Classical light obscuration instruments and MFI systems have their lower detection limit at about 1 µm. On the other hand, it is possible to determine aggregates <1 µm

semiquantitatively by dynamic light scattering and chromatographic methods. The chances and limitations of SEC have been reviewed extensively elsewhere [Barnard et al., 2010]. SEC measurements might lead to false negative results due to adsorption of protein to the column matrix, reversibility of aggregates, and inability of large aggregates to the pass column frit and underestimation of aggregate species with UV-detection [Carpenter et al., 2009; Philo, 2009]. Dynamic light scattering (DLS) on the other hand allows detection of aggregates sized between 10 nm and 1000 nm but due to the bulk nature of the measurement, the presence of a few large aggregates can dominate the entire size distribution and lead to artefacts [Demeester et al., 2005].

Hence, reproducible quantification, i.e. counting of particles in the submicron range of 0.1-1 µm is practically not possible [Carpenter et al., 2008].

At that point it is our intention to provide new insight into the performance of existing and new methods and to come to new recommendations how to proceed.

This study highlights the data generated with a new instrument promising to partly close the existing size gap below 1 µm and to provide particle counting from the lower µm range down to about 200 nm. A new two-detector-system, the AccuSizer FY nano® (PSS Nicomp, CA, USA), is marketed with nominal detection and counting limits of 0.15-10 µm [Nicomp, 2008].

The instrument itself dilutes the samples until an eligible count of particles is achieved, whereby coincidences of particles shall be avoided. A caveat is that protein aggregates that are reversible with dilution could be generally underestimated [Demeule et al., 2010]. The AccuSizer employs two detector systems: a light obscuration detector is counting particles from 610 nm to 10 µm. The second detector is a light scattering detector counting particles from 150 nm to 610 nm by sensing different intensities of scattered light which are related to defined sizes.

AccuSizer uses focused extinction for evaluation of results: only a few particles flowing through the focus located in a small fraction of the flow cell are counted. Those particle counts are recalculated to give the overall particle counts for the entire flow cell and finally the particle counts per ml of sample solution.

We rigorously assessed the AccuSizer in comparison to classical instruments: Four model proteins were stressed thermally, mechanically and by freeze-thawing. At defined time points samples were collected and analytics were performed. Particle count, monomer loss and turbidity were determined over time. Results of AccuSizer

(AS) were compared to the classical methods: Light obscuration (LO), Size-Exclusion Chromatography (SEC), Dynamic Light Scattering (DLS), turbidity or Optical density at 550 nm (OD).

Electrical sensing zone instruments (coulter counter, CC) also claim to have a detection limit below 1 µm, e.g. at about 400 nm. Our group has studied the performance of the CC technique versus LO before [Mück, 2002] and found a "usable" lower detection limit of about 700 nm, not 400 nm, due to high background signals at the smaller size channels from 400 nm to about 700 nm. It has been the conclusion in our previous studies that CC will not deliver more relevant information on particle formation compared to LO. In the previous study we successfully employed a novel concept to assess the performance of the particle counting method, that did not directly compare the absolute numbers of particles counted but the onset of particle formation when formulations were stressed over time: The ability of a counting method to reliably detect and quantify whether a formulation aggregates and forms particles after a certain amount of applied stress or not appears most important to us. This concept implies also the expectation that a method counting smaller particles might allow the earlier and more sensitive detection of aggregation. Counting smaller particles may allow to find "precursor" particles at an earlier time point compared to methods starting at >10 µm.

In summary, the aim of the study is first to decide whether a new method is really able to reliably count protein aggregates sized below 1 µm and secondly if data on particle counts below 10 µm or even below 1 µm would provide more useful information to the formulations scientist than the existing, traditional counting >10 µm.

3.2 Experimental setup

The protein formulations were filtered using a 0.1 µm Millex syringe-driven filter unit (Millipore, Carrigtwohill, Ireland) into a particle free beaker and filled into particle free vials. For each sampling point three vials with protein formulation and one vial with placebo were prepared. From each vial all used analytical methods were performed.
Four different proteins were stressed over time using three different stresses: Thermal and mechanical stress and freeze-thawing. During stress samples were taken and analytics were performed with five different methods: classical light obscuration (LO) at particle size channels ≥10 µm as required by USP and Ph.Eur. and at channel ≥1 µm in addition, Microflow imaging (MFI) at particle size channels ≥1 µm and ≥10 µm, dynamic light scattering (DLS), size-exclusion chromatography (SEC), optical density evaluation at 550 nm (OD) and AccuSizer (AS) measurements at particle size channels ≥250 nm, ≥500 nm, ≥750 nm, ≥1 µm, ≥2.5 µm, ≥5 µm and ≥7.5 µm. To avoid redissolution of aggregates standing times were kept as short as possible. Immediately after stressing all samples were measured with particle counters, starting with more sensitive AS. Maintaining this order made sure that comparability between measurements in case of redissolution was still given.
Results were evaluated and compared. We had a specific interest to assess the methods by their ability to detect changes in the formulation quality, i.e. the formation of larger aggregates and particles, at an early timepoint. Therefore we introduced the concept to determine “a point of detection” at which the applied stress resulted in formation of aggregates or particles or in loss of monomer content. The concept is visualized in figure 1.

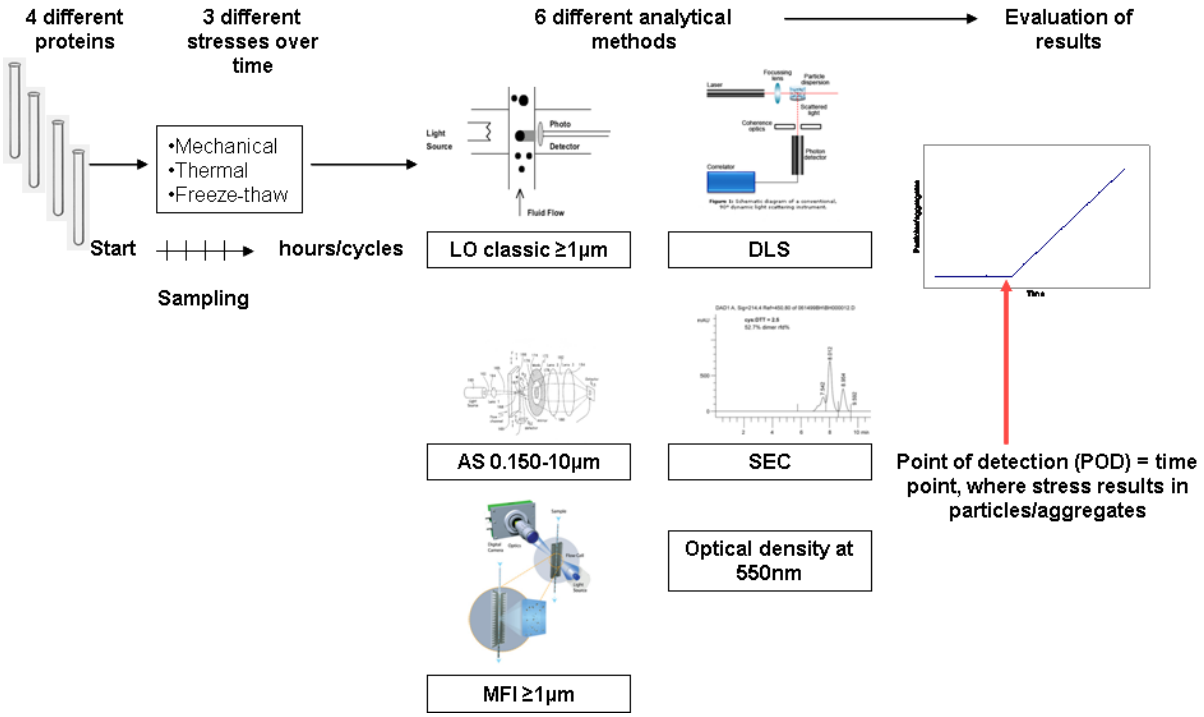

Fig. 1: Experimental setup

All in all we assessed for each Protein/stress combination (12 combinations) data at 6 or more time points and 6 methods. The results of the three particle counters were subdivided and different particle size classes were assessed: for LO and MFI particle size classes for particle ≥1 µm and ≥10 µm, for AS particle size classes for particles ≥250 nm, ≥500 nm, ≥750 nm, ≥1 µm, ≥2.5 µm, ≥5.0 µm and ≥7.5 µm (in total 11 data sets from particle counters for each time point). This huge amount of data sets (at least 84 for one single experiment; 12 experiments in total) can not completely be presented in this article. Therefore we evaluated raw data according to find the “point of detection”. The pre-evaluated data for all 12 experiments can be found in appendix (chapter 9).

3.3 Results and discussion

3.3.1 Light obscuration measurements with USP-qualified LO instruments in comparison to AS

The first study should elucidate how light obscuration measurements from traditional LO systems are compared to the new AccuSizer FY (AS) system.

First, we decided to use particle sizes of ≥1 µm to compare the systems. Both systems are technically very well able to count particles of this size class and we want to include as much particles of small size into the comparison as possible. Besides, though the upper detection limit of AS was declared by the manufacturer to be 10 µm any particles ≥7.5 µm were detected.

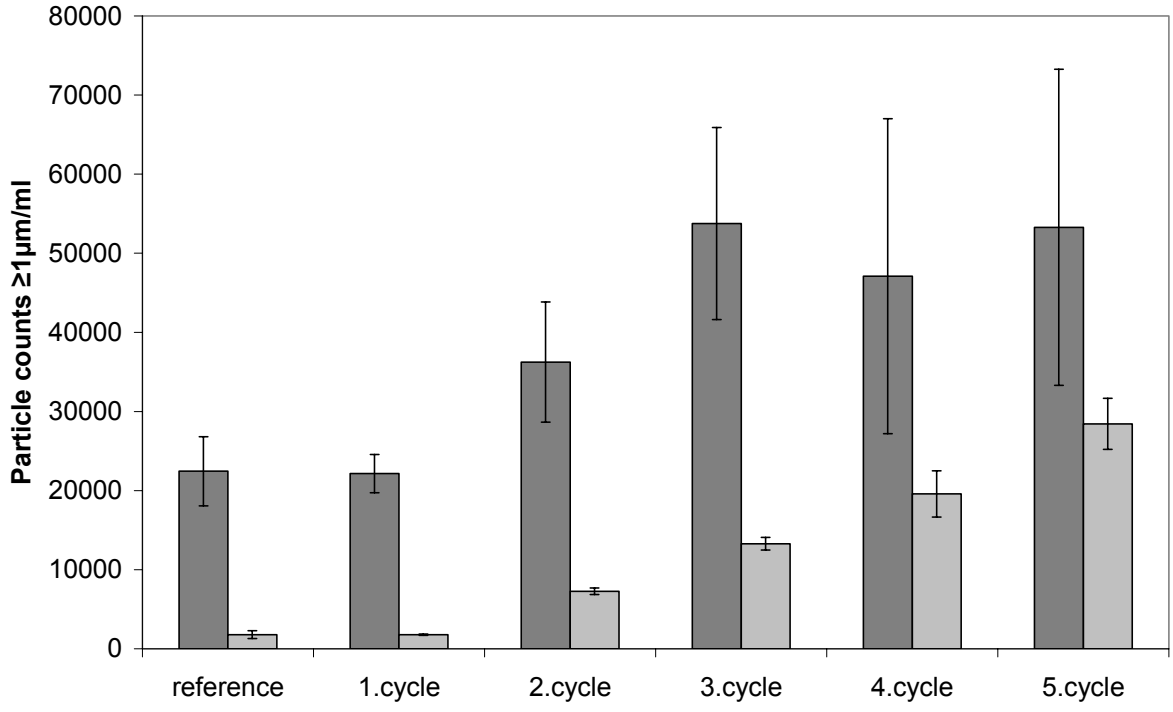

Fig. 2: Light obscuration measurements with LO instrument (light gray) and AccuSizer FY nano (dark grey) of freeze-thawed IgG_1-α; particles ≥1 µm; n = 3

Particle counts for particles ≥1 µm were taken after stresses were applied and plotted over stress. As the AccuSizer FY uses focused extinction and autodilution as special tools absolute counts of particles cannot be compared (figure 2). It is noticeable that AS detects up to 10-fold more particles in this size class than LO does. But

evaluation of the results clearly revealed that both instruments have the same trend of detecting the onset of particle formation. The Klotz instrument (LO) and the AccuSizer (AS) judged beginning aggregation in most of the cases at exactly the same time (table 1). Only in 2-3 cases of 12 protein/stress combinations the ability to determine the “point of detection” of LO and AS differed.

Table 1: Point of detection determined with LO and AS for particles ≥1 µm, more data in appendix

	LO*	AccuSizer*
IgG_1-α thermal	7	8
IgG_1-α mechanical	4	1
IgG_1-α freeze-thaw	**2**	**2**
IgG_1-ß thermal	**4**	**4**
IgG_1-ß mechanical	**1**	**1**
IgG_1-ß freeze-thaw	**2**	**2**
GCSF thermal	**1**	**1**
GCSF mechanical	2	1
GCSF freeze-thaw	**2**	**2**
Reteplase thermal	6	5
Reteplase mechanical	1	3
Reteplase freeze-thaw	2	1

* numbers express the point of detection

Interestingly a strong difference is seen in cases where mechanical stress had been applied. Two explanations are obvious. First, the standard deviation of the particle counts is compared to other samples very high for particle formation after mechanical stress. Second, autodilution and focused extinction by the AS system potentially leads to artefacts when measuring particles with a tendency for redissolution. Particles formed after mechanical stress show such a tendency [Kiese et al., 2010] and are therefore prone to being counted with high statistical error. In our studies high standard deviations can lead to a virtually later “time point of detection” (see 2.2.2.1.4).

Overall, the results after measuring four different proteins provide evidence that both LO instruments provide the same information when onset of particle formation is to be detected with the exception of samples after short term heavy mechanical stress.

3.3.2 Focused extinction and autodilution of AS

Although AS had a nominal counting limit of 10 µm it did not show any particle count for particles >7.5 µm. This might be explained by the focused extinction of AS. Focused extinction means that measurements are not performed counting all particles within the flow channel. Only a small spot of the channel is statistically evaluated and might lead to imprecise results in case the particle count is low. However, even in samples in which light obscuration is counting hundreds of particles >10 µm AS is not counting one single particle ≥7.5 µm (data not shown). Therefore, this rationale can not be adhered.

Autodilution can be considered as a disturbing factor for measurements of protein aggregates. There is the possibility that the measured aggregates within the samples are reversible by dilution and therefore not existent anymore during measurements. To evaluate this, measurements of stressed protein samples were performed with and without autodilution. Comparison showed that runs with autodilution did not result in different numbers for those measurements without autodilution. Curves of particle increase showed the same trend with small deviations to both sides (data not shown). From these results, autodilution can be excluded as a factor that resolves protein particles.

3.3.3 Is the very early onset of aggregation detectable with AS?

3.3.3.1 Lower detection limit of AS

AS is claimed to have a lower detection and counting limit of 150 nm. No other particle counting system for pharmaceutical use provides this opportunity at the moment. In a first step particle sizing standards were measured to confirm the correct setup of the device.

Figure 3 illustrates, that the instrument has the ability to detect particles in the nanometer range. AS can distinguish between particle *sizing* standards of 200 nm, 220 nm, 240 nm, 269 nm and 300 nm. The existence of a peak at 330 nm points to the presence of air bubbles, which was proven in former experiments (data not shown). Also particle sizing standards of 700 nm are detected. The lowest particle size detected is 160 nm, the particles used are declared as 150 nm. These results show that the lower detection limit has to be shifted slightly towards larger particle sizes but in general the system is able to work reliably at least at 200 nm and for larger particles.

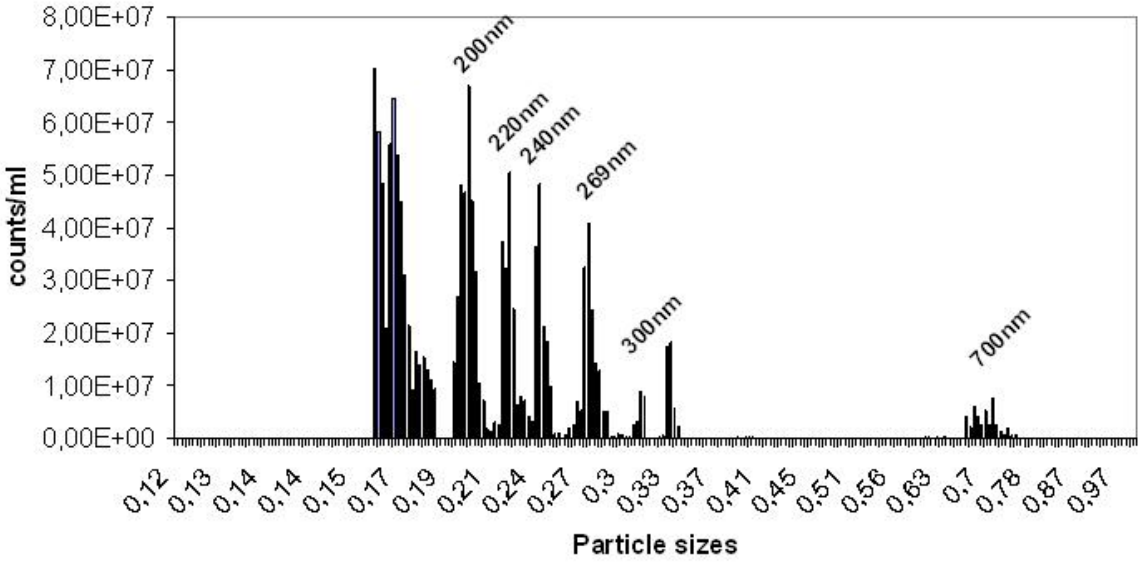

Fig. 3: Measurement of particle sizing standards: 150 nm, 200 nm, 220 nm, 240 nm, 269 nm, 300 nm and 700 nm

Furthermore the lower *counting* limit of AS had to be confirmed. For this purpose particle counting standards 300±6 nm and 498±5 nm were measured. The given concentration of particles in corresponding particle sizes are $1*10^9$ particles/ml.
For the standard 300 nm $1.13*10^9$ particles/ml ± $4.50*10^7$ particles/ml were counted; for the standard 498 nm $7.4*10^8$ particles/ml ± $1.82*10^7$ particles/ml were counted. This result shows that the AS is very well able to count particle in very low size ranges, at least from 300 nm upwards.

3.3.3.2 Onset of aggregation and particle formation

Further it should be assessed whether it is possible to get more information about the onset of aggregation by measuring extremely small particles in the upper nm range, i.e. below the 1 µm limit of traditional light obscuration counting with AS. In theory, small aggregates are considered as precursors or nuclei for aggregation [Golub et al., 2007; Mahler et al., 2005]. Hence, small particles should be earlier detectable than larger ones.

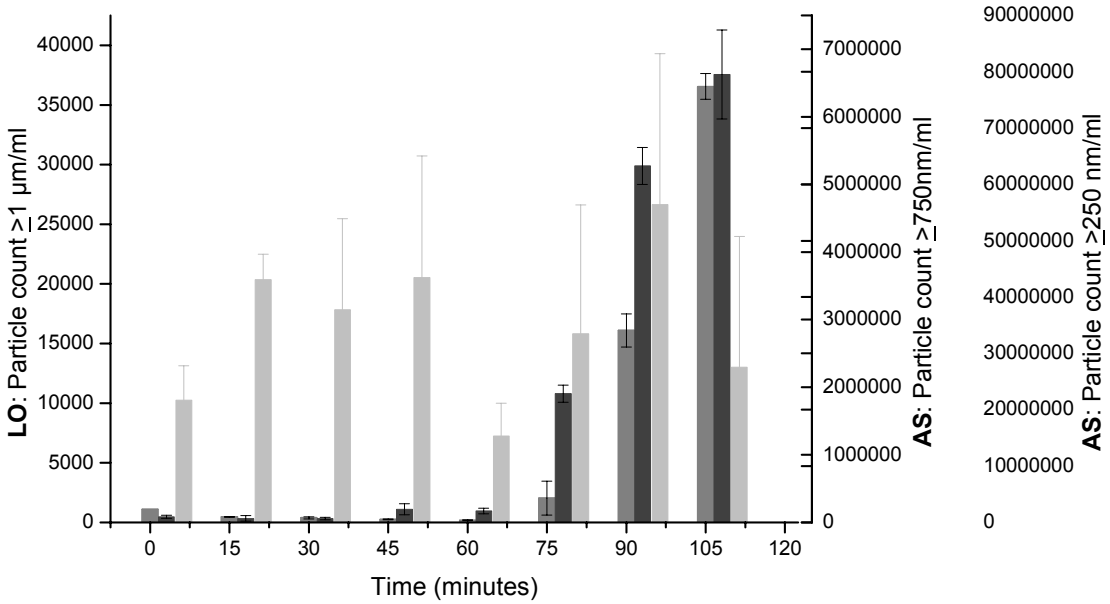

Fig. 4: Light obscuration measurements with Klotz instrument (LO particles ≥1 µm; grey) as well as light scattering measurement with AccuSizer (AS particles ≥750 nm, dark grey; AS particles ≥250 nm, light grey) of heated reteplase; n = 3; sampling every 15 minutes

However, despite the given ability of the AccuSizer FY to detect and count particles in the nanometer range, our experiments could not reveal reliable information about the early onset of aggregation. Only one out of 12 experiments resulted in an early increase of particle counts (“point of detection”) in the size class ≥0.25 µm (see appendix), whereas size classes ≥0.75 µm and ≥1.0 µm provided more information. Theoretically, small particles are expected to be earlier detectable than larger particles. High background noise makes it statistically almost impossible to detect small amounts of small aggregates.

rPA that is susceptible to heat stress was chosen as an example: Figure 4 shows a particle count increase for particles ≥1 µm measured with LO after 75 minutes, for particles ≥0.75 µm measured with AS after 45 minutes, whereas particles ≥0.25 µm measured with AS could not clearly show beginning aggregation due to the high background noise in the smaller particle size range.

The high background noise (figure 4) during measurements leads us to propose not to set value on the particle size channels close to the lower detection limit of AS. Only detection of particles ≥0.75 µm was found out to be meaningful. AccuSizer uses two detectors to count particles. The light obscuration detector is employed from 0.61 µm up to 10 µm and evidently works well. The light scattering detector (0.15 µm to 0.61 µm) is able to size but not to properly count protein aggregate particles. This

might be traced back to the fact that light scattering is not the best way to quantify particles of a wide size distribution as the AS software uses the amount of scattered light and the particle sizes to calculate particle numbers.
A comparable overall situation could be shown before with similar experiments with an electrical sensing zone instrument (CC) [Mück, 2002]. Proteins were stressed and samples were measured with classical LO instrument and Coulter Counter (CC). It was shown that the claimed lower detection limit of the CC did not give any additional information and had to be corrected from 0.4 µm to 0.7 µm.
For the time being we conclude that these measuring systems that are theoretically able to count particles in the upper nanometer range do not provide benefit over classic LO detection when particle formation in the course of protein aggregation is to be evaluated.
Further steps in the direction to count particles as an indicator for beginning protein aggregation would only be possible, if the background noise could be strongly reduced.

3.3.4 Aggregation theory

In theory, protein aggregation starts with building of small aggregates that accumulate to larger ones [Mahler et al., 2005].
Due to this theory aggregation after stressing proteins over time should first be detectable with particle size classes of ≥250 nm, then of LO ≥1 µm, later with particles size classes ≥10 µm. However, as elaborated in chapter 3.3.3 high background noise interferes with particle counts in the nanometer range. Therefore, interesting information about the onset of aggregation in the range <750 nm could not be provided.
When particle counts detected with classical LO instrument are compared, it turned out that particle counts in the size class ≥1 µm (figure 5) increases slightly earlier than in the size class ≥10 µm after e.g. freeze-thawing GCSF.

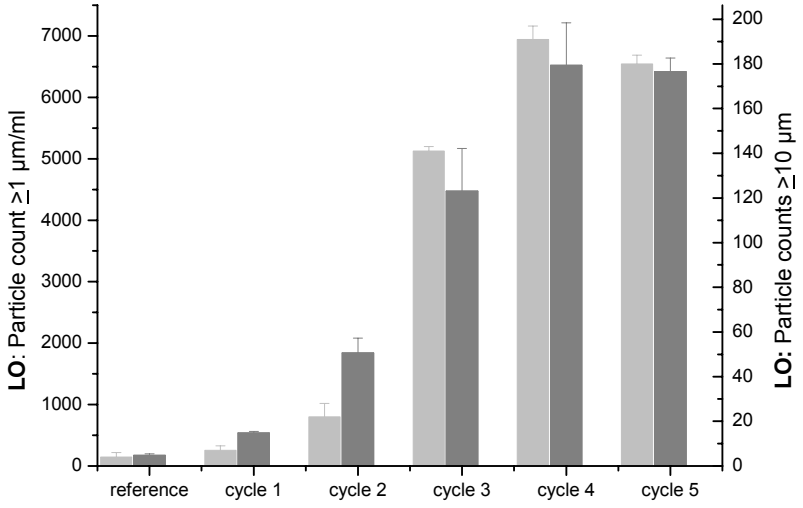

Fig. 5: Light obscuration measurements of freeze-thawed GCSF; particles ≥1 µm (dark grey) and ≥10 µm (light grey); n = 3

12 experiments were performed: four different proteins were stressed by freeze-thawing, heating and mechanically. An earlier increase of particle counts of particles >1 µm than for particles >10 µm was observable for six experiments (see bold prints in table 2). However, between detecting particles >1 µm and >10 µm only marginal delays are noticeable – four out of 12 experiments led to same time point of aggregation detection in both size classes, whereas in two out of 12 experiments even an earlier increase of the larger aggregates was detected.

But experiments with rPA and GCSF, which are supposed to be less stable, compared to antibodies, give evidence for the earlier formation of smaller particles than of larger ones. The more stable antibodies mainly show the same point of detection for particle formation.

For the time being, benefit of detecting particles >1 µm instead of particles >10 µm seems to be small, as it is not informative for all proteins. Detection of particle formation in antibody formulations, which are nowadays very important products and projects in pharmaceutical industry, does not deliver the wanted information. However, as LO measurements automatically delivers the additional information about particle formation of particles in the size class >1 µm, it would not be much more time effort to assess the available data.

Table 2: Point of detection determined with LO for particles ≥1 µm and ≥10 µm

	LO 1 µm*	LO 10 µm*
IgG_1-α thermal	7	7
IgG_1-α mechanical	4	1
IgG_1-α freeze-thaw	2	2
IgG_1-ß thermal	4	4
IgG_1-ß mechanical	1	1
IgG_1-ß freeze-thaw	**2**	**3**
GCSF thermal	**1**	**4**
GCSF mechanical	2	1
GCSF freeze-thaw	**2**	**3**
Reteplase thermal	**6**	**-****
Reteplase mechanical	**1**	**2**
Reteplase freeze-thaw	**2**	**3**

* numbers express the point of detection

** no detection of particles ≥10 µm during experiment, point of detection > 8

However, in another experiment IgG_1-α was freeze-thawed over five cycles to generate particles. Thereafter, solutions were stirred at different speeds. Figure 6 gives a hint, that large particles formed by freeze-thawing are crushed by stirring into smaller ones. Monitoring only particles ≥10 µm and ≥25 µm as required by the guidelines would disregard those small particles.

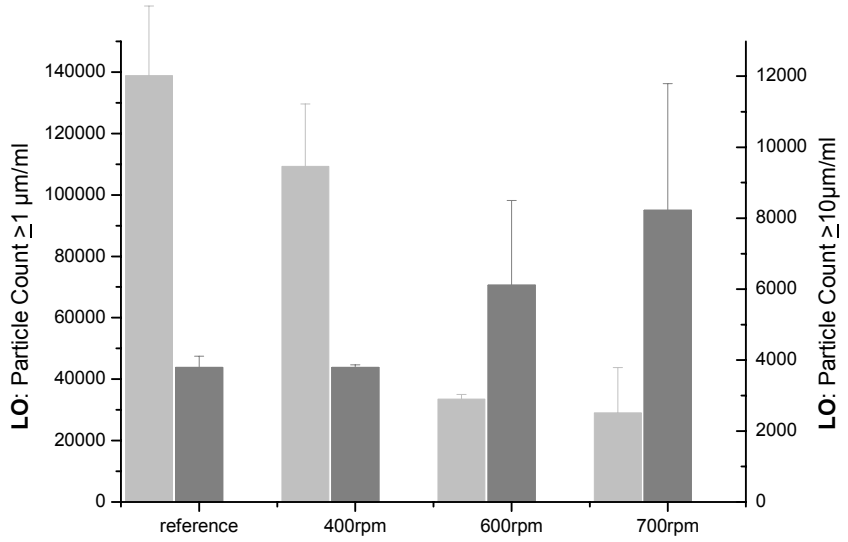

Fig. 6: Particle count of particles ≥1 µm (dark grey) and ≥10 µm (light grey) after stirring of freeze-thawed IgG_1-α; n = 3

3.3.5 Comparison of AS with DLS

As shown in chapter 3.3.3 it had not been possible to detect particles in nanometer size range with AS due to high background noise. Theoretically it could be possible, that there were no particles in the sizes <750 nm. This was checked by DLS measurements. Though DLS does not provide absolute particle counts, it is able to detect particles <750 nm, although the intensity of the DLS signal for larger particles is dominant compared to smaller ones [Demeester et al., 2005; Malvern, 2007].

To evaluate DLS data with regards to the "point of detection", Z-averages of the measured particle diameters [nm] were plotted over time. Using DLS, different changes in protein samples can be detected: shift of the monomer peak towards larger sizes and formation of an additional peak. In general we found that heat stressed antibody samples provide a monomer peak shift to larger sizes, whereas mechanically stressed or freeze-thawed antibody solutions present an additional peak caused by large particles.

DLS measurements of heat stressed IgG_1-α resulted in a peak shift and increase of Z-average after 20 minutes. This peak shift was still in the size range of an IgG_1 monomer, therefore theoretically not detectable with the AS. After 120 minutes heating at 65°C the peak shifted to higher sizes around 200 nm (figure 7), after 140 minutes an additional second peak (~1000 nm) was formed (figure 8). Both changes theoretically should have been detected by AS. Though, detection of particles >250 nm was only possible after 160 minutes (figure 9).

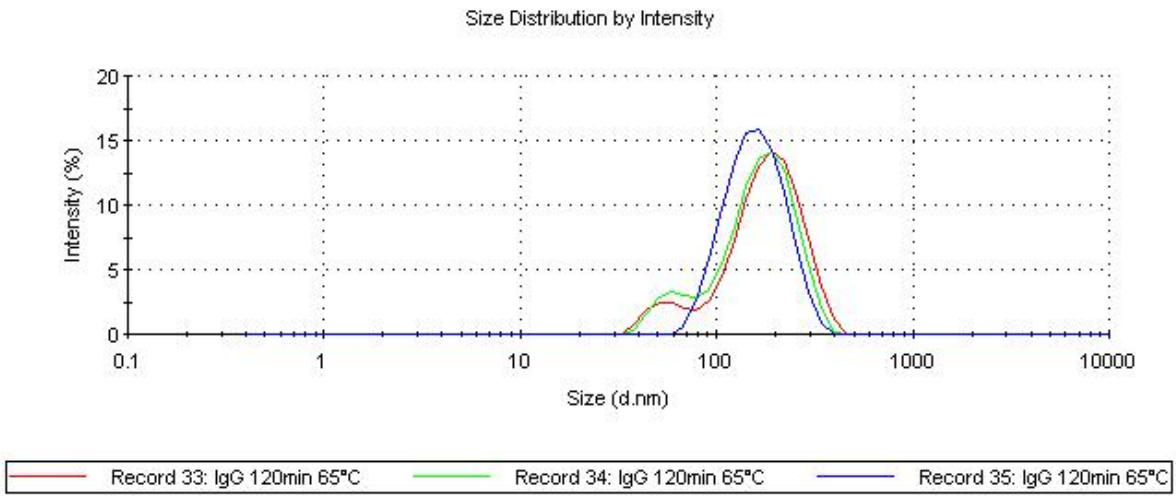

Fig. 7: DLS measurements after 120 minutes heat stress at 65°C IgG_1-α; peak shifted to ~200 nm

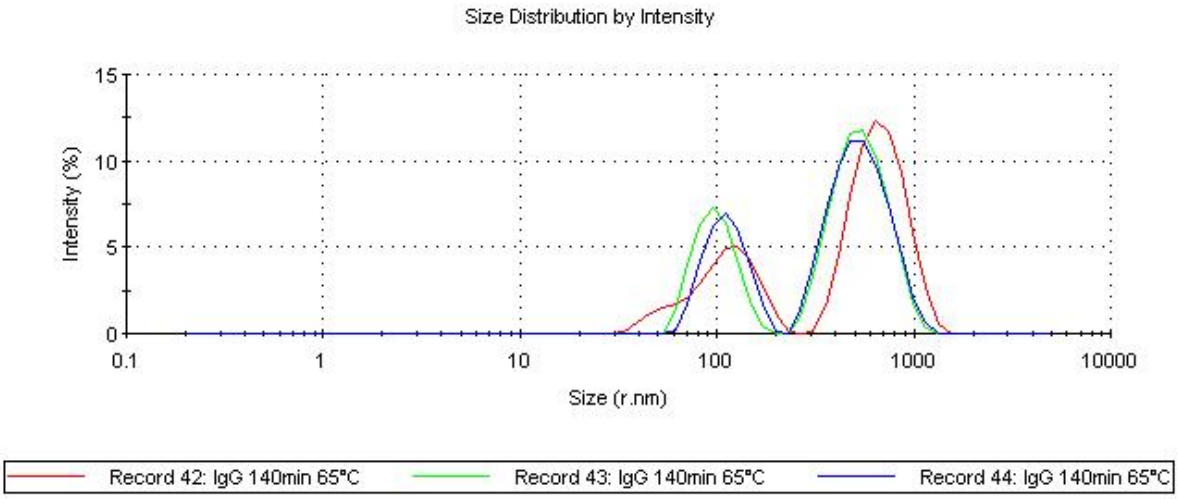

Fig. 8: DLS measurements after 140 minutes heat stress at 65°C IgG_1-α; peak shift and additional peak

	reference	20min	40min	60min	80min	100min	120min	140min	160min
SEC									
DLS									
OD_{550}									
LO ≥1.0 µm									
LO ≥10 µm									
AS ≥1.0 µm									
AS ≥0.25 µm									
AS ≥0.75 µm									
AS ≥0.50 µm									
AS ≥2.5 µm									
AS ≥5.0 µm									
AS ≥7.5 µm									

Fig. 9: Heat stress of IgG_1-α; detection power of different methods (results of particle counters were distinguished in different size classes, n = 3)

In another experiment, the effect of freeze-thaw stress on IgG_1-α was detected in larger particle size classes of both used particle counters after the 2nd cycle (figure 10), DLS measurements detected large particles only after the 3rd cycle (figure 11, see arrow). An increase of aggregates in the particle size class of particles ≥250 nm was not detected at all by AS. Similar observations could be made after mechanical stress (data not shown): Particle counters detected aggregates ≥0.75 µm resp. ≥1 µm before DLS instrument did, nanosized aggregates were not detected at all.

	reference	1.cycle	2.cycle	3.cycle	4.cycle	5.cycle
LO ≥10 µm						
LO ≥1.0 µm						
AS ≥1.0 µm						
AS ≥2.5 µm						
AS ≥0.50 µm						
AS ≥0.75 µm						
DLS						
OD 550						
SEC						
AS ≥5.0 µm						
AS ≥7.5 µm						
AS ≥0.25 µm						

Fig. 10: Freeze-thawing of IgG_1-α; detection power of different methods (results of particle counters were distinguished in different size classes; n = 3)

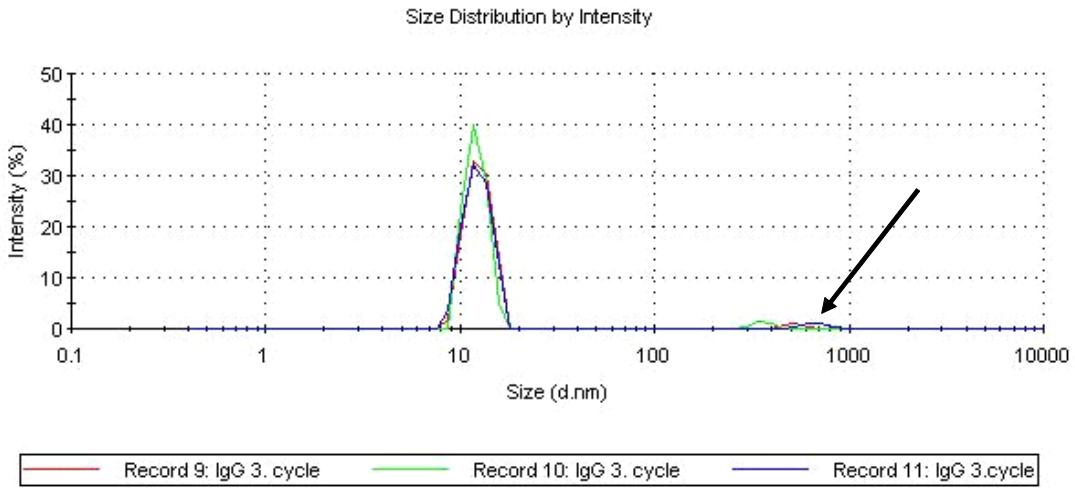

Fig. 11: DLS measurements after 3rd cycle freeze-thawing of IgG_1-α; generation of aggregates led to an additional peak; n = 3

All in all, DLS measurements showed a peak shift after heat stress of antibodies. The shifted peak theoretically should have been detected earlier by AS, as even the LO system revealed in its measurements for particles ≥1 µm and ≥10 µm an increased particle count.

A different situation is given after freeze-thawing and shaking of antibodies. LO and AS instruments were able to show increases of particle counts in µm ranges, though DLS measurements did not reveal a second peak. Anyhow, no changes in solution were detected by AS in the nanometer range.

Summarizing, DLS measurements after heat stress demonstrated that particles in nanometer range are existent.

3.3.6 Comparison of AS with turbidity measurements

Monitoring liquids for clarity/turbidity is also required by the pharmacopoeia (e.g. Ph.Eur.6.0, 2.2.1). Measuring turbidity is a very fast method, instruments are not expensive and easy to handle. Increasing turbidity is accompanied with an increasing amount of scattered light detected by a light detector is employed in a 90° angle. Particle or aggregate formation can lead to light deflection, which also diminishes the detected light. Therefore, turbidity measurements are taken into account for our studies and compared with detection abilities of AS.

Nephelometry is the method of choice; however needed sample volume is often too large as research and development have restricted sample availability. Therefore relationship between nephelometry and measurement of optical density (OD) at 550 nm is established. Measuring OD takes up only 100 µl sample volume.

Turbidity standards [European Directorate For The Quality of Medicine (EDQM), 2011a] were prepared and measured with both methods to obtain following relationship:

OD = 0.0007 * FNU (nephelometry) + 0.0266 (with R^2 = 0.9906; data not shown).

By definition turbid liquids have a FNU-value ≥3 FNU; therefore OD ≥0.0287 is the corresponding limit.

Turbidity theoretically directly correlates with generation of aggregates [Eckhardt et al., 1994]. Formed particles scatter incident light of an appropriate wavelength, thus turbidity increases with increasing particle count within the solution. However, a certain degree of OD or turbidity cannot be related to a certain particle size.

The onset of turbidity was measured for all 12 experiments: 4 different proteins and 3 different stress methods (data in appendix, chapter 9).

In our example a significant increase of OD after 80 minutes and a further steep increase of OD after 140 minutes can be found (figure 12). However, particles ≥250 nm were detected only after 160 minutes by AS (figure 9).

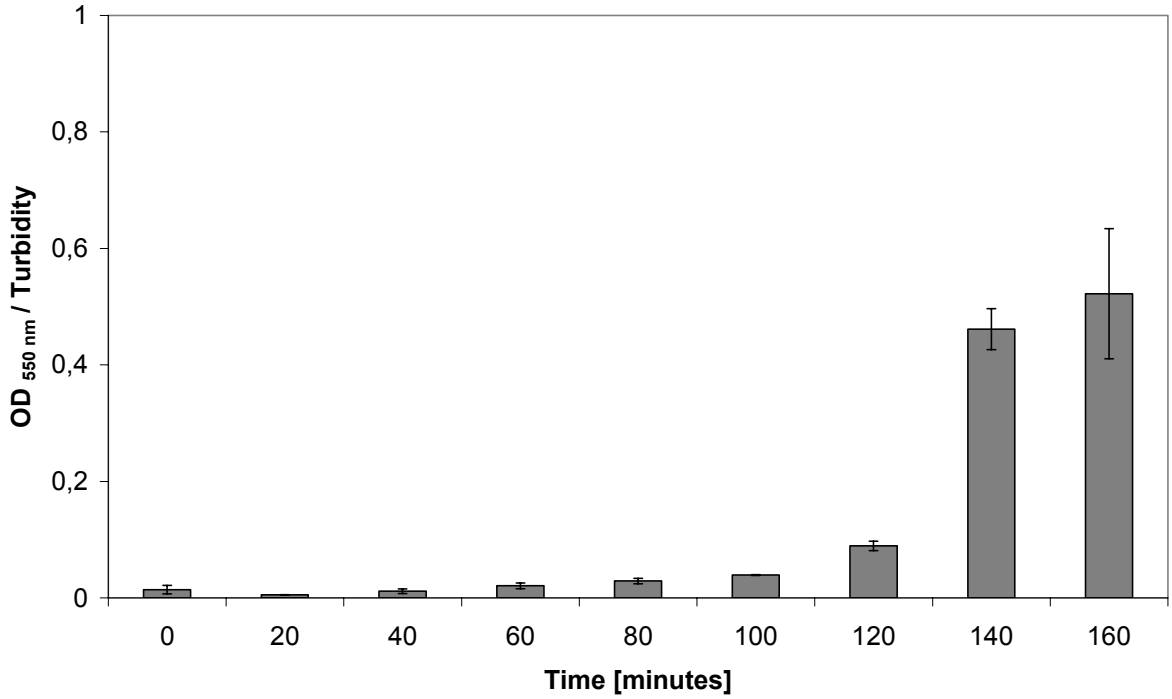

Fig. 12: OD measurements after 120 minutes heat stress at 65°C IgG_1-α; steep increase of OD after 140 minutes; n = 3

Table 3: Results from turbidity measurements

	Turbidity*
IgG_1-α thermal	4
IgG_1-α mechanical	1
IgG_1-α freeze-thaw	-**
IgG_1-ß thermal	2
IgG_1-ß mechanical	-**
IgG_1-ß freeze-thaw	-**
GCSF thermal	-**
GCSF mechanical	-**
GCSF freeze-thaw	-**
Reteplase thermal	6
Reteplase mechanical	2
Reteplase freeze-thaw	1

* numbers express the point of detection

** no detection of turbidity during experiment

Monitoring optical density is not as significant as e.g. counting particles: only six out of the 12 stress experiments causes an increase in optical density (table 3). Six stress experiments did not result in an increase of optical density.

Turbidity turned out to be a good indicator for thermally stressed antibodies – in these cases observing was reliable as turbidity increases reliably early. However, stressing antibodies by freeze-thawing did not lead to an increase of turbidity, whereas mechanical stress did only result in turbid samples of IgG_1-β. GCSF samples did not show turbidity after any stress, whereas rPA samples got turbid even after freeze-thawing.

Optical density measurement is an economical inspection method. Monitoring optical density/turbidity is fast and low priced, but provides no constant information about aggregation of proteins. Hence, it should not be the only method to depend on.

3.3.7 Comparison of AS with SEC

SEC is a common method to monitor protein aggregation. Though SEC is not able to give aggregate counts, it is a good method to give information about the relative amount of protein aggregation and protein monomer. In general, SEC turned out to be the best tested method to detect changes due to heat stress [Philo, 2009], see appendix. Heating proteins means supplying energy to the samples, this leads to the formation of small aggregates [Hawe et al., 2009].

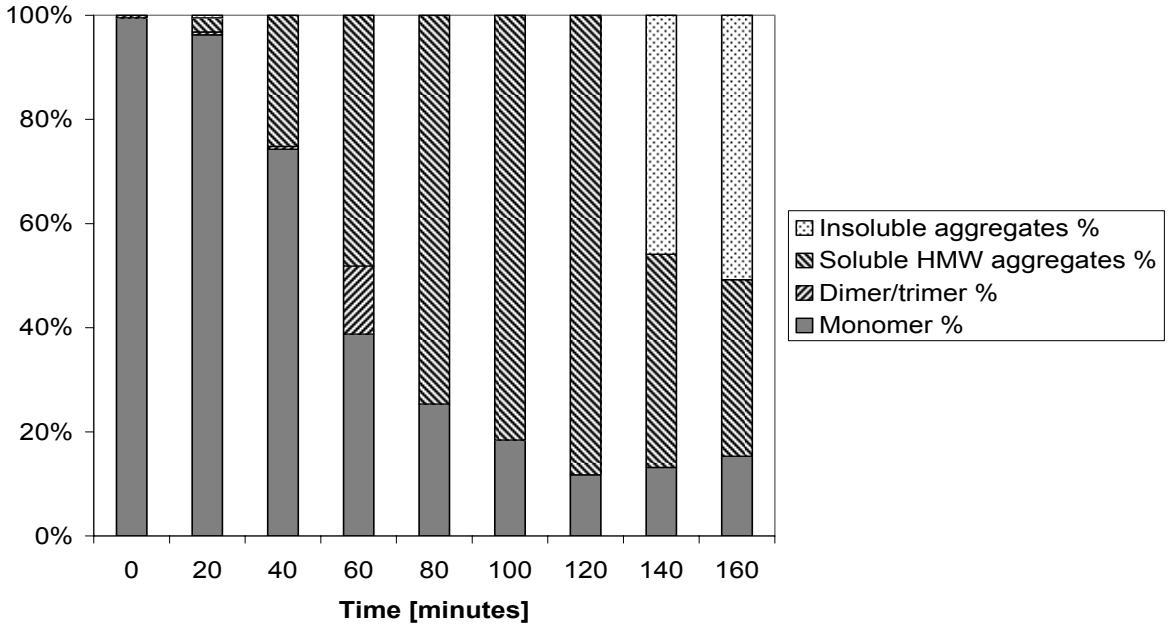

Fig. 13: SE-HPLC of 65°C stressed IgG_1-α; n = 3

Generation of soluble high molecular weight (HMW) aggregates and dimers/trimers started after 20 minutes heating IgG_1-α at 65°C (figure 13). Dimers and trimers could not have been detected by AS. Monomer (11 nm diameter) is decreasing over time, whereas aggregates are increasing. Insoluble aggregates are indirectly detected by

recovery rate after 140 minutes, which is fully congruent with LO data (figure 13 and figure 9). At least these large insoluble aggregates should also have been detected by the size class for particles ≥250 nm of AS, however particles were only detected after 160 min (figure 9).

SEC also turned out to be a good method to detect changes in GCSF- and rPA samples after mechanical and freeze-thaw stress. GCSF and rPA are more susceptible to stress than monoclonal antibodies are, therefore mechanical and freeze-thaw stress both led to the formation of higher amount of insoluble particles, visible as decreasing recovery rate (figure 14).

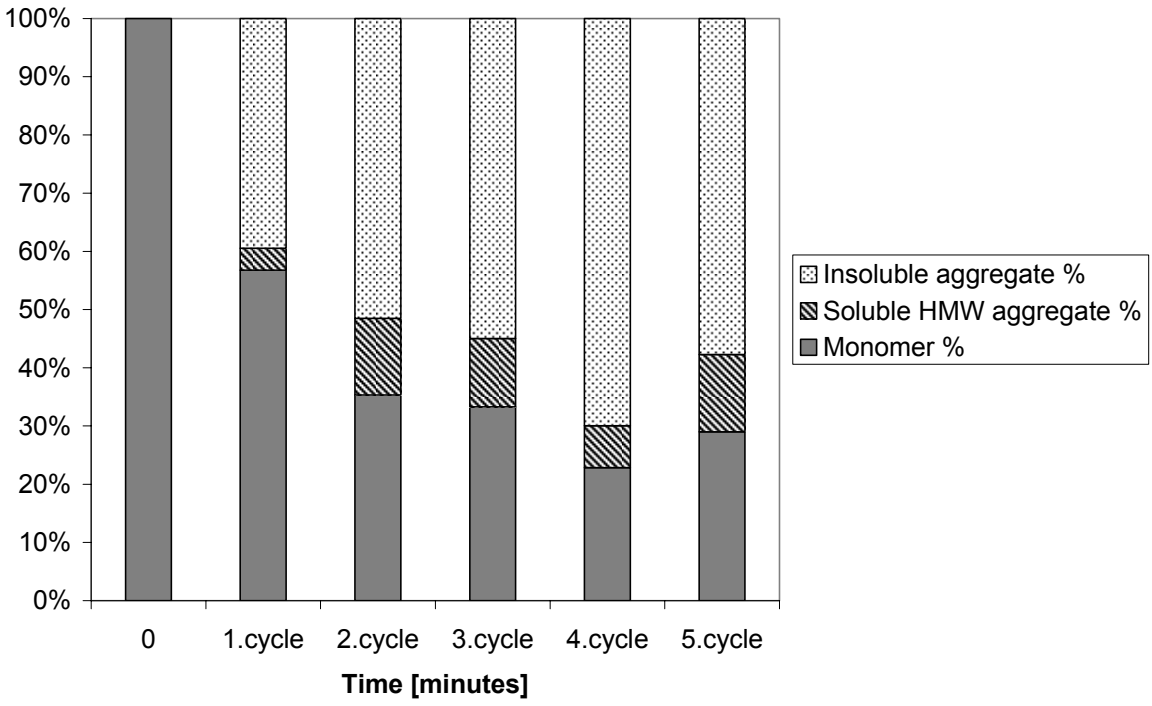

Fig. 14: SE-HPLC of freeze-thawed GCSF; n = 3

Shaking and freeze-thawing of monoclonal antibodies also assemble insoluble particles. Though, the absolute loss of protein was not high enough to become noticeable by SEC [Hawe et al., 2009]. Figure 15 shows an example: Freeze-thawing IgG_1-α does not result in an amount of insoluble protein particles high enough to be detectable by SEC. The absolute loss is calculated as recovery rate and related to protein monomer.

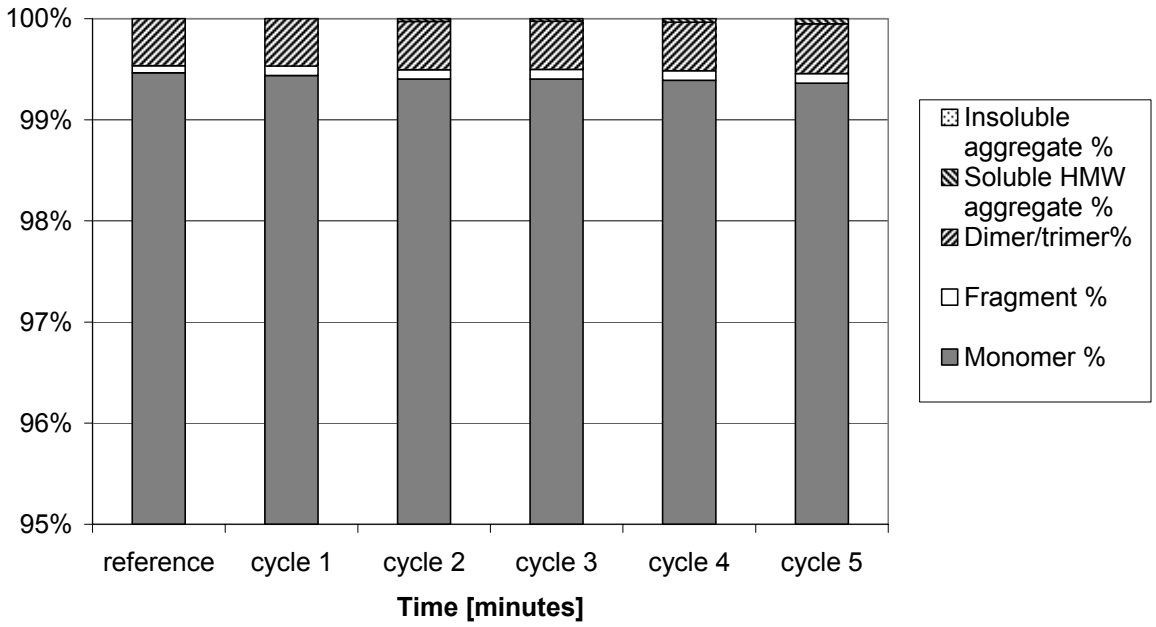

Fig. 15: Freeze-thawed IgG_1-α; n = 3

Concluding, all methods assessed are qualified to monitor changes in protein solutions. Reckoning the results of all measurements, an almost overall image is received. Though, one single method has a limited range of detection due to size limits, background noise, sensitivity or other interference factors. Further, the measurements provide different resulting parameters: count and size of aggregates, existence of changes, relative amount and size of aggregates. For the time being, evaluating results from one single method is not sufficient to get an overview about the aggregates in solution.

3.3.8 Does MFI deliver early information?

It is reported in literature, that MFI delivers more information regarding particle formation within protein formulation due to its higher sensitivity regarding translucent particles [Huang et al., 2008; Sharma et al., 2010].

Table 4 shows the results of MFI particle counting compared to classical LO particle counting, whereas the numbers indicate the quantity of first detection as a comparison of LO and MFI. The quantity of “point of detection” expresses the number of experiments with an earlier detection of particle formation than the respective other instrument. For example, a “2” for LO means that LO was in two experiments able to detect increasing particle formation earlier than MFI. It is already reported in literature

[Hawe et al., 2009] and also carved out in these experiments that particle counters are not dedicated to detect changes in protein formulations after thermal stress. Even MFI is not sensitive enough to detect those changes. From table 4 it can be concluded, that MFI is the best method to detect particle formation after freeze-thaw stress, whilst LO proved to be better at detecting particles formed during mechanical stress.

Table 4: Detection abilities of MFI compared to LO for particles ≥1 µm and ≥10 µm (the bigger the number the more sensitive the instrument)

	Particles ≥1 µm		Particles ≥10 µm	
	LO	MFI	LO	MFI
Freeze-thawing	2	**3**	1	**3**
Mechanical stress	**3**	2	**3**	1
Thermal stress	2	2	1	2

To further evaluate and explain these results, absolute particle counts and particle pictures of mechanical and freeze-thaw stress were checked for each protein. Due to above mentioned reasons we focused on particle formation after freeze-thawing and mechanical stress.

In chapter 2.2.2.1.4 it is explained how the “point of detection” after particle counting is evaluated. For these further evaluations we decided only to consider data points with standard deviations (SD). Due to high standard deviations after mechanical stress, a different picture about methods’ sensitivity can be drawn (table 5): again MFI is the most sensitive method to detect particle formation after freeze-thaw stress. After mechanical stress, both instruments seem to be equal regarding their detection sensitivity. Going more into detail, MFI is very sensitive in detection of GCSF-, rPA, and IgG_1-α-particles formed after both mechanical and freeze-thaw stress, whereas LO is more sensitive for particle detection of IgG_1-ß-particles.

Table 5: Detection abilities of MFI compared to LO for particles ≥1 µm and ≥10 µm without regard to averaged standard deviations

	Particles ≥1 µm		Particles ≥10 µm	
	LO	MFI	LO	MFI
Freeze-thawing	2	**3**	1	**3**
Mechanical stress	**3**	**3**	**4**	**4**

Further we scrutinized the pictures of protein particles taken by MFI. It became obvious, that protein particles formed after mechanical stress and freeze-thawing of

GCSF, rPA, and IgG_1-α are a mixture of both translucent and dark particles (example in figure 16).

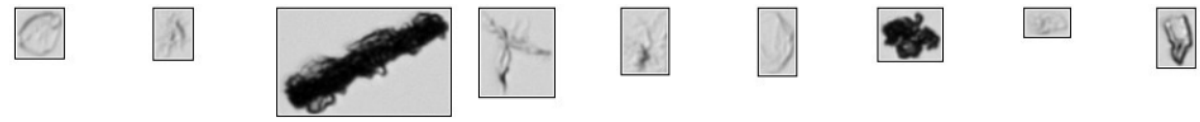

Fig. 16: Examples of GCSF particle pictures after mechanical stress

In contrast, IgG_1-ß particles after freeze-thawing and mechanical stress are consistently dark (example in figure 17).

Fig. 17: Examples of IgG_1-ß particle pictures after mechanical stress

To study the different effect of mechanical and freeze-thaw stress on IgG_1-ß, both IgG_1 formulations were compared with regards to their excipients. Both IgG_1 are formulated in histidine buffer and sugars. IgG_1-ß is stabilized with polysorbate 80 (PS-80), which obviously influences the appearance of protein particles.

Polysorbates are reported to protect protein formulations against the formation of protein aggregates although they bind negligible to immunoglobulins [Garidel et al., 2009]. Further it was found that PS can form peroxides [Ha et al., 2002] and fatty acids [Kishore et al., 2010], that on the opposite can destabilize proteins. During freeze-thawing PS-80 protects proteins by hindering destructive interactions with ice-crystals [Hillgren et al., 2002]. The existence of PS-80 is influencing the appearance of protein particles.

Summarizing the comparison of MFI and LO revealed that MFI is very sensitive for detection of translucent protein particles, as already addressed in literature [Huang et al., 2008; Sharma et al., 2010]. Proteins are prone to aggregation and obviously many protein formulations are generating translucent particles during stress, not detectable with LO. Hence, MFI is a valuable instrument for protein aggregate quantification. The microflow imaging method should be further evaluated with the view to adapt pharmacopoeial methods.

3.4 Conclusion

The scientific community has started a discussion about the gaps in analytical assessment of protein solutions [Carpenter et al., 2008; Giezen et al., 2008; Singh et al., 2010]. Development of more sensitive tools was postulated to close the gap. In that course the new instrument AccuSizer FY nano® theoretically able to measure in the range >150 nm and Microflow Imaging DPA 4200 were assessed.

From the present results it is evident that counting particles <1 µm with AS is not as promising as expected due to the high background noise. Although DLS and SEC measurements showed changes in the nanometer range after thermal stress, AS did not detect any protein denaturation. Indeed it is possible to detect particles in the range >150 nm using particle size standards, however counting is not accurate.

A potential particle count increase is covered with high particle counts from background noise. The nominal lower detection limit of 150 nm could not be confirmed with the described experiments. A lower size limit of 750 nm can be provided which is not far from the lower size limit of the classically used light obscuration instruments. Previous work in this field [Mück, 2002] showed that also instruments with electrical sensing zones (Coulter Counter) can not provide the nominal lower detection limit due to high background noises. Early events of aggregation could only be detected at 700 nm which is close to the detection limit of our experiments and also close to the lower detection limit of light blockage instruments. Regarding the new AccuSizer FY nano® instrument there is reasonable suspicion that light blockage detector is operating and counting well, whereas light scattering detector is not adequate for counting particles within performed experiments.

Results from particle counting with MFI delivered slightly more information with regard to subvisible particles than particle counting with classical LO. Particles formed during mechanical stress and freeze-thawing from an IgG_1 formulated with PS-80 are different to those formed during freeze-thawing and mechanical stress from proteins not protected with PS-80. Proteins formulated without PS-80 form both translucent and dense particles during stress, therefore MFI is more sensitive than LO. IgG_1 under PS-80 protection forms consistently dense and dark particles which are perfectly detectable with LO.

USP <788> is requiring not to have more than 6000 particles ≥10 µm and more than 600 particles ≥25 µm in a container. There is reason to think that this is too insensitive. Former studies figured out, that particles ≥1 µm and ≥10 µm were detected at absolutely the same time [Singh et al., 2010]. However, results from this study show that a correlation between particle formation in the size classes in the USP-required ranges and particle formation in the size ranges ≥1 µm/≥750 nm is depending on the protein. Stressing sensitive proteins, leads to an earlier formation of smaller particles than of larger ones. Antibodies did confirm the mentioned studies from Singh: particles in size classes ≥1 µm and ≥10 µm were detected at the same time.

There is also evidence for the fact that e.g. stirring shears larger particle to smaller ones. We found, that particles ≥10 µm built by freeze-thawing are crushed into smaller ones after stirring even at low stirring speeds (e.g. 400 rpm); altering of large particles to smaller ones over storage time was found recently [Kiese et al., 2010]. Stirring at higher speeds (600 rpm or 700 rpm) leads to faster crushing of large particles. This implies that stir stress experiments lead to large amounts of smaller particles but not to “out-of-specification” results. Increasing amount of larger particles would occur after long and faster stirring; though small particles are already existent after short time or lower stir speed. An aggregated protein solution could therefore also pass the USP requirements, when large aggregates have been crushed to smaller ones during stirring.

For the time being, it is recommendable to use classic light obscuration (10 µm) in combination with SEC [den Engelsman et al., 2011]. This allows in all cases studied most sensitive analytic for the moment. However, e.g. crushing large particles into smaller ones during stirring makes it reasonable to reconsider pharmacopoeial requirement sooner or later. Stirring is an essential manufacturing step; the formed smaller particles are not assessed within the guidelines.

For the future it is recommended to include MFI measurements in the ranges ≥1 µm as standard requirements into pharmacopoeias. MFI measurements deliver more and earlier information about beginning protein aggregation; MFI is a helpful and informative method.

Measurements in the submicron range of AccuSizer do not lead to higher sensitivity and relevant more information with available equipment.

3.5 Reference List

1. Barnard,J.G., Singh,S., Randolph,T.W., Carpenter,J.F., 2010. Subvisible particle counting provides a sensitive method of detecting and quantifying aggregation of monoclonal antibody caused by freeze-thawing: Insights into the roles of particles in the protein aggregation pathway. J Pharm. Sci., 100, 492-503.

2. Bee,J.S., Chiu,D., Sawicki,S., Stevenson,J.L., Chatterjee,K., Freund,E., Carpenter,J.F., Randolph,T.W., 2009. Monoclonal antibody interactions with micro- and nanoparticles: adsorption, aggregation, and accelerated stress studies. J Pharm. Sci., 98, 3218-3238.

3. Bee,J.S., Davis,M., Freund,E., Carpenter,J.F., Randolph,T.W., 2010. Aggregation of a monoclonal antibody induced by adsorption to stainless steel. Biotechnol. Bioeng., 105, 121-129.

4. Bhatnagar,B.S., Bogner,R.H., Pikal,M.J., 2007. Protein stability during freezing: separation of stresses and mechanisms of protein stabilization. Pharm. Dev. Technol., 12, 505-523.

5. Carpenter,J.F., Randolph,T.W., Jiskoot,W., Crommelin,D.J., Middaugh,C.R., Winter,G., 2009. Potential inaccurate quantitation and sizing of protein aggregates by size exclusion chromatography: Essential need to use orthogonal methods to assure the quality of therapeutic protein products. J Pharm. Sci., 99, 2200-2208.

6. Carpenter,J.F., Randolph,T.W., Jiskoot,W., Crommelin,D.J., Middaugh,C.R., Winter,G., Fan,Y.X., Kirshner,S., Verthelyi,D., Kozlowski,S., Clouse,K.A., Swann,P.G., Rosenberg,A., Cherney,B., 2008. Overlooking subvisible particles in therapeutic protein products: Gaps that may compromise product quality. J Pharm. Sci., 98, 1-5.

7. Chi,E.Y., Weickmann,J., Carpenter,J.F., Manning,M.C., Randolph,T.W., 2005. Heterogeneous nucleation-controlled particulate formation of recombinant human platelet-activating factor acetylhydrolase in pharmaceutical formulation. J Pharm. Sci., 94, 256-274.

8. Das,T., Nema,S., 2008. Protein particulate issues in biologics development. Am. Pharm. Rev., 11, 52, 54-52, 57.

9. Demeester,J., de Smedt,S.S., Sanders,N.N., Haustraete,J., 2005. Light scattering. In: Jiskoot,W., Crommelin,D.J. (Eds.), AAPS, Arlington, 245-275.

10. Demeule,B., Messick,S., Shire,S.J., Liu,J., 2010. Characterization of particles in protein solutions: reaching the limits of current technologies. AAPSJ, 12, 708-715.

11. den Engelsman,J., Garidel,P., Smulders,R., Koll,H., Smith,B., Bassarab,S., Seidl,A., Hainzl,O., Jiskoot,W., 2011. Strategies for the assessment of protein aggregates in pharmaceutical biotech product development. Pharm. Res., 28, 920-933.

12. Eckhardt,B.M., Oeswein,J.Q., Yeung,D.A., Milby,T.D., Bewley,T.A., 1994. A turbidimetric method to determine visual appearance of protein solutions. J Pharm. Sci. Technol., 48, 64-70.

13. Eppler,A., Weigandt,M., Hanefeld,A., Bunjes,H., 2010. Relevant shaking stress conditions for antibody preformulation development. Eur. J Pharm. Biopharm., 74, 139-147.

14. European Directorate For The Quality of Medicine (EDQM), 2011a. Ph.Eur.2.2.1 Clarity and degree of opalescence of liquids.

15. European Directorate For The Quality of Medicine (EDQM), 2011b. Ph.Eur.2.9.19 Particulate contamination: subvisible particles.

16. Fradkin,A.H., Carpenter,J.F., Randolph,T.W., 2009. Immunogenicity of aggregates of recombinant human growth hormone in mouse models. J Pharm. Sci., 98, 3247-3264.

17. Garidel,P., Hoffmann,C., Blume,A., 2009. A thermodynamic analysis of the binding interaction between polysorbate 20 and 80 with human serum albumins and immunoglobulins: a contribution to understand colloidal protein stabilisation. Biophys. Chem., 143, 70-78.

18. Giezen,T.J., Mantel-Teeuwisse,A.K., Straus,S.M., Schellekens,H., Leufkens,H.G., Egberts,A.C., 2008. Safety-related regulatory actions for biologicals approved in the United States and the European Union. JAMA, 300, 1887-1896.

19. Golub,N., Meremyanin,A., Markossian,K., Eronina,T., Chebotareva,N., Asryants,R., Muronets,V., Kurganov,B., 2007. Evidence for the formation of start aggregates as an initial stage of protein aggregation. FEBS Lett., 581, 4223-4227.

20. Ha,E., Wang,W., Wang,Y.J., 2002. Peroxide formation in polysorbate 80 and protein stability. J Pharm. Sci., 91, 2252-2264.

21. Hawe,A., Kasper,J.C., Friess,W., Jiskoot,W., 2009. Structural properties of monoclonal antibody aggregates induced by freeze-thawing and thermal stress. Eur. J Pharm. Sci., 38, 79-87.

22. Hillgren,A., Lindgren,J., Alden,M., 2002. Protection mechanism of Tween 80 during freeze-thawing of a model protein, LDH. Int. J Pharm., 237, 57-69.

23. Huang,C.T., Sharma,D., Oma,P., Krishnamurthy,R., 2008. Quantitation of protein particles in parenteral solutions using micro-flow imaging. J Pharm. Sci., 98, 3058-3071.

24. Jones,L.S., Kaufmann,A., Middaugh,C.R., 2005. Silicone oil induced aggregation of proteins. J. Pharm. Sci., 94, 918-927.

25. Kiese,S., Pappenberger,A., Friess,W., Mahler,H.C., 2010. Equilibrium studies of protein aggregates and homogeneous nucleation in protein formulation. J Pharm. Sci., 99, 632-644.

26. Kishore,R.S., Pappenberger,A., Dauphin,I.B., Ross,A., Buergi,B., Staempfli,A., Mahler,H.C., 2010. Degradation of polysorbates 20 and 80: Studies on thermal autoxidation and hydrolysis. J Pharm. Sci., 100, 721-731.

27. Mahler,H.C., Friess,W., Grauschopf,U., Kiese,S., 2008. Protein aggregation: Pathways, induction factors and analysis. J Pharm. Sci., 98, 2909-2934.

28. Mahler,H.C., Muller,R., Friess,W., Delille,A., Matheus,S., 2005. Induction and analysis of aggregates in a liquid IgG1-antibody formulation. Eur. J Pharm. Biopharm., 59, 407-417.

29. Malvern., 2007, Dynamic light scattering; technical note. http://www.malvern.com/labeng/technology/dynamic_light_scattering/dynamic_light_scattering.htm .

30. Mück, C., 2002, Analytik von Proteinaggregation mittels Coulter-Prinzip: Vergleich mit der Lichtblockade-Messung. Department of Pharmacy, LMU Munich, [Diploma].

31. Narhi,L.O., Jiang,Y., Cao,S., Benedek,K., Shnek,D., 2009. A critical review of analytical methods for subvisible and visible particles. Curr. Pharm. Biotechnol., 10, 373-381.

32. Nicomp., 2008, Accusizer Theory. http://www.pssnicomp.com/accutheory.htm .

33. Philo,J.S., 2009. A critical review of methods for size characterization of non-particulate protein aggregates. Curr. Pharm. Biotechnol., 10, 359-372.

34. Philo,J.S., Arakawa,T., 2009. Mechanisms of protein aggregation. Curr. Pharm. Biotechnol., 10, 348-351.

35. Rosenberg,A.S., 2006. Effects of protein aggregates: an immunologic perspective. AAPSJ, 8, E501-E507.

36. Schellekens,H., 2003. Immunogenicity of therapeutic proteins. Nephrol. , Dial. , Transplant., 18, 1257-1259.

37. Schellekens,H., 2005. Factors influencing the immunogenicity of therapeutic proteins. Nephrol. , Dial. , Transplant., 20, vi3-vi9.

38. Sharma,D.K., King,D., Oma,P., Merchant,C., 2010. Micro-flow imaging: flow microscopy applied to sub-visible particulate analysis in protein formulations. AAPSJ, 12, 455-464.

39. Singh,S.K., Afonina,N., Awwad,M., Bechtold-Peters,K., Blue,J.T., Chou,D., Cromwell,M., Krause,H.J., Mahler,H.C., Meyer,B.K., Narhi,L., Nesta,D.P., Spitznagel,T., 2010. An industry perspective on the monitoring of subvisible particles as a quality attribute for protein therapeutics. J Pharm. Sci., 99, 3302-3321.

40. Thirumangalathu,R., Krishnan,S., Ricci,M.S., Brems,D.N., Randolph,T.W., Carpenter,J.F., 2009. Silicone oil- and agitation-induced aggregation of a monoclonal antibody in aqueous solution. J Pharm. Sci., 98, 3167-3181.

41. Tyagi,A.K., Randolph,T.W., Dong,A., Maloney,K.M., Hitscherich,C., Jr., Carpenter,J.F., 2008. IgG particle formation during filling pump operation: A case study of heterogeneous nucleation on stainless steel nanoparticles. J Pharm. Sci., 98, 94-104.

42. United States Pharmacopeia, 2009. Particulate Matter in Injections <788>.

4. Dilution of Stressed Protein Solutions into Serum: Effects on Particle counting

4.1 Introduction

Proteins are mainly administered subcutaneously or intravenously. In both cases, it is obvious that colloidal stability and other factors determining the quality of the drug will change after administration compared to the situation *in vitro*, i.e. in the formulation. Typically such effects are neglected as due to dilution on the one hand and the fact that the respective body fluids represent aqueous buffer systems no immediate risk exists on the other. However, in certain cases formulations with non-physiological pH, very high or low ionic strength, or solvent content precipitation of the drug either immediately or soon after the injection should be considered. Such effects might affect pharmacokinetics and/or lead to immunologically relevant complications [Buttel et al., 2011; Schellekens, 2005]. Proteolytic enzymes can also alter protein's efficacy. Alternatively dissolution of aggregates and particulate matter in the formulated drug product may take place and may render compromised in vitro quality attributes rather irrelevant *in vivo*.

In the scientific community discussions have started about the right track to deal with aspects of advanced formulation assessment in future [Jiskoot et al., 2011]. Different analytical approaches were chosen, aiming to characterize the fate of therapeutical proteins in physiological fluids. However, e.g. results regarding adsorption of serum components onto therapeutical proteins are not clear yet. Further studies found similar sedimentation coefficients for IgE in PBS and serum, suggesting that binding of serum components to IgE was very small or even not existing [Demeule et al., 2009]. Other studies, using fluorescence single particle tracking, discovered that serum components seemed to adsorb to protein aggregates [Filipe et al., 2011].

In this study, we wanted to evaluate the potential of particle counters to determine protein particles in physiological media. Serum solutions with its yellowish appearance might diminish the possibility that particles are detected as particle counting relies on a sufficient difference of refractive index between particle and surrounding medium. Furthermore, particle counting is evaluated to follow the fate of

aggregated therapeutical proteins in different media, such as serum solution. Particle counts of stressed therapeutical proteins were monitored over 20 hours to judge whether there is an adsorption of serum components accompanied with increasing particle counts. In fact, proteins are not expected to circulate unmodified up to 20 hours in blood [Yoo et al., 2010]. They are opsonised by macrophages before. However, in a first approach contact of therapeutical proteins and serum is allowed for 20 hours to study all possible changes and adsorptions.

In a first approach we studied the effects of dilution into serum solution and reference buffer solutions on particulate matter in IgG_1-α-solutions. Therefore, protein solutions were stressed mechanically, thermally or by freeze-thawing and stressed samples were diluted 1:50 into serum solution (pH 7.4) and buffer solutions (matching formulation buffer and phosphate buffer at pH 7.4). Samples were analyzed directly after dilution and after up to 20 h incubation times.

4.2 Experimental setup

Serum solution containing 10 mg/ml bovine serum albumin (BSA) in 5 mM phosphate buffer at 7.4 was prepared; matching placebo buffer was also prepared at pH 7.4. Phosphate buffer concentration was chosen according to physiological conditions [MedizInfo, 2011]: human blood contains 0.5 mM phosphate buffer; as it was not possible to simulate haemoglobin buffer and bicarbonate buffers, phosphate buffer concentration was chosen 10-fold higher as found in human blood.

The formulations of three therapeutic proteins (IgG_1-α (5 mg/ml), GCSF (0.5 mg/ml) and rPA (1.0 mg/ml)) were filtered through a 0.2 µm Millex syringe-driven filter unit (Millipore, Carrigtwohill, Ireland) into a particle free beaker and filled into particle free vials.

The protein samples were submitted to different stresses: freeze-thawing, mechanical and thermal stress. Stressed protein was diluted 1:50 into different (physiological) media: corresponding formulation buffer, BSA in phosphate buffer at pH 7.4 (“serum solution”), or phosphate buffer at pH 7.4 (each n = 3). Each sample with stressed protein in different media was analyzed after 0 and 20 hours (figure 1) using LO and MFI. The dilution step was performed to simulate the administration of comparably small amounts therapeutical protein into large amounts of serum.

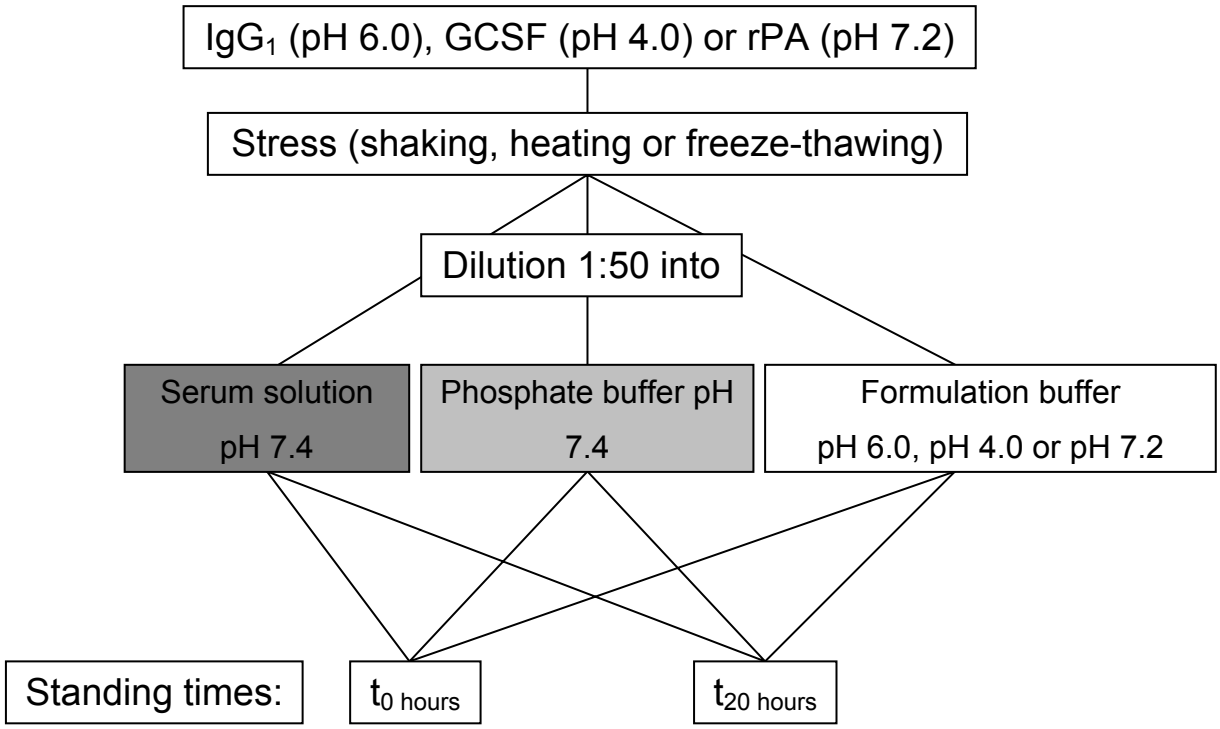

Fig. 1: Experimental setup

4.3 Results and discussion

Particle counting was performed using LO and MFI. Three vials per sampling point (0 and 20 hours) were analyzed; each with one measurement performed with MFI, two measurements with LO. First run of LO was taken as rinsing. We compared particle counts for both instruments at t_0 and t_{20} for particles ≥1 µm and ≥10 µm. Furthermore, standard deviations were considered into interpretations with regards to changes or trends: Small standard deviations and clear particle count decrease or increase was considered as a change. In case standard deviations were high, raw data were checked. If one outlier differed strongly and seemed unreasonable, a change in particle counts over time although not statistically significant was then claimed as a change. Strongly differing values pointed only to a trend.
If not further mentioned, graphs show particle counts after dilution of therapeutic protein into serum or buffer solutions.

4.3.1 Mechanical stress and dilution of IgG_1

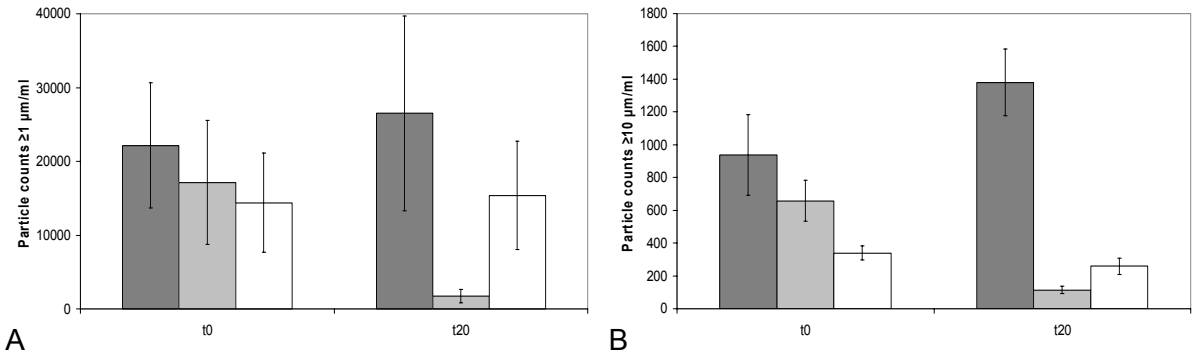

Fig. 2: LO results after dilution of mechanically stressed IgG_1-α into serum-solution (dark grey), phosphate buffer (light grey) and formulation buffer (white);
A: particles ≥1 µm/ml B: particles ≥10 µm/ml

Stressing IgG_1-α mechanically and diluting into different media delivered surprising results: Dilution into phosphate buffer at pH 7.4 led to a strong decrease in particle count over time for all particle size classes, whereas particles diluted into serum-solution (pH 7.4) tend to increase and particles diluted into formulation buffer (pH 6.0) were more stable (figure 2). Particle count in serum-solution and formulation buffer did not change significantly. Same results were found for MFI measurements (data not shown).

The phenomenon of decreasing particle count in phosphate buffer was scrutinized in chapter 5 (Buffer-screening: Effects of dilution, pH and standing time on particulate matter in IgG_1-solution).

4.3.2 Freeze-thawing and dilution of IgG_1

Freeze-thawing IgG_1-α and diluting the stressed samples into the three different media resulted in a decrease of particle counts over 20 hours in all size classes, except particles ≥10 µm in serum-solution. According to LO results, particle counts for these particles increased over 20 hours (figure 3A/B).

MFI measurements did not show any trend (figure 3C/D). Particle in all tested media at both particle size classes seemed to be stable.

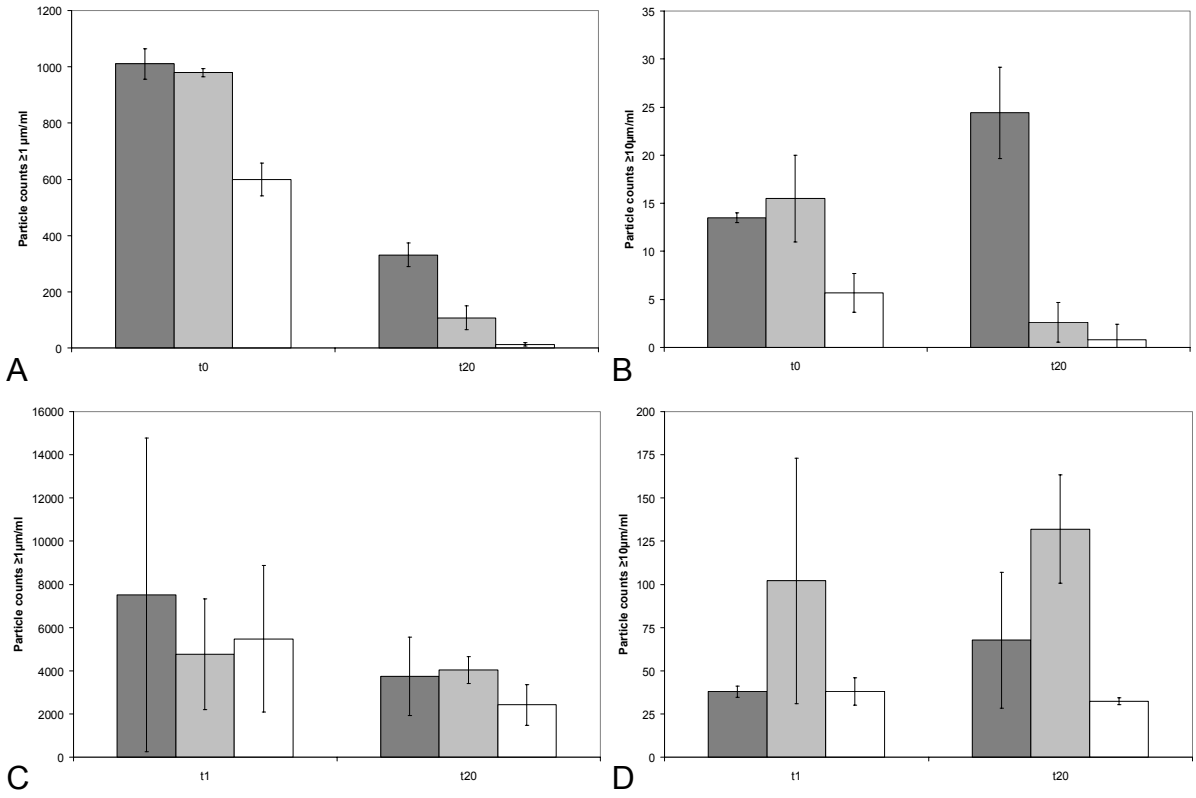

Fig. 3: LO (upper serial; A/B) and MFI (bottom serial; C/D) results after dilution of freeze-thawed IgG_1-α into serum-solution (dark grey), phosphate buffer (light grey) and formulation buffer (white)
A/C: particles ≥1 µm/ml B/D: particles ≥10 µm/ml

4.3.3 Mechanical stress and dilution of GCSF

GCSF particles formed during mechanical stress showed different trends. Whereas, LO measurements revealed a decrease in particle counts for particles in all tested media and all particle size classes over time (figure 4A/B), MFI results showed different changes: particle counts (≥1 µm and ≥10 µm) significantly increased during 20 hours in serum (figure 4C/D). Particle counts (≥1 µm) in phosphate buffer and

formulation buffer showed an increasing trend over time (figure 4C). Particle counts (particles ≥10 µm) in phosphate buffer and formulation buffer did not show any changes. It is already reported in literature that MFI is more sensitive with regards to translucent particles than LO. A minimal refractive index difference between protein particle and solution medium is required for particle detection with both instruments. The required difference for MFI is smaller than for LO [Huang et al., 2008; Sharma et al., 2010a; Sharma et al., 2010b]. It is already discussed in literature that MFI is much more sensitive to translucent particles than LO [Barnard et al., 2012; Huang et al., 2008; Mire-Sluis et al., 2011; Sharma et al., 2011; Sharma et al., 2010a]. Particles formed by mechanically stressed GCSF became translucent over time (figure 4); therefore they were not detectable any more using LO, whereas MFI could still detect an increase of particles in serum solution. Figure 5 shows examples of pictures found after mechanical and freeze-thaw stress of GCSF. After a standing time of 20 hours, particles became more translucent, as already indicated with particle counting results of LO and MFI.

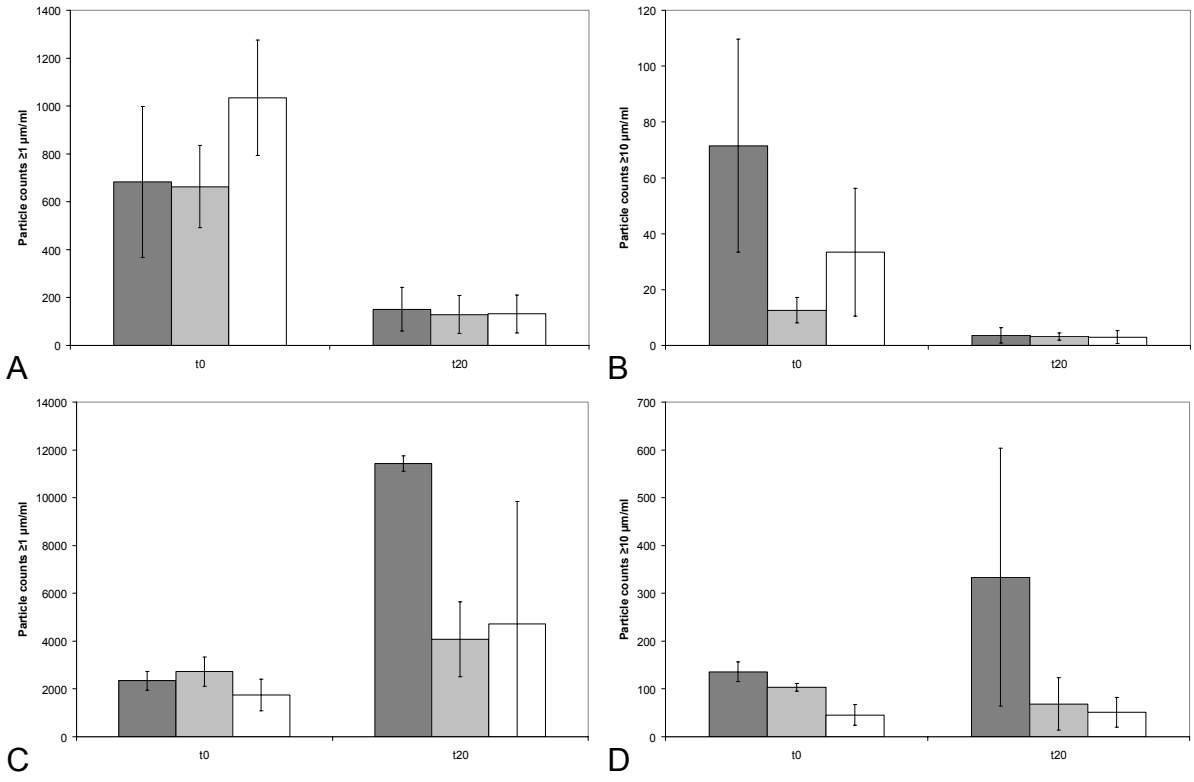

Fig. 4: LO (upper serial; A/B) and MFI (bottom serial; C/D) results after dilution of mechanically stressed GCSF into serum-solution (dark grey), phosphate buffer (light grey) and formulation buffer (white) A/C: particles ≥1 µm/ml B/D: particles ≥10 µm/ml

	Examples of translucent particles found at t_0	Examples of translucent particles found at t_{20}
Mechanically stressed GCSF; diluted in formulation buffer		
Mechanically stressed GCSF; diluted in phosphate buffer		
Mechanically stressed GCSF; diluted in Serum		
Freeze-thawed GCSF; diluted in formulation buffer		
Freeze-thawed GCSF; diluted in phosphate buffer		
Freeze-thawed GCSF; diluted in Serum		

Fig. 5: Examples of translucent particles found with MFI directly (t_0) and 20 hours (t_{20}) after diluting mechanically stressed or freeze-thawed GCSF into formulation buffer, phosphate buffer or serum solution

4.3.4 Freeze-thawing and dilution of GCSF

According to LO measurements, freeze-thawing GCSF and dilution into serum-solution, phosphate buffer, or formulation buffer resulted in a decrease of particle count for all particle size classes (figure 6A/B), whereas MFI measurements did not show significant trends over time (figure 6C/D).

However, a trend towards decreasing particle counts found in formulation buffer for both particle size classes could be detected, whereas particle counts in serum-solution and phosphate buffer were more or less the same after 20 hours. Again, stressed GCSF particles became more translucent in all tested media and particle size classes (see also figure 5).

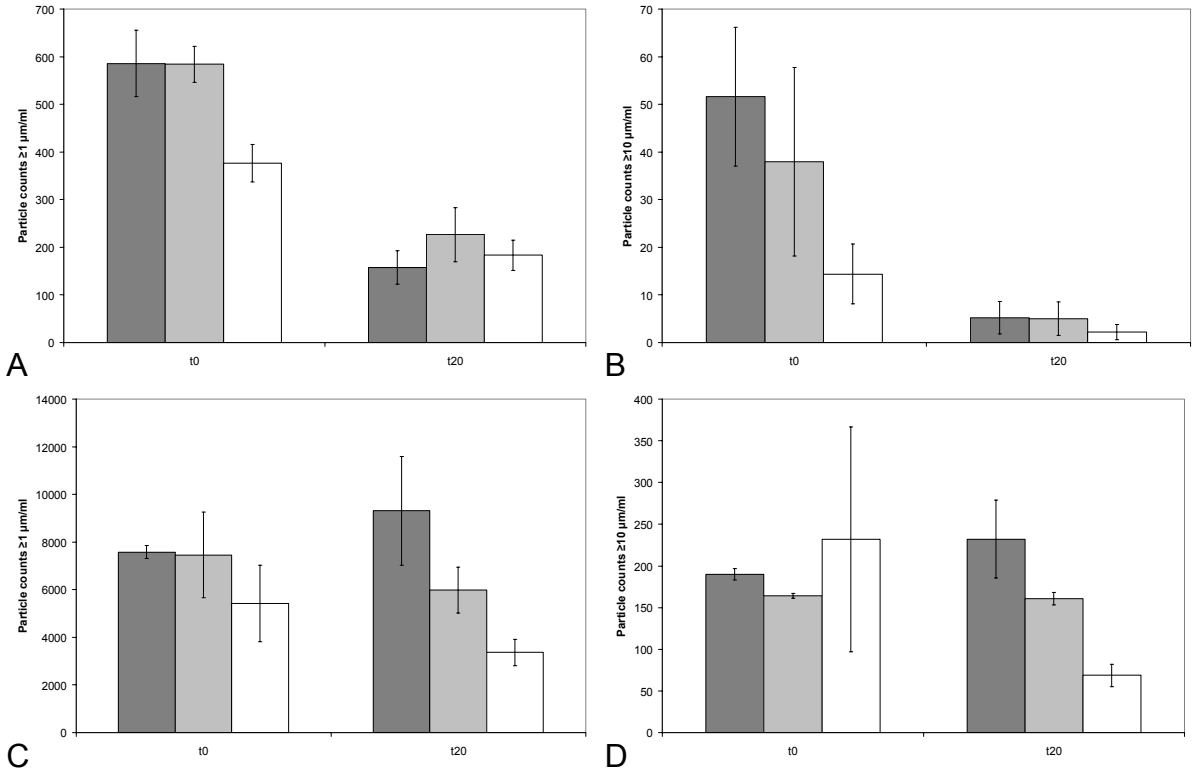

Fig. 6: LO (upper serial) and MFI (bottom serial) results after dilution of freeze-thawed GCSF into serum-solution (dark grey), phosphate buffer (light grey) and formulation buffer (white) A/C: particles ≥1 µm/ml B/D: particles ≥10 µm/ml

In summary, particle formation and resulting particle count increase can be found after diluting stressed GCSF solution into serum-solution. Particles becoming translucent, clearly confirmed with MFI. Diluting stressed GCSF solution into phosphate buffer or formulation buffer did not show increasing particle counts. Particles were stable or showed a decreasing trend in count.

The fact, that protein particles become translucent over time and can not be detected with LO but only with MFI is alarming, as particle count measurements according to pharmacopoeias is performed using e.g. classical LO. Protein particles might be overlooked.

4.3.5 Mechanical stress and dilution of rPA

Mechanical stress of rPA and dilution into the different media again showed different trends and changes (figure 7).

LO measurements showed a decrease in particle counts (≥1 µm) in formulation buffer (figure 7A) and also decreasing particle counts (≥10 µm) in all tested media (figure 7B), whilst small particles in serum and phosphate buffer are clearly increasing. MFI measurements revealed no changes for particles ≥1 µm in all media

(figure 7C) and for particles >10 µm in formulation buffer, whereas larger particles in serum-solution and phosphate buffer are increasing (figure 7D). Consequently, smaller particles are becoming less translucent and more dense over time, whilst larger particles are becoming more transparent (figure 7), only detectable using MFI (figure 8).

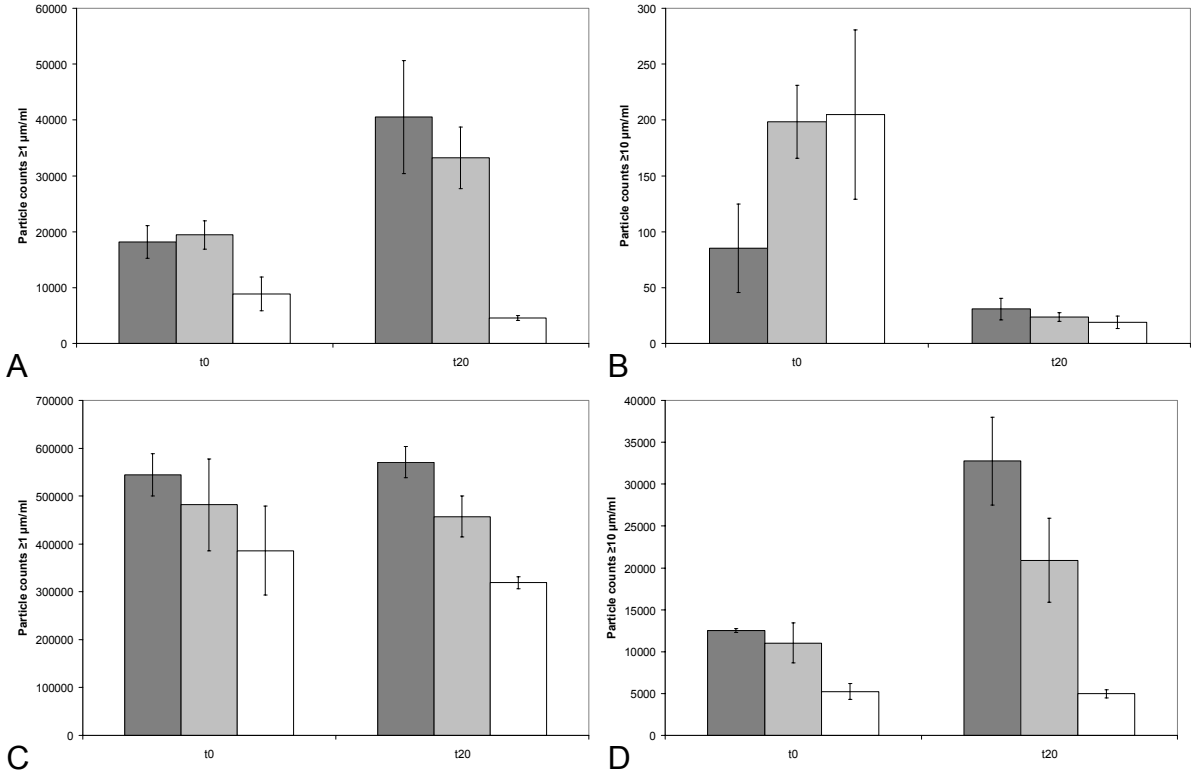

Fig. 7: LO (upper serial) and MFI (bottom serial) results after dilution of mechanically stressed rPA into serum-solution (dark grey), phosphate buffer (light grey) and formulation buffer (white)
A/C: particles ≥1 µm/ml B/D: particles ≥10 µm/ml

	Examples of translucent particles found at t_0	Examples of translucent particles found at t_{20}
Mechanically stressed rPA; diluted in formulation buffer		
Mechanically stressed rPA; diluted in phosphate buffer		
Mechanically stressed rPA; diluted in Serum		
Freeze-thawed rPA; diluted in formulation buffer		
Freeze-thawed rPA; diluted in phosphate buffer		
Freeze-thawed rPA; diluted in Serum		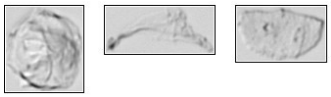

Fig. 8: Examples of translucent particles found with MFI directly (t_0) and 20 hours (t_{20}) after diluting mechanically stressed or freeze-thawed rPA into formulation buffer, phosphate buffer or serum solution

4.3.6 Freeze-thawing and dilution of rPA

Freeze-thawing and diluting rPA-samples delivered another trend in particle formation. LO measurements for particles ≥1 µm showed a decrease over 20 hours in phosphate and formulation buffer, whereas particles in serum-solution seemed to be more stable and showed no differences in count over time (figure 9A).

Larger particles did also show a decrease in particle count (figure 9B). According to MFI results, larger particles showed no differences in count over time (figure 9D) and consequently became more translucent (see figure 8). Particles ≥1 µm in formulation buffer decreased and particles in serum increased and also became more transparent (figure 9C).

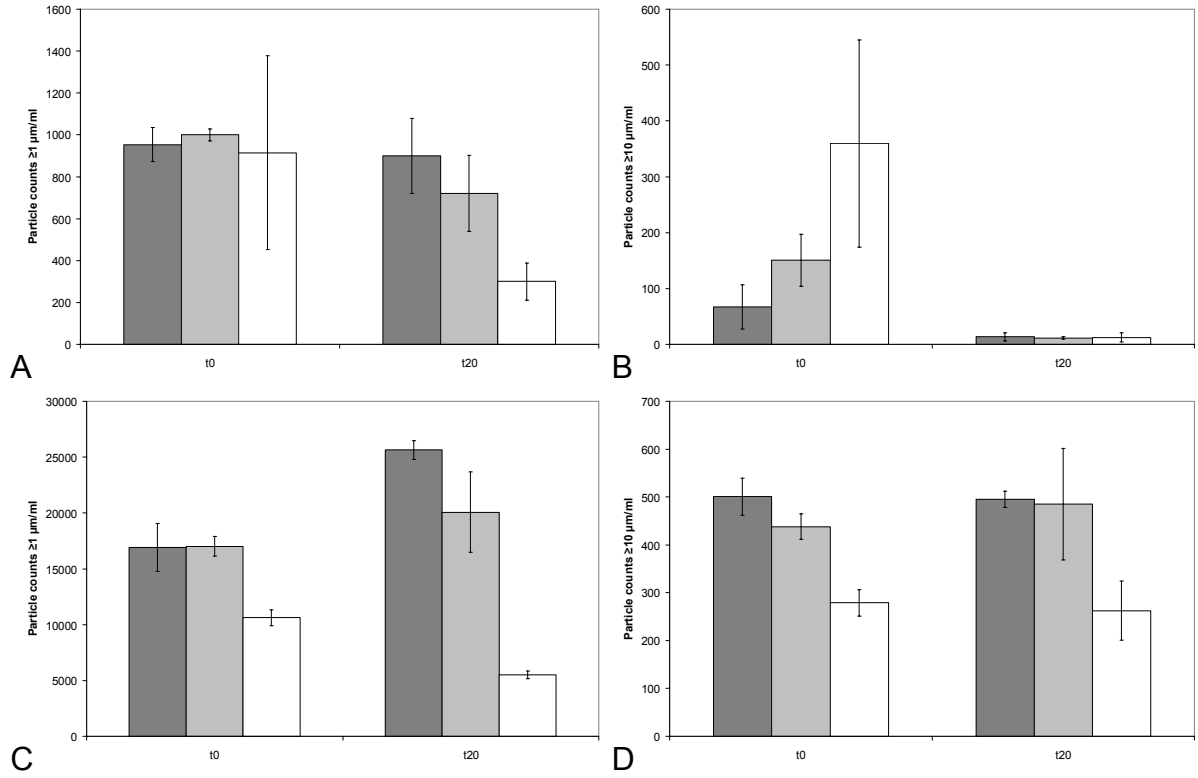

Fig. 9: LO (upper serial) and MFI (bottom serial) results after dilution of freeze-thawed rPA into serum-solution (dark grey), phosphate buffer (light grey) and formulation buffer (white)
A/C: particles ≥1 µm/ml B/D: particles ≥10 µm/ml

Summarizing, particle counts detected with LO decreased over time in all tested media, except small particles found after mechanical stress and dilution into serum solution and phosphate buffer at pH 7.4. Particle counts detected with MFI were more stable or increased in serum and phosphate buffer over time. Particles again became more translucent over time, except small particles after mechanical stress diluted into serum solution and phosphate buffer, which became less translucent. Particle counts of particles ≥10 µm in serum solution and phosphate buffer even increased over time.

4.3.7 Thermal stress

Heating IgG_1-α-solution and diluting it into the three media resulted in a clear particle count decrease in all size classes and all media (figure 10A/B).

As thermally stressed IgG_1-α forms covalently linked aggregates particle redissolving was not expected [Hawe et al., 2009]. MFI results showed no clear trend in decrease or increase of particle counts (data not shown).

Heating and diluting GCSF did not deliver any trends in decrease or increase of particle counts using LO and MFI (data not shown).

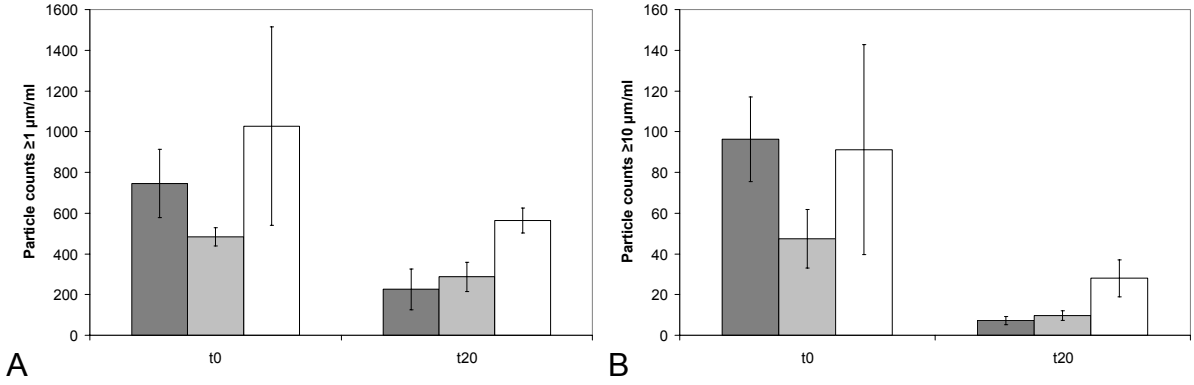

Fig. 10: LO results after dilution of thermally stressed IgG_1-α into serum-solution (dark grey), phosphate buffer (light grey) and formulation buffer (white)
A: particles ≥1 µm/ml B: particles ≥10 µm/ml

Heating and diluting rPA resulted in a decrease of particle counts (≥1 µm) in all media and for both instruments, LO and MFI (figure 11A/C). Information regarding particle counts for particles ≥10 µm differed: LO measurements resulted in a particle count decrease (figure 11B), whereas MFI measurements resulted in a particle count increase (figure 11D).

The expectation was that particles are becoming more translucent as seen for mechanical and freeze-thaw stress. Surprisingly, standing times after thermal stress resulted in dense and dark particles, which should have been detectable with LO. The dense particles mainly have been detected after diluting into serum and phosphate buffer at pH 7.4 (figure 12). Obviously, particle counters do not give consistent information after thermal stress, as already mentioned in chapter 3.

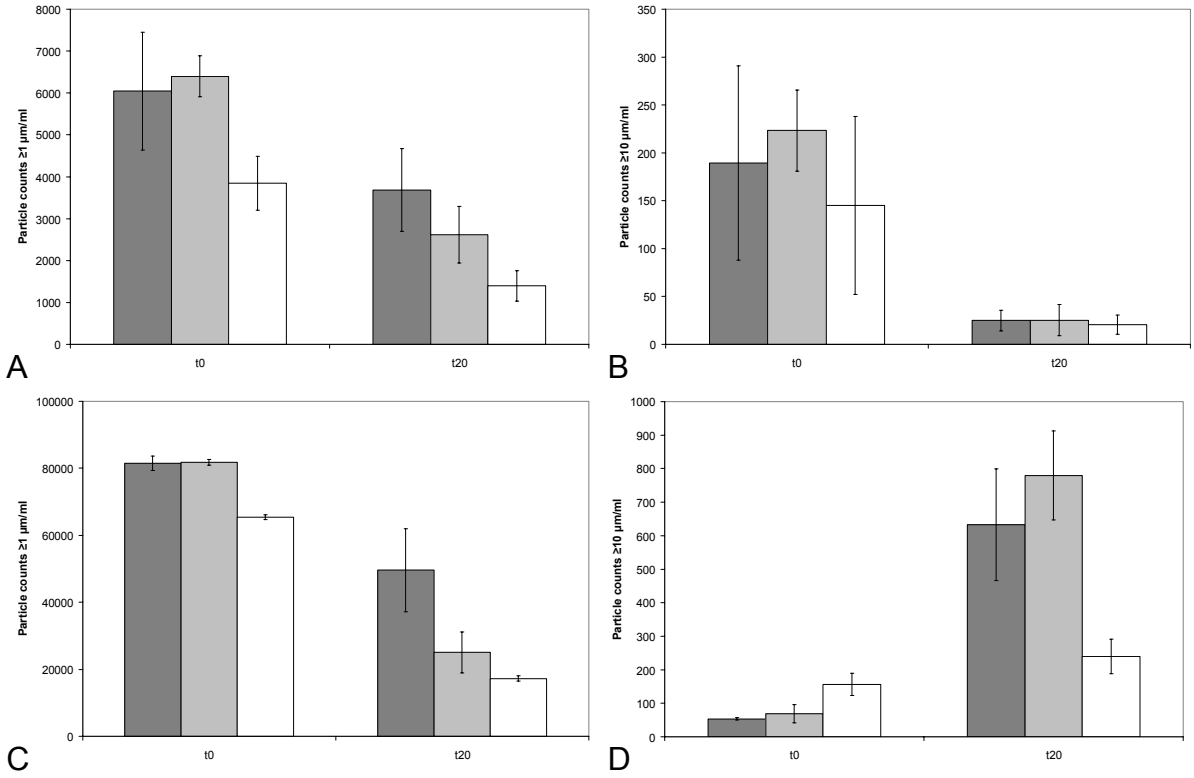

Fig. 11: LO (upper serial) and MFI (bottom serial) results after dilution of thermally stressed rPA into serum-solution (dark grey), phosphate buffer (light grey) and formulation buffer (white)
A/C: particles ≥1 µm/ml B/D: particles ≥10 µm/ml

	t_0	t_{20}
Thermal stressed; diluted in Placebo		
Thermal stressed; diluted in Phosphatebuffer		
Thermal stressed; diluted in Serum		

Fig. 12: Examples of particles found with MFI directly (t_0) and 20 hours (t_{20}) after diluting mechanically stressed or freeze-thawed rPA into formulation buffer, phosphate buffer or serum solution

4.3.8 Kinetics

In the described experiments we investigated trends in particle counts after 20 hours. The results are in fact very interesting. However, proteins are not circulating 20 hours in human blood. Therefore, we studied the trend after one, two and four hours for a selected set of experiment.

Examining mechanical stress of rPA and comparing figure 7 and figure 13 makes clear that e.g. particle count increases in serum and phosphate buffer are already taking place within the first hour after dilution and particle counts remaining stable afterwards; although it was previously published that particle equilibrium is only adjusted after months of storage [Kiese et al., 2010].

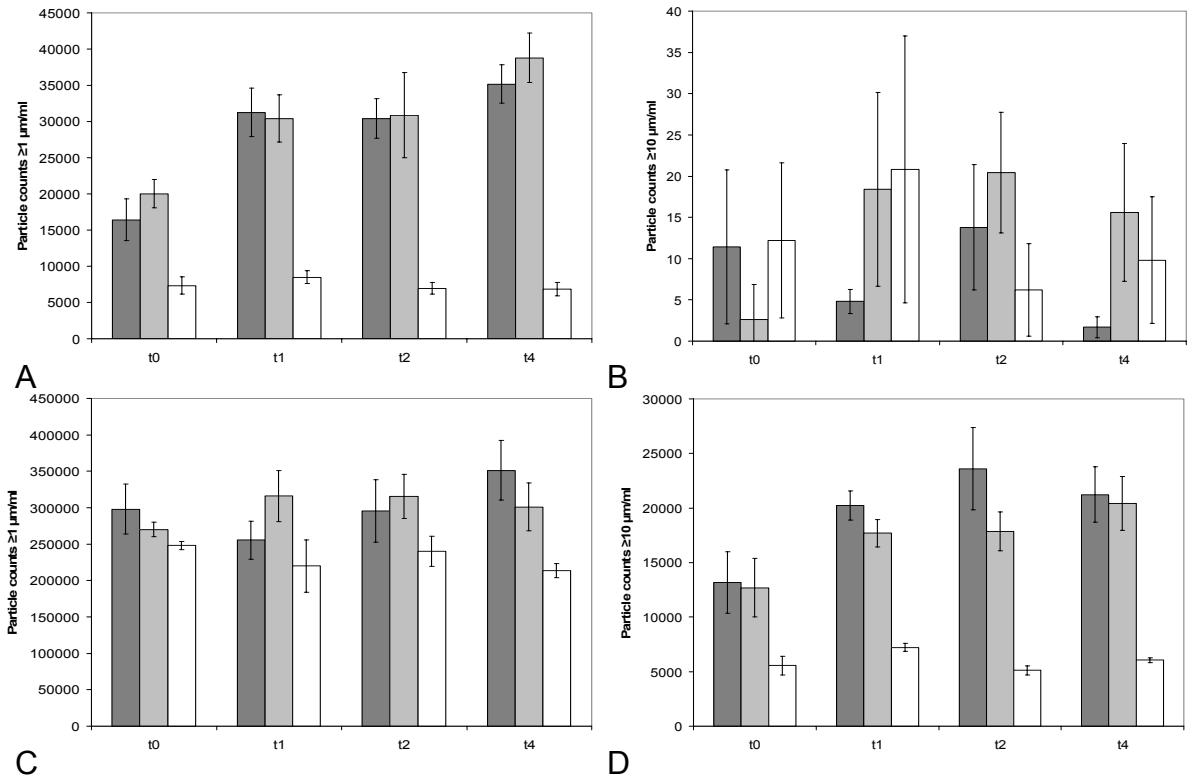

Fig. 13: Kinetic. LO (upper serial) and MFI (bottom serial) results after dilution of mechanically stressed rPA into serum-solution (dark grey), phosphate buffer (light grey) and formulation buffer (white) A/C: particles ≥1 µm/ml B/D: particles ≥10 µm/ml over time

4.4 Conclusion

One aim of this study was the evaluation of potential of particle counters to determine protein particles in physiological media. Particle counting was absolutely possible with both tested particle counters: LO and MFI. Presence of serum had no influence on the measurements.

The main aim of this study was to assess the fate of protein particles after dilution into different (physiological) media. To simulate the administration into humans, stressed protein solutions were diluted 1:50 into different media. In order to have enough protein particles after dilution, the proteins had to be extremely stressed. During measurements of undiluted solutions the detection limit of the particle counters was reached.

We can not draw clear conclusions regarding the adsorption of serum components to pharmaceutical protein particles and accompanied increasing aggregate counts. The aggregate counts after administration into serum solutions increased, which can mean that protein aggregates may trigger further aggregation or serum may bind to studied proteins. However we can not exclude effects like pH changes, as particle counts also increase after dilution into phosphate buffer. The possibility of serum components to adsorb onto protein particles was already studied by analytical ultra centrifugation [Demeule et al., 2009]. The sedimentation coefficient in serum and in PBS was found to be similar, which points to the fact that serum components are not binding to the therapeutic antibody studied. However, different results were found in other studies: interactions between and adducts of therapeutic proteins and human serum albumin were found, verified by ELISA [Braun et al., 1997; Kumarasamy et al., 1994].

From our results it can be further concluded that particulate matter in aggregated protein solutions may change after dilution into different (physiological) media: obviously, a significant amount of preformed aggregates is redissolved; other aggregates grow further, particularly in serum. Consequently, aggregation is still relevant with regards to dilution *in vitro* or *in vivo*. After dilution into phosphate buffer or placebo the situation may be different due to changes of pH and ionic strength

[Sahin et al., 2010], time [Kiese et al., 2008; Kiese et al., 2010], or pure dilution effects [Carpenter et al., 2009]. However, for simulations of proteins administration into human body only serum solution effects were of utmost interest for us.
Three different proteins were tested in this study: IgG_1, GCSF and rPA. Particularly GCSF and rPA are susceptible to stress; particles formed from these two proteins were becoming translucent over time and the particle count increased. These particles were only detectable using MFI. Particles formed by IgG_1-α were more stable and the particle count did not further increase. Formed particles did not show the tendency to become translucent over time and were detectable with MFI and LO after 20 hours.

From the first experiments with IgG_1-α solution it was concluded that aggregation after typical in vitro stress tests might not be overly relevant when such formulations are diluted in vitro or in vivo. However, studying GCSF and rPA as further proteins, these conclusions have to be revised and change to the opposite. We found increasing particle counts and increasing particle transparency after dilution of stressed protein solutions into physiological media. The fact, that protein particles can become translucent over time is alarming. Particle counts are currently monitored with e.g. classical LO, while translucent particles can only be detected with MFI. This means in reverse, that aggregation of proteins has to be avoided in any case as the aggregates are not redissolved after administration into human body but even increased.

4.5 Reference List

1. Barnard,J.G., Rhyner,M.N., Carpenter,J.F., 2012. Critical evaluation and guidance for using the coulter method for counting subvisible particles in protein solutions. J Pharm. Sci., 101, 140-153.

2. Barnard,J.G., Singh,S., Randolph,T.W., Carpenter,J.F., 2010. Subvisible particle counting provides a sensitive method of detecting and quantifying aggregation of monoclonal antibody caused by freeze-thawing: Insights into the roles of particles in the protein aggregation pathway. J Pharm. Sci., 100, 492-503.

3. Braun,A., Alsenz,J., 1997. Development and use of enzyme-linked immunosorbent assays (ELISA) for the detection of protein aggregates in interferon-alpha (IFN-alpha) formulations. Pharm. Res., 14, 1394-1400.

4. Buttel,I.C., Chamberlain,P., Chowers,Y., Ehmann,F., Greinacher,A., Jefferis,R., Kramer,D., Kropshofer,H., Lloyd,P., Lubiniecki,A., Krause,R., Mire-Sluis,A., Platts-Mills,T., Ragheb,J.A., Reipert,B.M., Schellekens,H., Seitz,R., Stas,P., Subramanyam,M., Thorpe,R., Trouvin,J.H., Weise,M., Windisch,J., Schneider,C.K., 2011. Taking immunogenicity assessment of therapeutic proteins to the next level. Biologicals, 39, 100-109.

5. Carpenter,J.F., Randolph,T.W., Jiskoot,W., Crommelin,D.J., Middaugh,C.R., Winter,G., 2009. Potential inaccurate quantitation and sizing of protein aggregates by size exclusion chromatography: Essential need to use orthogonal methods to assure the quality of therapeutic protein products. J Pharm. Sci., 99, 2200-2208.

6. Demeule,B., Shire,S.J., Liu,J., 2009. A therapeutic antibody and its antigen form different complexes in serum than in phosphate-buffered saline: a study by analytical ultracentrifugation. Anal. Biochem, 388, 279-287.

7. Filipe,V., Poole,R., Kutscher,M., Forier,K., Braeckmans,K., Jiskoot,W., 2011. Fluorescence single particle tracking for the characterization of submicron protein aggregates in biological fluids and complex formulations. Pharm. Res., 28, 1112-1120.

8. Fradkin,A.H., Carpenter,J.F., Randolph,T.W., 2009. Immunogenicity of aggregates of recombinant human growth hormone in mouse models. J Pharm. Sci., 98, 3247-3264.

9. Fradkin,A.H., Carpenter,J.F., Randolph,T.W., 2011. Glass particles as an adjuvant: a model for adverse immunogenicity of therapeutic proteins. J Pharm. Sci., 100, 4953-4964.

10. Hawe,A., Kasper,J.C., Friess,W., Jiskoot,W., 2009. Structural properties of monoclonal antibody aggregates induced by freeze-thawing and thermal stress. Eur. J Pharm. Sci., 38, 79-87.

11. Huang,C.T., Sharma,D., Oma,P., Krishnamurthy,R., 2008. Quantitation of protein particles in parenteral solutions using micro-flow imaging. J Pharm. Sci., 98, 3058-3071.

12. Jiskoot,W., Randolph,T.W., Volkin,D.B., Middaugh,C.R., Schöneich,C., Winter,G., Friess,W., Crommelin,D.J.A., Carpenter,J.F., 2012. Protein instability and immunogenicity: Roadblocks to clinical application of protein delivery systems. J Pharm. Sci., 101, 946-954.

13. Kiese,S., Pappenberger,A., Friess,W., Mahler,H.C., 2010. Equilibrium studies of protein aggregates and homogeneous nucleation in protein formulation. J Pharm. Sci., 99, 632-644.

14. Kiese,S., Papppenberger,A., Friess,W., Mahler,H.C., 2008. Shaken, not stirred: mechanical stress testing of an IgG1 antibody. J Pharm. Sci., 97, 4347-4366.

15. Kumarasamy,R., Bausch,J., Kopcha,D., Patel,S., McGonigle,E., 1994. An enzyme-linked immunosorbent assay (ELISA) for quantitation of adducts of granulocyte-macrophage colony stimulating factor (GM-CSF) and human serum albumin (HSA) in stressed solution mixtures. Pharm. Res., 11, 365-371.

16. MedizInfo., 2011, http://www.medizinfo.de/labormedizin/elektrolyte/phosphat.shtml.

17. Mire-Sluis,A., Cherney,B., Madsen,R., Polozova,A., Rosenberg,A., Smith,H., Arora,T., Narhi,L., 2011. Analysis and Immunogenic Potential of Aggregates and Particles. BioProcess International, 9, 38-54.

18. Rosenberg,A.S., 2006. Effects of protein aggregates: an immunologic perspective. AAPSJ, 8, E501-E507.

19. Sahin, E., Grillo, A.O., Perkins, M.D., and Roberts, C.J., 2010, Comparative effects of pH and ionic strength on protein-protein interactions, unfolding, and aggregation for IgG1 antibodies. J.Pharm.Sci., 99, 4830-4848.

20. Schellekens,H., 2003. Immunogenicity of therapeutic proteins. Nephrol. , Dial. , Transplant., 18, 1257-1259.

21. Schellekens,H., 2005. Factors influencing the immunogenicity of therapeutic proteins. Nephrol. , Dial. , Transplant., 20, vi3-vi9.

22. Sharma,D.K., Oma,P., Pollo,M.J., Sukumar,M., 2010a. Quantification and characterization of subvisible proteinaceous particles in opalescent mAb formulations using Micro-Flow Imaging. J Pharm. Sci., 99, 2628-2642.

23. Sharma, D., Merchant, C., Oma, P., King, D., and Thomas, D., 2011, Analysis of subvisible particles in protein therapeutics using Micro-flow Imaging. Abstracts of Papers, 241st ACS National Meeting & Exposition, Anaheim, CA, United States, March 27-31, 2011 , BIOT-353.

24. Sharma,D.K., King,D., Oma,P., Merchant,C., 2010b. Micro-flow imaging: flow microscopy applied to sub-visible particulate analysis in protein formulations. AAPSJ, 12, 455-464.

25. Yoo,J.W., Chambers,E., Mitragotri,S., 2010. Factors that control the circulation time of nanoparticles in blood: challenges, solutions and future prospects. Curr. Pharm. Des, 16, 2298-2307.

5. Buffer-Screening: Effects of Dilution, pH and Standing Time on Particulate Matter in IgG_1-Solution

5.1 Introduction

As described in Chapter 4 (“Dilution of stressed protein solutions into serum: Effects on particulate matter“) decreasing particle counts could be found when diluting mechanically stressed IgG_1-α particles into serum-buffer (phosphate-buffer) at pH 7.4 over time. However, particles were more stable when diluted into formulation buffer at pH 6.0. It is already reported in literature that buffers can have an immense effect on proteins [Katayama et al., 2006].

This buffer-screening is intended to investigate the effects of dilution, pH, ionic strength, and standing time on particulate matter in an IgG_1-α-solution. All factors are reported in literature to have a strong effect on protein solution [Carpenter et al., 2009; Kiese et al., 2010; Sahin et al., 2010]. Phosphate-buffers at pH 4.0 (acidic pH), pH 6.0 (formulation pH of IgG_1-α-solution) pH 7.0 (close to physiological tissue pH) and pH 9.0 (close to isoelectric point = pH 8.81) were chosen, each at ionic strengths of 10 mM or 75 mM according to chapter 4. Mechanical stress was applied on the IgG_1-α-solution and consequently stressed samples were diluted 1:50 into phosphate buffers (experiment 1). In a further experiment (experiment 2), IgG_1-α-solution was first diluted 1:50 into the different phosphate buffers and then stressed mechanically. In both experiments standing times from 0 to 48 h were applied until particle counting was performed.

5.2 Experimental setup

The protein formulation (IgG_1-α) was filtered through a 0.2 µm Millex syringe-driven filter unit (Millipore, Carrigtwohill, Ireland) into a particle free beaker and finally filled into particle free Zinsser vials and sealed with screw caps (Zinsser Analytic, Frankfurt, Germany). 5 h shaking stress was applied at 1000 rpm.

The protein samples were exposed to mechanical stress followed by an 1:50 dilution into the respective buffer.

8 Phosphate buffers with different pH (pH 4.0 (acidic pH), pH 6.0 (formulation pH) pH 7.0 (close to physiological pH) and pH 9.0 (close to isoelectric point) and different ionic strengths (10 mM and 75 mM) were applied.

In a first experiment, IgG_1-α-solution (5 mg/ml) was mechanically stressed over 5 hours at 1000 rpm. The stressed IgG_1-α-solution was diluted 1:50 into buffers (n = 3) to obtain a final concentration of 0.1 mg/ml. Particle counting was performed using light obscuration and Microflow Imaging after 0, 24 and 48 hours.

In a second experiment IgG_1-α-solution (5 mg/ml) was diluted 1:50 into buffer (n = 3). Diluted IgG_1-α samples (0.1 mg/ml) were mechanically stressed over 5 hours at 1000 rpm and particles were counted after 0, 24 and 48 hours.

5.3 Results and discussion

5.3.1 Experiment 1

5.3.1.1 Results of particle counting: LO and MFI

LO measurements resulted in decreased particle counts (particles ≥1 µm) over time for all tested pH-values and ion concentrations (figure 1 A/C). This effect is even stronger at alkaline pH. In parallel, particle counts (particles ≥10 µm) increased over time (figure 2 B/D). Small particles grow into larger ones, which is more pronounced at alkaline pH and higher buffer molarity.

However, different information is obtained from MFI measurements. MFI particle count measurements were not as consistent as LO measurements (figure 2). Particle counts slightly decreased over time (particles ≥1 µm and ≥10 µm, both ionic strengths). Furthermore, fewer particles were found at alkaline pH and high ionic strengths.

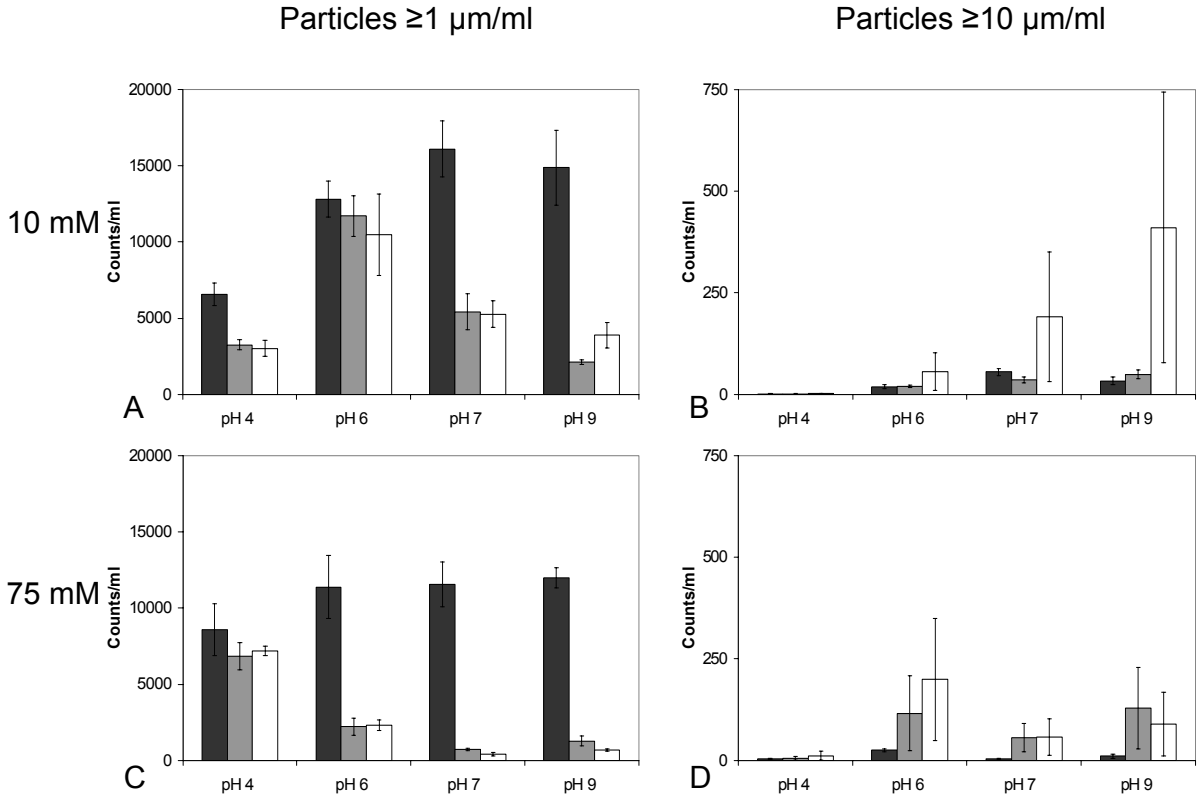

Fig. 1: Light obscuration results for experiment 1: stressed sample was diluted in different phosphate buffers and measurement was performed after 0 (dark grey), 24 (light grey) and 48 (white) hours

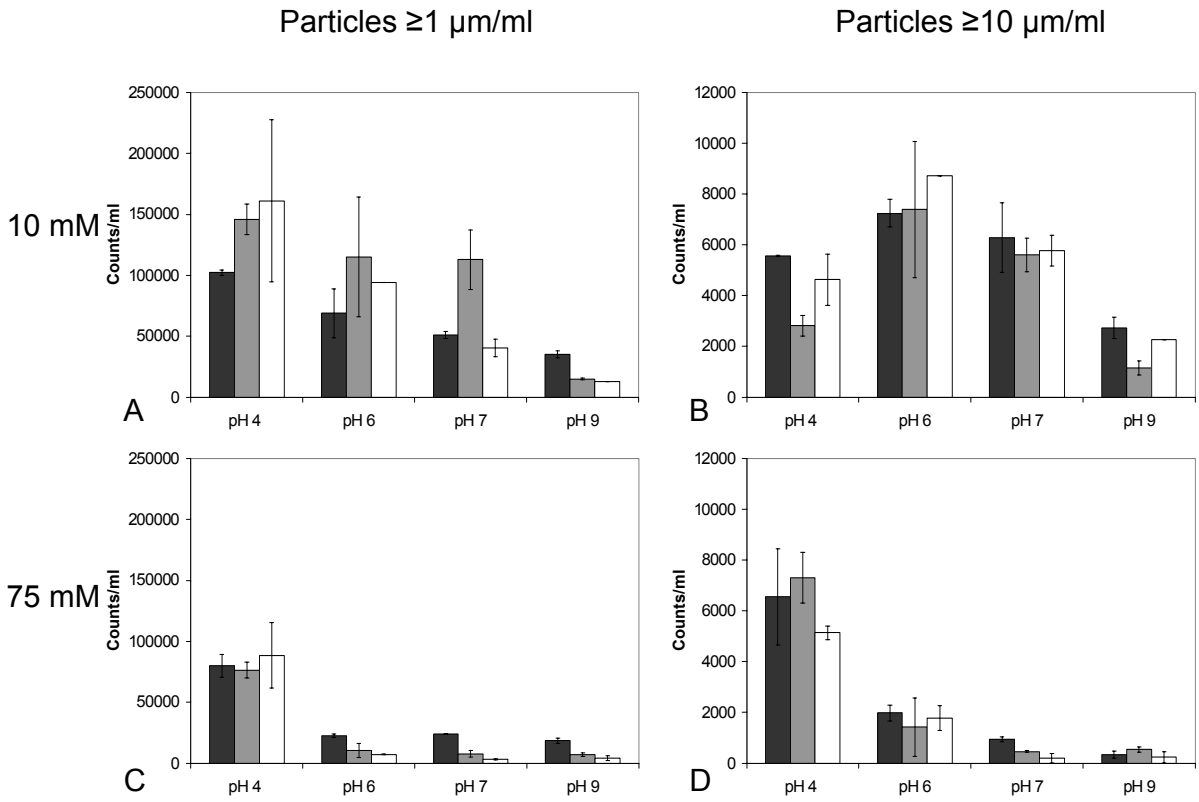

Fig. 2: Micro-flow Imaging results for experiment 1: stressed sample was diluted in different phosphate buffers and measurement was performed after 0 (dark grey), 24 (light grey) and 48 (white) hours

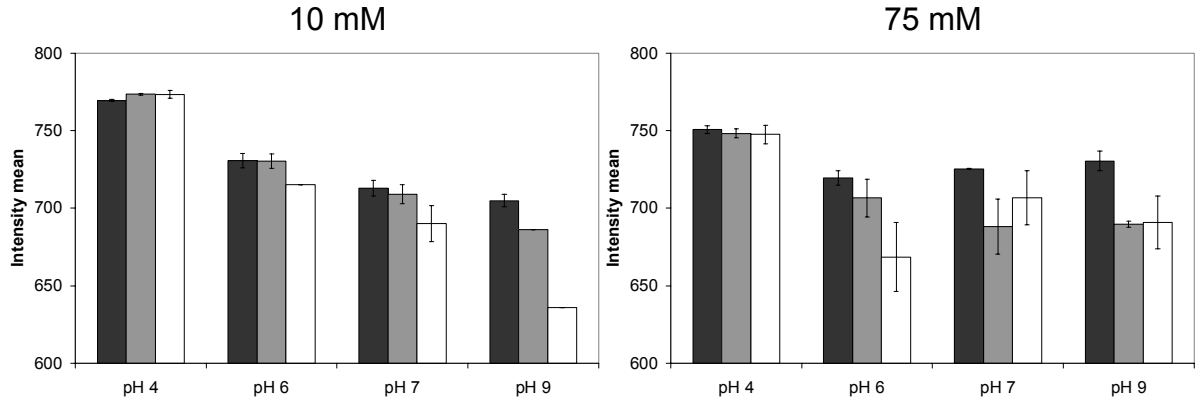

Fig. 3: Microflow-Imaging results (Intensity mean) for experiment 1: stressed sample was diluted in different phosphate buffers and measurement was performed after 0, 24 and 48 hours

MFI also gives information on particle appearance like particle form or intensity mean (IM). IM values give information about the amount of light passing through the protein particles. High IM values are found when particles are translucent and are letting pass more light from the light source. On the contrary, lower IM values are found for more dense particles that absorb more light. Monitoring IM, it turned out that with increasing pH also IM values decrease over time (figure 3). To make sure that only proteinacious particles are monitored, a software filter was used to exclude air

bubbles, and large edge particles. Air bubbles are known to be circular; therefore all detected particles with a circularity ≥0.85 were excluded [Sharma et al., 2009]. Large edge proteins are often stuck to the flow cell and detected more than once, therefore all detected particles ≥ 80 µm were also excluded. Recently, the development of an improved filter was reported [Strehl et al., 2011].

Low intensity mean values are found at alkaline pH. IM values decrease over time, which suggests that particles become denser, further particles are denser at alkaline pH. This explains the comparable low particle count (particles ≥1 µm) detected with LO at pH 4.0 (t_0): particles are too translucent to be detected with LO (figure 1A/C).

5.3.1.2 Effect of dilution on pH

After dilution of serum into buffer solutions, pH was controlled (table 1). The buffer capacity of the higher molar buffer is clearly noticeable: pH values were kept almost constant. Diluting the small amount of IgG solution 1:50 into the 10 mM buffers, only the pH value within the neutral buffer was kept constant, whereas acidic pH values slightly increased and alkaline pH values decreased. This implies that pH values given for the low molecular buffers in figures 1 and 2 are slightly different from stated pH values. In lower molar buffers, the pH differences are not as strong as in higher molar buffers; this explains the stronger effect of the higher molar buffer on the dilution of smaller particles.

Table 1: pH values after pH adjustment of buffers (buffer) and directly after addition of stressed IgG solution (controlled)

		pH 4	pH 6	pH 7	pH 9
10mM	buffer	4.06	6.05	6.86	8.72
	controlled	4.45	6.20	6.86	8.10
75mM	buffer	3.84	5.93	6.72	8.69
	controlled	3.92	5.99	6.73	8.42

5.3.1.3 Dilution effect on particulate matter

To evaluate the influence of dilution, mechanically stressed and undiluted samples are measured as control (table 2). The particle numbers after dilution (table 3) were compared with the particle numbers before dilution. To recalculate the 1:50 dilution, the particle numbers before dilution were divided by 50, printed in bold. It is obvious, that for particles ≥1 µm the detection limit has been reached: all diluted samples reveal a higher particle count than undiluted and recalculated samples. Hence, for small particles an assessment regarding the dilution effect is not possible. For larger

particles the result is different: the undiluted and recalculated solution exposes a higher particle count than diluted samples. This implies that larger particles are dissolved immediately upon dilution.

Table 2: Particle counts and standard deviations after mechanical stress; undiluted and recalculated samples

	Undiluted	Undiluted, divided by 50
Particles ≥1µm/ml	166283 ± 7943	**3326**
Particles ≥10µm/ml	26621 ± 4429	**532**

Table 3: Particle counts and standard deviations after mechanical stress and dilution in respective buffers

		Diluted in 10 mM buffer	Diluted in 75 mM buffer
Particles ≥1µm/ml	pH 4	6571 ± 730	8573 ± 1703
	pH 6	12814 ± 1171	11375 ± 2062
	pH 7	16091 ± 1833	11557 ± 1475
	pH 9	14880 ± 2455	11980 ± 666
Particles ≥10µm/ml	pH 4	1 ± 1	4 ± 1
	pH 6	19 ± 5	25 ± 3
	pH 7	55 ± 9	4 ± 1
	pH 9	33 ± 9	11 ± 5

5.3.1.4 Zeta potential measurements

Summarizing, the different information between LO and MFI results have to be further evaluated.

In a first approach, zeta potential (ZP) theory is dedicated to clarify results. In theory, close to isoelectric point (IEP) ZP values are low [Chiti, 2006; Jachimska et al., 2008], the protein carries no net charge, and van der Waal's forces are outweighing and protein particles tend to aggregate [Calamai et al., 2003; Chiti et al., 2006]. Zeta potential is strongly dependent from pH: at acidic pH zeta potential is positive, at more alkaline pH zeta potential values become negative and at IEP zeta potential is zero [Arakawa et al., 1984; Ruppert et al., 2001] as schematically shown in figure 4.

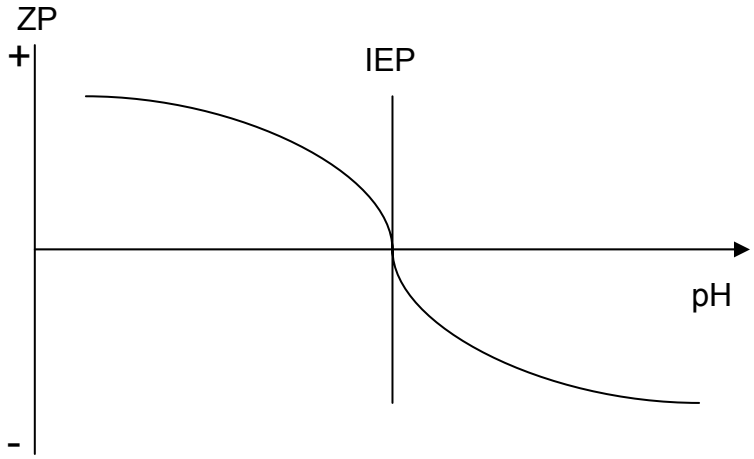

Fig. 4: Zeta potential (ZP) theory as a function of pH

Practically, ZP titrations should be performed at protein concentrations of 4-10 mg/ml and ionic strengths of maximum 20 mM. Hence, ZP titrations of diluted samples (0.1 mg/ml) were not possible, as well as titration in 75 mM phosphate buffer. Therefore ZP of IgG_1-α was measured in bulk concentration (5 mg/ml) after buffer exchange to 10 mM histidine at pH 6.0 (figure 5), which is the formulation buffer.

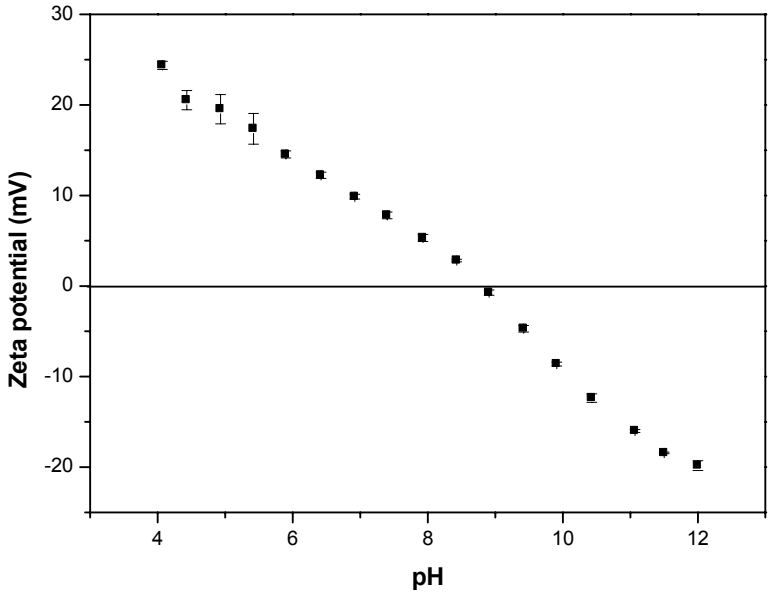

Fig. 5: Zeta potential (5 mg/ml IgG_1 in 10 mM histidine pH 6.0) as a function of pH

ZP titration revealed the IEP at pH 8.81. Different pH and ionic strengths influence ZP of protein [Zhu et al., 2007]. However, further considerations are made on the basis of the performed titration.

Theoretically, at pH 8.81 net charge of protein is zero and aggregation of particles is predominant over repulsion.

On the one hand, LO measurements perfectly fit in: particle counts for particles ≥1 µm increased with increasing pH at t_0. Particle counts for particles ≥1 µm/ml at t_1 and t_{24} are smaller at pH 9.0 than at pH 4.0, however, particles ≥10 µm/ml are increasing with increasing pH. Smaller particles seem to aggregate to larger ones close to IEP. On the other hand, results of MFI measurements show a particle count decrease close to IEP not explainable with ZP theory. Furthermore, it seems that aggregates are even redissolving close to IEP, where the protein solution is theoretically most instable and aggregation should be predominant. MFI results show a particle count decrease with increasing pH for both particle size classes.

Interestingly, IM is increasing with increasing zeta potential (figure 6). This implies that particles are more translucent with increasing zeta potential and increasing stability of solutions. The less the solution stability is, the denser protein particles are.

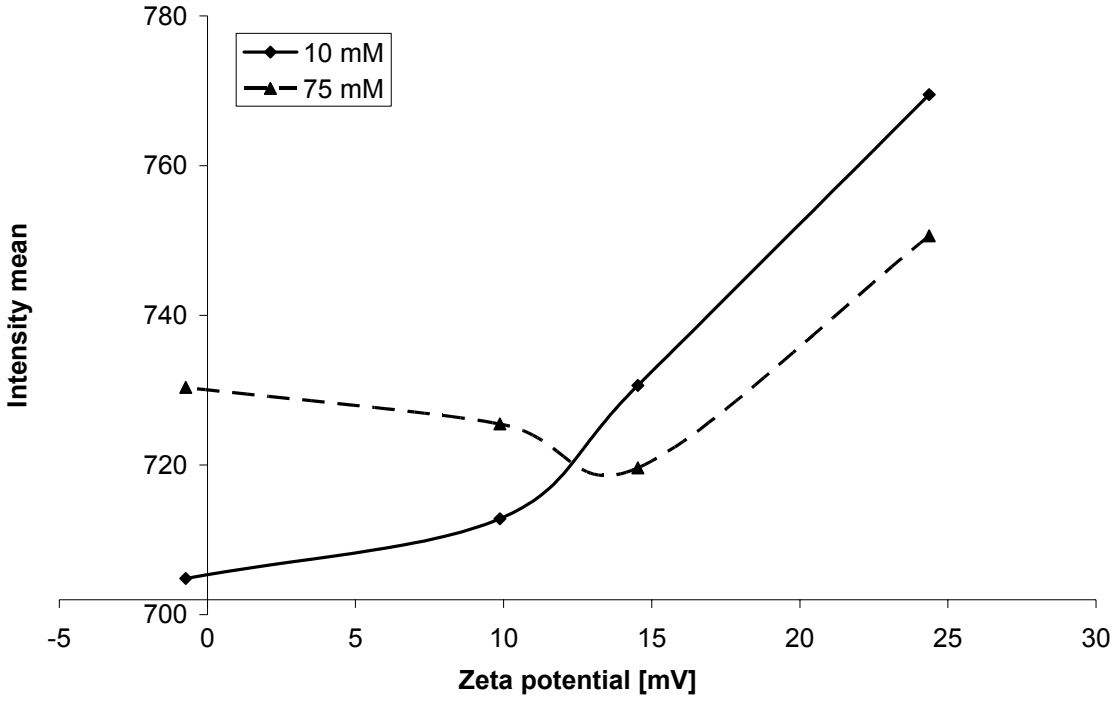

Fig. 6: Intensity mean as a function of zeta potential: Found IM values for 10 mM and 75 mM are plotted over zeta potential values from titrations after buffer exchange (see above)

It is already addressed in literature that MFI is more sensitive to transparency of particles [Huang et al., 2008; Sharma et al., 2011; Sharma et al., 2010].

However, in this case MFI obviously is not detecting particles that are expected due to zeta potential theory [Chiti, 2006; Jachimska et al., 2008] and also are detected by LO.

5.3.1.5 Microscopic results

Zeta potential titrations offered valuable clues on protein aggregation dependencies, however, it has not been clarified yet, whether particle counts from LO or MFI has to be conceded as true. An important difference to examine is the increasing (LO; figure 1 B/D) respectively decreasing (MFI; figure 2B/D) particle count of larger particles over time.

Stressed protein was diluted into phosphate buffer at pH 4.0 and pH 9.0 at both ionic strengths, further characterization was performed at t_0 and t_{24}.

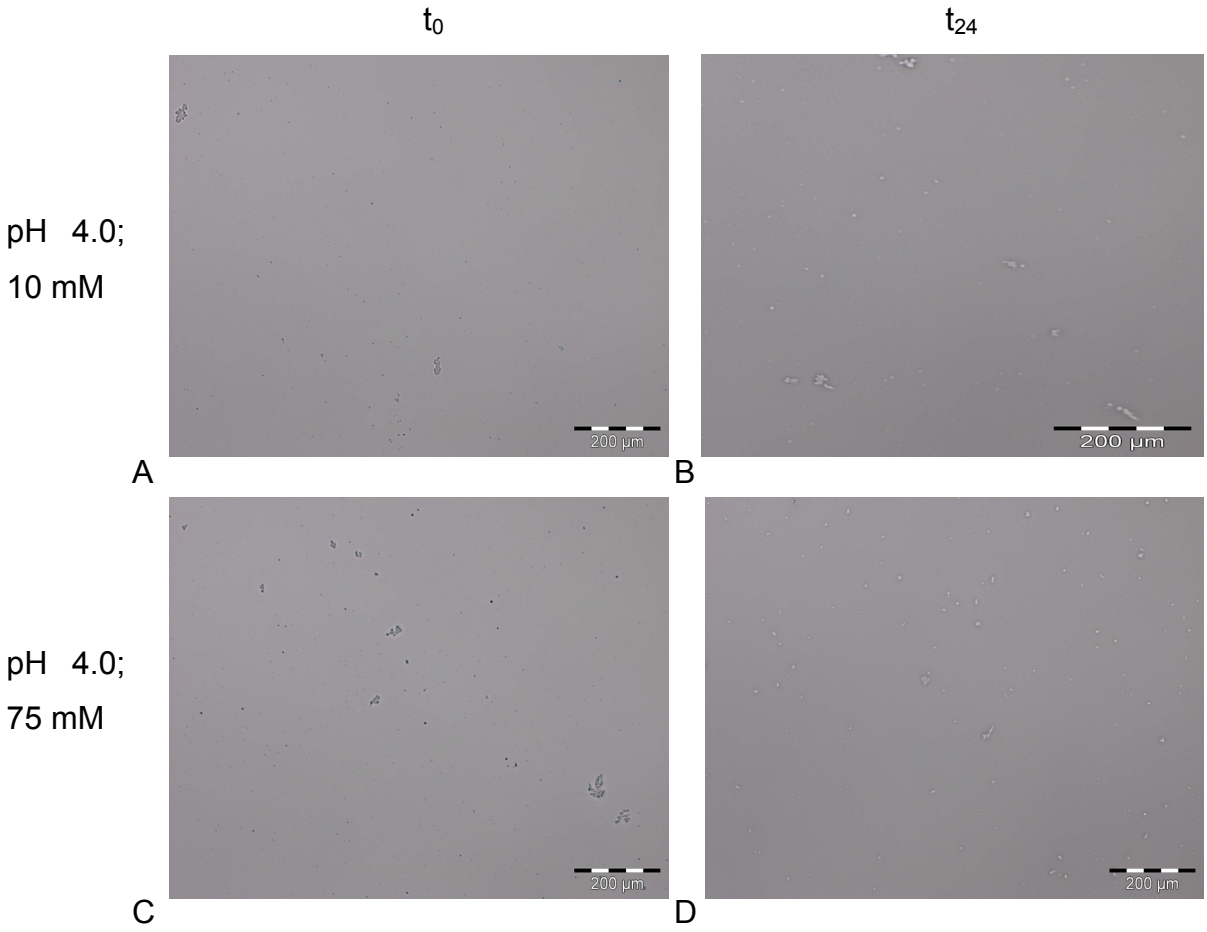

Fig. 7: Microscope pictures of stressed IgG_1-α diluted into phosphate buffer at pH 4.0

10 µl of each sample were put on a microscope slide, dried and examined under the microscope. Drying should allow examination of all particles in one layer. With this

experiment not the absolute particle number but a trend of particle counts decrease or increase over time should be evaluated.

Microscope pictures confirmed IM results found with MFI: particles at pH 4.0 at both ionic strengths are more translucent than particles at pH 9.0 at both ionic strengths. Also IM values are higher at acidic pH, proving particles at pH 4.0 to be translucent. Further, microscope pictures confirm the trend for particles ≥10 µm found with LO and ZP theory: larger particles are increasing over time. Figure 7 and 8 show particles of diluted protein samples at t_0 and t_{24}. Both figures show an increasing trend for particles, more pronounced at pH 9.0 (figure 8), which fits to LO results.

Of course, as samples are neither filtered nor proteinacious particles are selectively stained, this trend has to be examined with caution. MFI results are not explainable, especially as for pilot experiments in chapter 4 MFI showed same results as LO.

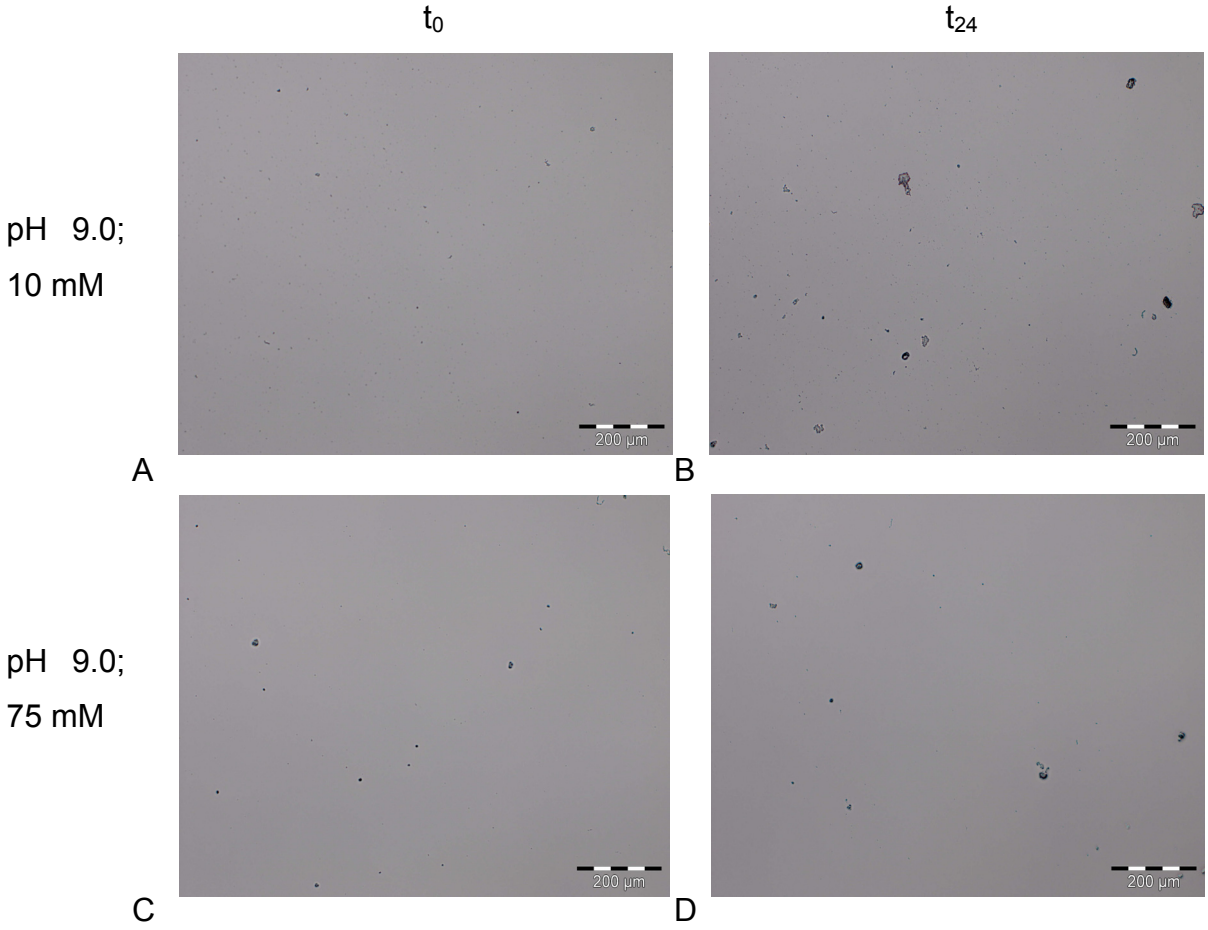

Fig. 8: Microscope pictures of stressed IgG_1-α diluted into phosphate buffer at pH 9.0

5.3.2 Experiment 2

5.3.2.1 Results of particle counting: LO and MFI

In general, stressing diluted protein solutions does not lead to high amounts of aggregates as protein monomers are not crossing each others ways often [Shire et al., 2004]. Therefore, experiment 2 does not lead to comparable particle counts as experiment 1.

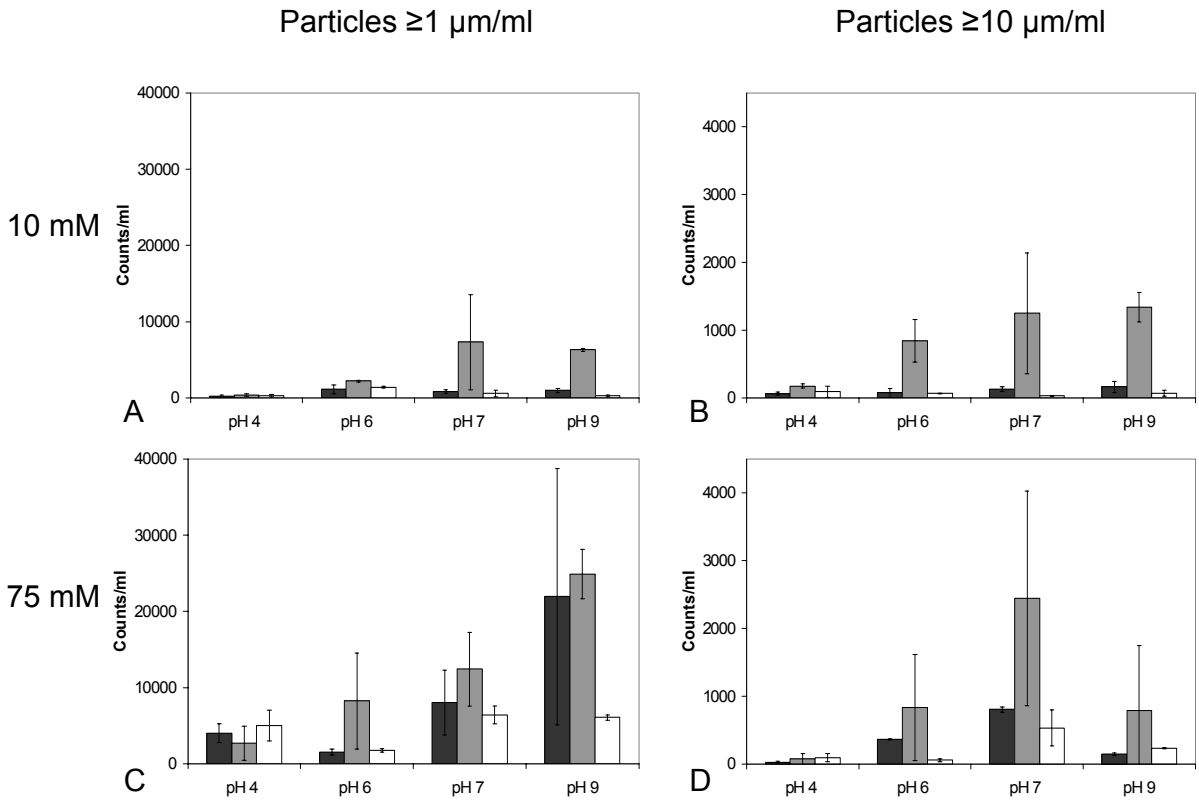

Fig. 9: Light obscuration results for experiment 2: diluted sample was stressed in different phosphate buffers and measurement was performed after 0 (dark grey), 24 (light grey) and 48 (white) hours

LO measurements revealed high standard deviations after mechanical stress (figure 9). Particle counts for particles ≥1 µm and ≥10 µm found in 10 mM samples seem to increase after 24 hours and to decrease again after 48 hours to the initial value or even below. In general, in 10 mM samples, particle count is at a low level.

LO measurements in 75 mM samples discovered even higher standard deviations than in 10 mM samples in both particle size classes. However, there are still same trends observable: particle counts seem to increase after 24 hours and to decrease again after 48 hours. The particle level is higher than in 10 mM samples. Particle counts seem to increase (not significantly) with increasing pH.

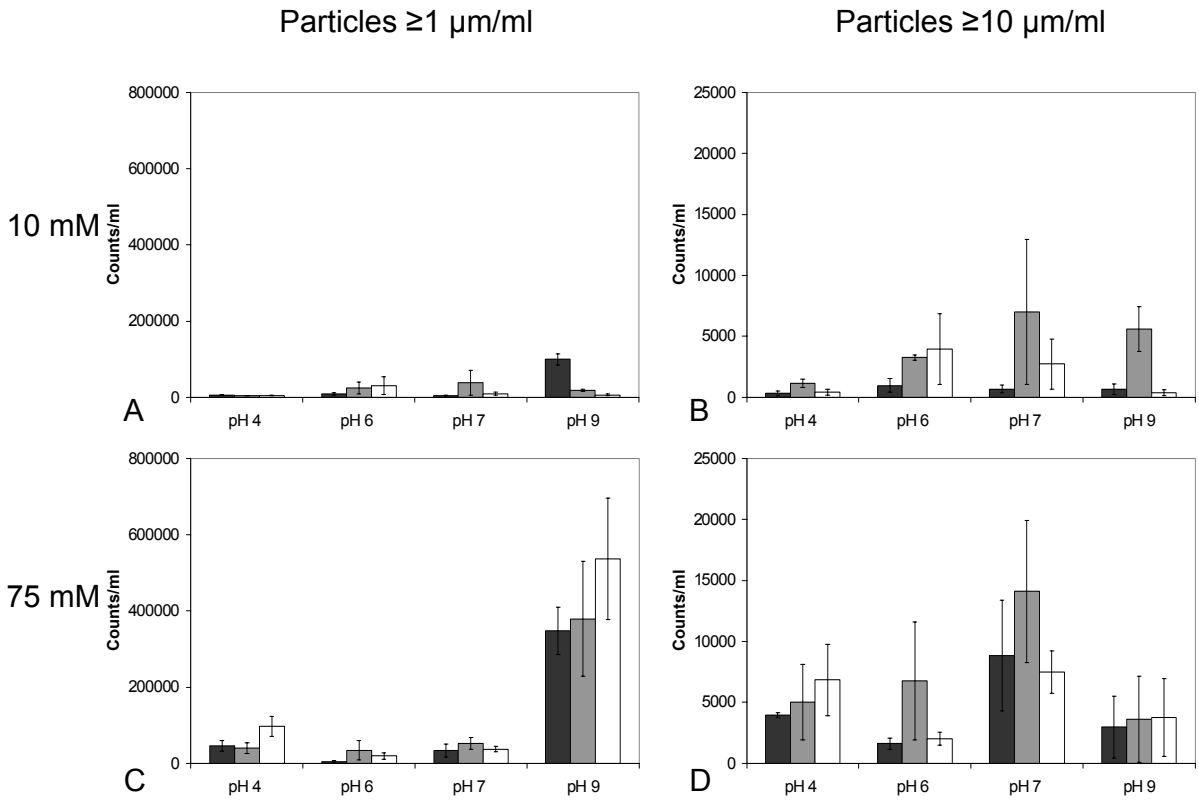

Fig. 10: Micro-flow Imaging results for experiment 2: diluted sample was stressed in different phosphate buffers and measurement was performed after 0 (dark grey), 24 (light grey) and 48 (white) hours

MFI measurements also showed high standard deviations, especially in the 75 mM samples (figure 10). For the 10 mM samples particle levels were low, there is also the trend of increasing and then decreasing particle count over time. In 75 mM samples particle count is also low for particles ≥1 µm, except at pH 9.0. In these samples high amounts (~400000) of small particles were found, also visible with LO.

However, in general LO and MFI results of experiment 2 fit to zeta potential theory: particle counts are increasing with increasing pH. Close to IEP more particles are found than at acidic pH at which the protein solution is more stable.

5.4 Conclusion

Stressing diluted solutions does not result in high amounts of aggregates. Amongst other reasons, protein aggregation is strongly dependent on protein concentration [Minton, 2005; Shire et al., 2004]. Therefore, experiment 2 (applying stress on diluted protein solutions) is not appropriate to determine effects of different pH, standing times and dilution of proteins. However, one trend was dominant: particle counts seemed to increase first and then decrease again over time. Further, close to IEP particle count is higher than at larger zeta potential values.

Stressing IgG_1-α bulk solution, diluting it into different phosphate buffers and monitoring the effect of time, ionic strength and pH delivered interesting results. Particles ≥1 µm decrease over time and increasing pH, whilst larger particles ≥10 µm increase at the same time, confirmed by microscopic experiments. Concluding, the small particles grow into larger ones. This effect is more pronounced at alkaline pH, as well as higher buffer molarities. At acid pH larger particles are dissolved. IEP is determined at pH 8.81; protein particles are not charged and tend to aggregate and form larger particles. MFI results show that alkaline pH values dissolves particles, whereas the more acidic pH values more or less do not have any effect. These results could not be confirmed with orthogonal methods.
Generally we can conclude that at pH 4.0 used IgG_1-formulation is prevented from aggregation due to large positive zeta potential values and involved repelling forces. Worst pH is alkaline pH 9.0 close to IEP. Proteins are charged less and aggregate with each other. Changing the pH has a huge impact on protein particles: at a pH value close to IEP aggregation is predominant over dissolving. At other pH values protein particles can be redissolved.
Dilution of mechanically stressed protein solution directly leads to redissolving of larger particles. The impact of dissolution on smaller particles could not be assessed with these experiments as the detection limit of LO was reached.

MFI-images of samples were analyzed for mean intensity (proportional to transparency). Intensity of particles is described in illumination intensity levels [Huang

et al., 2008]. Earlier it was found that intensities of proteinaceous particles differ as a function of size and mode of generation [Sharma et al., 2010]. These studies show intensity as a function of pH and time. Mean intensity decreases over increasing pH and also over time.
With increasing zeta potential intensity mean is also increasing. Particles are more translucent at stable formulations and denser close to IEP. Close to IEP particles tend to aggregate. Hence, the more stable aggregates are, the denser they appear.

The studies described within chapter 5 were performed to enlighten the decreasing particle count after diluting mechanically stressed IgG_1 into phosphate buffer. As an overall conclusion it can be stated, that small particles diluted into phosphate buffers with different ionic strengths and pH values decrease over 20 hours (table 4).

		5 mM	10 mM	75 mM
pH 7.0	LO	N/A	decrease	decrease
	MFI	N/A	**increase**	decrease
pH 7.4 (from chapter 4)	LO	decrease	N/A	N/A
	MFI	decrease	N/A	N/A
pH 9.0	LO	N/A	decrease	decrease
	MFI	N/A	decrease	decrease

Table 4: Particle count over 20 hours after dilution into different phosphate buffers; particles ≥1 µm

With increasing ionic strength and increasing pH larger particles tend to increase over 20 hours (table 5). Increasing particle count of larger particles at increasing pH is caused by isoelectric point at pH 8.81. Protein molecules are not charged and can aggregate.

		5 mM	10 mM	75 mM
pH 7.0	LO	N/A	decrease	**increase**
	MFI	N/A	**stable**	decrease
pH 7.4 (from chapter 4)	LO	decrease	N/A	N/A
	MFI	decrease	N/A	N/A
pH 9.0	LO	N/A	**increase**	**increase**
	MFI	N/A	decrease	**stable**

Table 5: Particle count over 20 hours after dilution into different phosphate buffers; particles ≥10 µm

5.5 Reference List

1. Arakawa,T., Timasheff,S.N., 1984. Mechanism of protein salting in and salting out by divalent cation salts: balance between hydration and salt binding. Biochemistry, 23, 5912-5923.

2. Calamai, M., Taddei, N., Stefani, M., Ramponi, G., and Chiti, F., 2003, Relative Influence of Hydrophobicity and Net Charge in the Aggregation of Two Homologous Proteins. Biochemistry 42[51], 15078-15083.

3. Carpenter,J.F., Randolph,T.W., Jiskoot,W., Crommelin,D.J., Middaugh,C.R., Winter,G., 2009. Potential inaccurate quantitation and sizing of protein aggregates by size exclusion chromatography: Essential need to use orthogonal methods to assure the quality of therapeutic protein products. J Pharm. Sci., 99, 2200-2208.

4. Chiti,F., Dobson,C.M., 2006. Protein misfolding, functional amyloid, and human disease. Annu. Rev. Biochem, 75, 333-366.

5. Chiti, F., 2006, Relative importance of hydrophobicity, net charge, and secondary structure propensities in protein aggregation. Protein Rev. 4[Protein Misfolding, Aggregation, and Conformational Diseases, Part A], 43-59.

6. Huang,C.T., Sharma,D., Oma,P., Krishnamurthy,R., 2008. Quantitation of protein particles in parenteral solutions using micro-flow imaging. J Pharm. Sci., 98, 3058-3071.

7. Jachimska,B., Wasilewska,M., Adamczyk,Z., 2008. Characterization of globular protein solutions by dynamic light scattering, electrophoretic mobility, and viscosity measurements. Langmuir, 24, 6866-6872.

8. Katayama,D.S., Nayar,R., Chou,D.K., Valente,J.J., Cooper,J., Henry,C.S., Vander Velde,D.G., Villarete,L., Liu,C.P., Manning,M.C., 2006. Effect of buffer species on the thermally induced aggregation of interferon-tau. J Pharm. Sci., 95, 1212-1226.

9. Kiese,S., Pappenberger,A., Friess,W., Mahler,H.C., 2010. Equilibrium studies of protein aggregates and homogeneous nucleation in protein formulation. J Pharm. Sci., 99, 632-644.

10. Minton,A.P., 2005. Influence of macromolecular crowding upon the stability and state of association of proteins: predictions and observations. J Pharm. Sci., 94, 1668-1675.

11. Ruppert,S., Sandler,S.I., Lenhoff,A.M., 2001. Correlation between the osmotic second virial coefficient and the solubility of proteins. Biotechnol. Prog., 17, 182-187.

12. Sahin, E., Grillo, A.O., Perkins, M.D., and Roberts, C.J., 2010, Comparative effects of pH and ionic strength on protein-protein interactions, unfolding, and aggregation for IgG1 antibodies. J.Pharm.Sci. 99[12], 4830-4848.

13. Sharma, D., Merchant, C., Oma, P., King, D., and Thomas, D., 2011, Analysis of subvisible particles in protein therapeutics using Micro-flow Imaging. Abstracts of Papers, 241st ACS National Meeting & Exposition, Anaheim, CA, United States, March 27-31, 2011 , BIOT-353.

14. Sharma,D.K., Oma,P., Krishnan,S., 2009. Silicone microdroplets in protein formulations. Detection and enumeration. Pharm. Technol., 33, 74-76, 78.

15. Sharma, D.K., Oma, P., Pollo, M.J., and Sukumar, M., 2010, Quantification and characterization of subvisible proteinaceous particles in opalescent mAb Formulations Using Micro-Flow Imaging. J.Pharm.Sci. 99[6], 2628-2642.

16. Shire,S.J., Shahrokh,Z., Liu,J., 2004. Challenges in the development of high protein concentration formulations. J Pharm. Sci., 93, 1390-1402.

17. Strehl,R., Rombach-Riegraf,V., Diez,M., Egodage,K., Bluemel,M., Jeschke,M., Koulov,A.V., 2011. Discrimination Between Silicone Oil Droplets and Protein Aggregates in Biopharmaceuticals: A Novel Multiparametric Image Filter for Sub-visible Particles in Microflow Imaging Analysis. Pharm. Res., 29, 594-602.

18. Zhu,X., Fan,H., Li,D., Xiao,Y., Zhang,X., 2007. Protein adsorption and zeta potentials of a biphasic calcium phosphate ceramic under various conditions. J Biomed. Mater. Res. B Appl. Biomater., 82, 65-73.

6. Comparison of TopLyo® (Schott) Vials with Standard Glass Type I Vials concerning repression or enhancement of particle formation

6.1 Introduction

During protein formulation finding the most adequate packaging material is a challenging task. As proteins are prone to aggregation, primary packaging material should not be enhancing unfolding or adsorption and accompanying aggregation.
Recently TopLyo® vials have been developed. TopLyo® vials have a hydrophobic coating on the inside surface. The hydrophobic surface is coated using the Plasma Impulse Chemical Vapor Deposition (PICVD) technique (figure 1). TopLyo® vials are proposed to optimize efficiency of lyophilization processes. Due to their homogenous hydrophobic surfaces and optimized geometry adhesion of substances and interactions of substances with vials is minimized. The cake after lyophilization should be prevented from collapsing and the residual volume is then almost completely reduced.

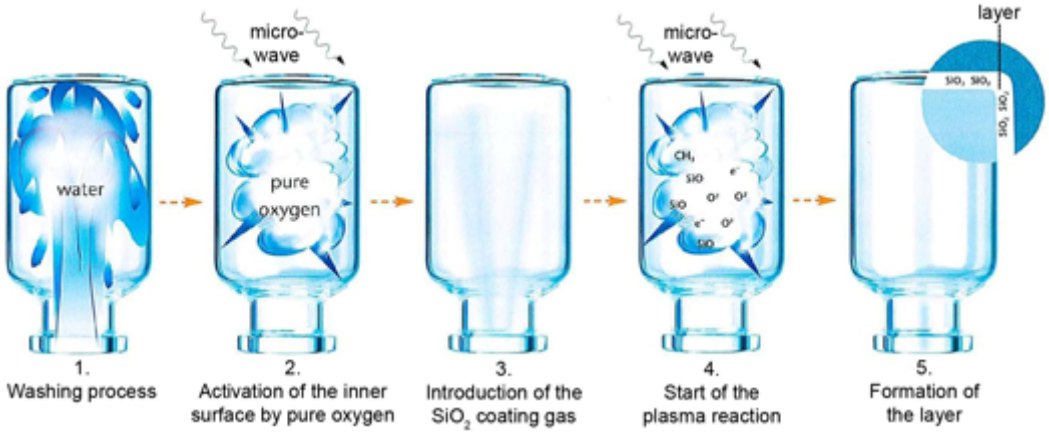

Fig. 1: PICVD Coating process, developed and patented by Schott

The main focus of this study lies on the evaluation of particulate matter and its connection to protein adsorption onto surfaces in TopLyo® vials after freeze-drying.
On the one hand, highly chemically resistant coatings are reported to offer a benefit with regards to subvisible particle formation [Iacocca et al., 2010].

On the other hand, hydrophobically coated TopLyo® vials theoretically make the proteins unfold more easily than uncoated glass vials. Freeze-drying partly removes the hydration layer of dried proteins and therefore disturbs protein's native state [Mukherjee et al., 2009]. During freeze-drying non-covalent and covalent aggregates can be formed, which can be inhibited with stabilizers like sugars [Crowe et al., 1990; Wang et al., 2010]. During freezing non-freezable water is not removed, whereas drying very well removes this water, which results in changes of physical properties. Unfolding can be a consequence of e.g. temperature, pH change, or interfacial adsorption, resulting in aggregation [Bhatnagar et al., 2007; Chang et al., 1996; Gomez et al., 2001; Strambini et al., 1996]. Unfolded proteins can further aggregate [Manning et al., 1989; Manning et al., 2010; Wang et al., 2007; Wang et al., 2010] or adsorb to vial surfaces [Johnston, 1996; Wu et al., 1989]. In order to reduce the loss of protein upon adsorption, addition of polysorbates is reported [Kueltzo et al., 2008; Mahler et al., 2005; Mahler et al., 2008; Wang et al., 2008].

The authors wanted to evaluate whether TopLyo® vials prevent or might even promote formation of particles during the lyophilization process. In a first approach a therapeutical protein (IgG_1-α) and its respective placebo were filled into TopLyo® vials and standard glass type I vials. The protein was freeze-dried, and particle counts in the reconstituted solutions were taken afterwards.

6.2 Sample preparation and experimental setup

IgG_1-α solution in histidine buffer (5 mg/ml) at pH 6.0 was filtered through a 0.2 µm Millex syringe-driven filter unit (Millipore, Carrigtwohill, Ireland) into a particle free beaker and filled into particle free vials.

3 ml protein solution was filled into TopLyo® vials and classic glass type I 5 ml vials (both Schott, St. Gallen, Switzerland), respective placebo solution was also filled in both vial types.

20 TopLyo® and 20 classic glass vials were freeze-dried; two vials of both types were filled with placebo solution and were also freeze-dried. Untreated protein-formulation (references) was kept in both vials and stored at 2-8°C; the freeze-drying process was controlled using sensors in additional vials filled with protein solutions.

After freeze-drying Karl-Fisher titrations and DSC measurements were performed (n = 3) to determine residual moisture and glass transition temperature of the samples.

Particle counts were taken from freeze-thawed and freeze-dried samples and references using LO and MFI.

Further, zeta potential titrations of the IgG_1-α in 10 mM histidine buffer at pH 6.0 were performed, as well as protein adsorption studies. Protein adsorption studies were performed using the freeze-thawed samples and references. Adsorbed protein was desorbed using 0.05% SDS in PBS buffer at pH 7.2. The exact amount of desorbed protein was calculated using a 6-point calibration (0.0001-0.01 mg/ml) after SE-HPLC performance. The desorbed amount of protein was calculated related to the surface of respective vial [mg/m^2].

6.3 Results and discussion

6.3.1 Physicochemical properties of lyophilizates

Table 1 shows the residual water [%] and glass transition temperature [Duddu et al., 1997] of the protein. It is obvious that IgG_1-α and its placebo formulations do not show significant differences in both vial types.

Table 1: Physicochemical properties of lyophilizates

Protein-vial-combination	Residual moisture ± SD (%)[a]	Tg ± SD (%)[b]
Placebo TopLyo®	1.25 ± 0.17	38,3 ± 1,5
IgG_1-α TopLyo®	1.25 ± 0.18	38,5 ± 1,9
Placebo standard glass	1.12 ± 0.13	39,7 ± 10,2
IgG_1-α standard glass	1.58 ± 0.14	47,4 ± 8,05

[a]Determined by Karl Fischer titration, n = 3
[b]Determined by DSC, n = 3

6.3.2 Particle counting after freeze-drying IgG_1-α

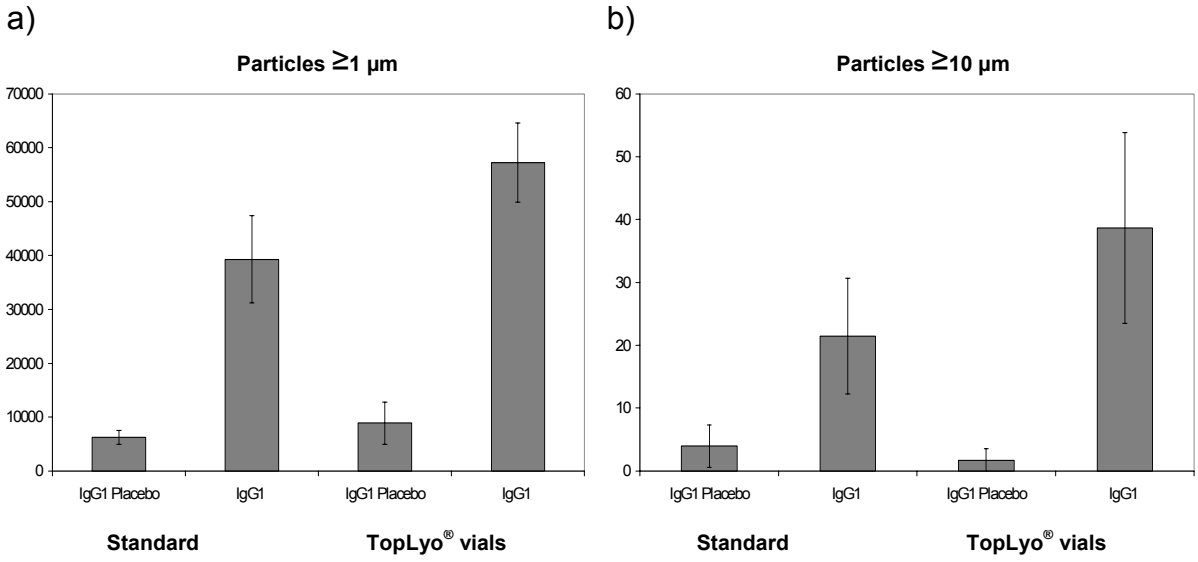

Fig. 2: Particle counting of PAMAS for a) particles ≥1 µm/ml and b) particles ≥10 µm after freeze-drying IgG_1-α: Comparing standard vials with TopLyo® vials

Particle counting using LO revealed that freeze-drying is a strong stress factor for IgG_1-α with regards to particle formation. Indeed, it was elaborated earlier that antibodies can be unstable during lyophilization [Hagiwara et al., 2000].

Measurements of untreated IgG_1-α reference showed less than 1000 particles ≥1 µm/ml (data not shown), whereas even freeze-dried placebo solutions contained more particles after freeze-drying than IgG_1-α reference; particles can be contaminants from freeze-drying chamber or caused by glass corrosion or delamination of glass.

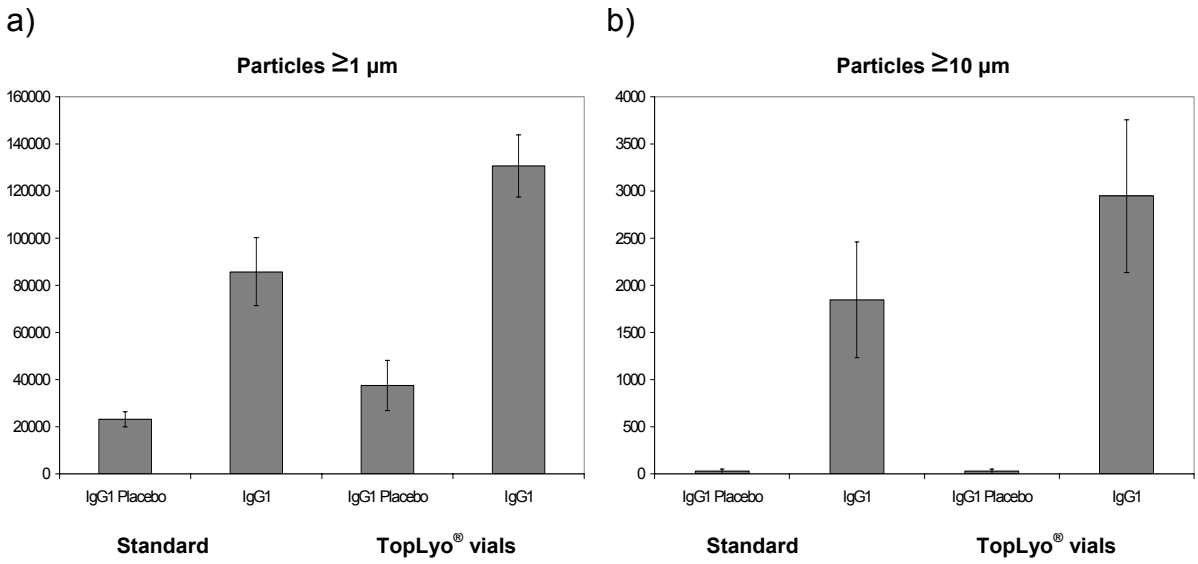

Fig. 3: Particle counting of MFI for a) particles ≥1 µm/ml and b) particles ≥10 µm/ml after freeze-drying IgG_1-α: Comparing standard vials with TopLyo® vials

MFI measurements showed same trend as LO measurement. Counts of particles ≥10 µm again did not show differences between the two compared vials, whereas particle counts of particles ≥1 µm emphasized that TopLyo® vials are not the best choice for preventing IgG_1-α-formulation from particle formation during freeze-drying.

Concluding, particles ≥10 µm did not show any differences between TopLyo® vials and standard vials. MFI and LO delivered comparable results. More particles ≥1 µm were found in TopLyo® vials than in glass type I vials.
Overall, standard glass type I vials are more adequate for freeze-drying IgG_1-α than TopLyo® vials, which have more hydrophobic surfaces. Proteins can be unstable during freeze-drying and can unfold [Wang, 1999]. Unfolding results in presenting normally buried hydrophobic surfaces to the outside [Chi et al., 2003] and might lead to adsorption of IgG_1-α-solution onto TopLyo® vial surfaces during freeze-drying.

6.3.3 Zeta potential

Zeta potential (ZP) measurements of proteins and vials deliver information about net charge at formulation pH [Jachimska et al., 2008; Lehermayr et al., 2011].

We found that IgG_1-α, formulated at pH 6.0, is more prone to aggregation during freeze-thawing in TopLyo® vials than in classic glass type I vials.

ZP measurements of IgG_1-α were not feasible in formulation used for freeze-thawing studies due to high ionic strength. Therefore, the IgG_1-α formulation buffer was exchanged into 10 mM histidine buffer at pH 6.0. The pH titration (figure 4) delivers information about the isoelectric point with a zeta potential of 0 mV at pH 8.81. At formulation pH 6.0 zeta potential is +14.5 mV.

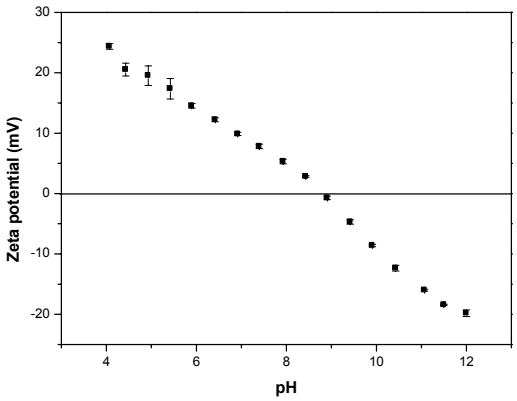

Fig. 4: Zeta potential titration of IgG_1-α

6.3.4 Desorption of protein

We were interested to find a further rationale to elucidate the larger amount of particles formed during freeze-drying the IgG_1-α-formulation in TopLyo® vials.

Adsorption of proteins on solid surfaces like glass vials is dependent from surface qualities like hydrophilicity and electrical state [Haynes et al., 1994]. It is described in literature that most protein adsorption is by non-specific binding, except at hydrophilic surfaces [Milthorpe, 2005].

Desorption of proteins adsorbed to vial surfaces delivers further information. This method carefully and qualitatively determines the amount of protein that is adsorbed to the inner vial surfaces during incubation time. The incubation time for freeze-dried samples is as long as the freeze-drying and reconstitution processes take. The references are kept in liquid state at 2-8°C. To equalize the glass contact of untreated references and freeze-dried samples, desorption of protein in references

was determined as soon as samples in lyophilisation chamber were frozen. Protein solutions were carefully removed from the vials.

Protein desorption from vial surfaces is accomplished with SDS in PBS buffer at pH 7.2. SDS as a surfactant preserves proteins from adsorption to surfaces [Mizutani et al., 1978] and hence increases sample stability [Mizutani, 1980]. Further, SDS in running buffers leads to better resolution and increased accuracy, which is important in terms of analyzing very small desorbed amounts of proteins [Welling-Wester et al., 1988]. Most importantly for these experiments, SDS at concentrations above critical micelle concentration (CMC) [Froeberg et al., 1999; Santos et al., 2011] has a strong eluting force for proteins on glass [Mizutani, 1980]. CMC of surfactants decrease with increasing ionic strengths, therefore reported results are consistent: The CMC of SDS in water was reported to be at 8.08 mM (with M_{SDS} = 288.4 g/mol the resulting concentration is 0.23%) [Fuguet et al., 2005]; the CMC in PBS buffer at pH 7.2 and 25 °C was earlier found [Mathes, 2010] at 0.94 mM (0.027%). To quantitatively desorb the protein from vial surfaces, a SDS concentration above CMC of 0.05 % was chosen for experiments.

The desorbed protein amounts were calculated via Size-Exclusion Chromatography (SEC) with fluorescence detector using a 6-point calibration. Calculations were performed using ChemStation. 6-point calibrations from 0.0001-0.01 mg/ml for each protein were performed to calculate the exact amount of desorbed protein. Desorption amounts were related to adsorption surfaces of respective vials [mg/m²], listed in table 2. The adsorption surface is the contact surface from glass and IgG_1-α solution.

In table 2 both vial types can easily be compared directly with each other as the respective pairs are listed together.

The desorbed amount of IgG_1-α proved to be significantly less from standard glass vial surfaces than from TopLyo® vial surfaces. Obviously, a larger protein amount adsorbed to TopLyo® vials with hydrophobic surfaces. This could have led to the formation of a larger amount of protein aggregates than in classic glass type I vials. It is already reported in literature [Bee et al., 2011] that adsorption to interfaces can cause protein aggregation.

Proteins exist in equilibrium state of folded and unfolded protein molecules [Wang et al., 2010]. The unfolded molecules can present their lipophilic residues, which are buried during folded state, to the outer face. The lipophilic residues then can adsorb

to surfaces, shifting the equilibrium towards unfolded molecules. The more hydrophobic the surfaces are the more likely unfolded protein molecules can adsorb. During freeze-drying proteins might be detached from those surfaces due to e.g. pH-shifts [Norde et al., 1986]. The unfolded proteins then can form aggregates with each other [Brange, 2000]. Understandably, a high adsorption amount can lead to a higher amount of protein aggregates.

Interestingly, larger protein amounts has been desorbed from reference TopLyo® vials than from freeze-dried sample in TopLyo® vials. Obviously, during freeze-drying the protein has been detached from vial surfaces, although proteins can adsorb irreversibly and in a native state [Hoehne et al., 2010]. The detached and possibly unfolded [Chi et al., 2003] protein could easily form aggregates. In classic glass type I vials the amount of desorbed protein in reference and in freeze-dried samples is equal (~4.8 mg/m^2). This points to the fact that during freeze-drying the adsorbed protein is not detached from classic glass type I vials and therefore does not from as much aggregates as found after freeze-drying in TopLyo® vials.

Table 2: Desorption of proteins from vial surfaces (n=3)

			Desorption [mg/m²]	Standard-deviation
IgG_1-α	**TopLyo®**	**reference**	**8,420**	**0,551**
IgG_1-α	Standard glass	reference	4,825	0,310
IgG_1-α	**TopLyo®**	**freeze-dried**	**7,118**	**0,840**
IgG_1-α	Standard glass	freeze-dried	4,879	0,487

6.4 Conclusion

This study aimed to assess the hydrophobically coated TopLyo® vials with regard to formation of particulate matter during freeze-drying of one model protein. TopLyo® vials were compared with classic glass type I vials.

In hydrophobically coated TopLyo® vials the particle counts for all particle size classes were significantly higher than in standard glass type I vials.

It was found that particle formation during freeze-drying strongly depends on the amount of proteins adsorbed to vial surfaces. In general, low adsorption/desorption of protein to vial surfaces lead to less particle formation during freeze-drying.

6.5 Reference List

1. Bee,J.S., Randolph,T.W., Carpenter,J.F., Bishop,S.M., Dimitrova,M.N., 2011. Effects of surfaces and leachables on the stability of biopharmaceuticals. J Pharm. Sci., 100, 4158-4170.

2. Bhatnagar,B.S., Bogner,R.H., Pikal,M.J., 2007. Protein stability during freezing: separation of stresses and mechanisms of protein stabilization. Pharm. Dev. Technol., 12, 505-523.

3. Brange,J., 2000. Physical Stability of Proteins. In: Frokjaer,S., Hovgaard,L. (Eds.), Taylor & Francis, London, 89-112.

4. Chang,B.S., Kendrick,B.S., Carpenter,J.F., 1996. Surface-induced denaturation of proteins during freezing and its inhibition by surfactants. J Pharm. Sci., 85, 1325-1330.

5. Chi,E.Y., Krishnan,S., Randolph,T.W., Carpenter,J.F., 2003. Physical stability of proteins in aqueous solution: mechanism and driving forces in nonnative protein aggregation. Pharm. Res., 20, 1325-1336.

6. Crowe,J.H., Carpenter,J.F., Crowe,L.M., Anchordoguy,T.J., 1990. Are freezing and dehydration similar stress vectors? A comparison of modes of interaction of stabilizing solutes with biomolecules. Cryobiology, 27, 219-231.

7. Duddu,S.P., Dal Monte,P.R., 1997. Effect of glass transition temperature on the stability of lyophilized formulations containing a chimeric therapeutic monoclonal antibody. Pharm. Res., 14, 591-595.

8. Froeberg,J.C., Blomberg,E., Claesson,P.M., 1999. Desorption of Lysozyme Layers by Sodium Dodecyl Sulfate Studied with the Surface Force Technique. Langmuir, 15, 1410-1417.

9. Fuguet, E., Rafols, C., Roses, M., and Bosch, E., 2005, Critical micelle concentration of surfactants in aqueous buffered and unbuffered systems. Anal.Chim.Acta 548[1-2], 95-100.

10. Gomez,G., Pikal,M.J., Rodriguez-Hornedo,N., 2001. Effect of initial buffer composition on pH changes during far-from-equilibrium freezing of sodium phosphate buffer solutions. Pharm. Res., 18, 90-97.

11. Hagiwara, H., Yuasa H., and Yamamoto, Y., 2000, Stabilized human monoclonal antibody preparation. [US6165467].

12. Haynes,C.A., Norde,W., 1994. Globular proteins at solid/liquid interfaces. Colloids and Surfaces B: Biointerfaces, 2, 517-566.

13. Hoehne,M., Samuel,F., Dong,A., Wurth,C., Mahler,H.C., Carpenter,J.F., Randolph,T.W., 2010. Adsorption of monoclonal antibodies to glass microparticles. J Pharm. Sci., 100, 123-132.

14. Iacocca,R.G., Toltl,N., Allgeier,M., Bustard,B., Dong,X., Foubert,M., Hofer,J., Peoples,S., Shelbourn,T., 2010. Factors affecting the chemical durability of glass used in the pharmaceutical industry. AAPS. PharmSciTech., 11, 1340-1349.

15. Jachimska,B., Wasilewska,M., Adamczyk,Z., 2008. Characterization of globular protein solutions by dynamic light scattering, electrophoretic mobility, and viscosity measurements. Langmuir, 24, 6866-6872.

16. Johnston,T.P., 1996. Adsorption of recombinant human granulocyte colony stimulating factor (rhG-CSF) to polyvinyl chloride, polypropylene, and glass: effect of solvent additives. PDA. J Pharm. Sci. Technol., 50, 238-245.

17. Kueltzo,L.A., Wang,W., Randolph,T.W., Carpenter,J.F., 2008. Effects of solution conditions, processing parameters, and container materials on aggregation of a monoclonal antibody during freeze-thawing. J Pharm. Sci., 97, 1801-1812.

18. Lehermayr,C., Mahler,H.C., Mader,K., Fischer,S., 2011. Assessment of net charge and protein-protein interactions of different monoclonal antibodies. J Pharm. Sci., 100, 2551-2562.

19. Mahler,H.C., Friess,W., Grauschopf,U., Kiese,S., 2008. Protein aggregation: Pathways, induction factors and analysis. J Pharm. Sci., 98, 2909-2934.

20. Mahler,H.C., Muller,R., Friess,W., Delille,A., Matheus,S., 2005. Induction and analysis of aggregates in a liquid IgG1-antibody formulation. Eur. J Pharm. Biopharm., 59, 407-417.

21. Manning,M.C., Chou,D.K., Murphy,B.M., Payne,R.W., Katayama,D.S., 2010. Stability of protein pharmaceuticals: an update. Pharm. Res., 27, 544-575.

22. Manning,M.C., Patel,K., Borchardt,R.T., 1989. Stability of protein pharmaceuticals. Pharm. Res., 6, 903-918.

23. Mathes, J.M., 2010, Protein Adsorption to Vial Surfaces - Quantification, Structural and Mechanistic Studies. Department of Pharmacy, LMU Munich, [PhD].

24. Milthorpe, B., 2005, Protein Adsorption to Surfaces and Interfaces. Surfaces and Interfaces for Biomaterials , 763-781.

25. Mizutani,T., 1980. Decreased activity of proteins adsorbed onto glass surfaces with porous glass as a reference. J Pharm. Sci., 69, 279-282.

26. Mizutani, T. and Mizutani, A., 1978, Adsorption of a protein on glass surfaces in detergent solutions. J.Non-Cryst.Solids 27[3], 437-439.

27. Mukherjee,S., Chowdhury,P., Gai,F., 2009. Effect of dehydration on the aggregation kinetics of two amyloid peptides. J Phys. Chem. B, 113, 531-535.

28. Norde,W., MacRitchie,F., Nowicka,G., Lyklema,J., 1986. Protein adsorption at solid-liquid interfaces: Reversibility and conformation aspects. Journal of Colloid and Interface Science, 112, 447-456.

29. Santos,O., Svendsen,I.E., Lindh,L., Arnebrant,T., 2011. Adsorption of HSA, IgG and laminin-1 on model titania surfaces--effects of glow discharge treatment on competitively adsorbed film composition. Biofouling., 27, 1003-1015.

30. Strambini,G.B., Gabellieri,E., 1996. Proteins in frozen solutions: evidence of ice-induced partial unfolding. Biophys. J, 70, 971-976.

31. Wang,W., 1999. Instability, stabilization, and formulation of liquid protein pharmaceuticals. Int. J Pharm., 185, 129-188.

32. Wang,W., Nema,S., Teagarden,D., 2010. Protein aggregation--pathways and influencing factors. Int. J Pharm., 390, 89-99.

33. Wang,W., Singh,S., Zeng,D.L., King,K., Nema,S., 2007. Antibody structure, instability, and formulation. J Pharm. Sci., 96, 1-26.

34. Wang,W., Wang,Y.J., Wang,D.Q., 2008. Dual effects of Tween 80 on protein stability. International Journal of Pharmaceutics, 347, 31-38.

35. Welling-Wester,S., Kazemier,B., Orvell,C., Welling,G.W., 1988. Effect of detergents on the structure of integral membrane proteins of Sendai virus studied with size-exclusion high-performance liquid chromatography and monoclonal antibodies. J Chromatogr., 443, 255-266.

36. Wu,C.S., Chen,G.C., 1989. Adsorption of proteins onto glass surfaces and its effect on the intensity of circular dichroism spectra. Anal. Biochem, 177, 178-182.

7. Simulation of Stir Stress and Prediction of Resulting Particle Formation in IgG_1-Solutions

7.1 Introduction

Due to the presumed correlation of immunogenicity and aggregation of protein pharmaceuticals [Patten et al., 2003; Rosenberg, 2006; Schellekens, 2003; Schellekens, 2005] the evaluation of protein aggregation and resulting particle formation is becoming a more and more important factor for quality of protein drug products [Carpenter et al., 2008; Wang, 2005]. In this thesis, it was evaluated whether aggregation and particle formation resulting from stir stress can be described and predicted by fitting data to a theoretical model and how such prediction could be used for process upscaling.

One typical stress factor for biopharmaceuticals during manufacturing, storage and handling is mechanical stress like occurring during stirring [Kiese et al., 2008]. Stirring speed is a classic set parameter for mixing larger volumes of protein solutions and adjusting this parameter is a typical issue during upscaling in the course towards commercial production.

Applying computational fluid dynamics [Sundström et al., 2010] stirring processes can be simulated and the stress produced by stirring can be quantified. Stress can be quantitatively expressed as “stress tensor” [Pa] in the liquid phase. The determination of a correlation between particle formation and stress tensor values was of high interest. In a further step, it was investigated whether prediction of particle formation during upscaling processes is possible. Former approaches to predict aggregation rates and shelf life mainly concentrated on conformational and colloidal stabilities or accelerated stability studies [Roberts et al., 2003; Weiss et al., 2009] or spectroscopic and calorimetric methods [Youssef, 2010].

Stirring at six different stirring speeds (150 rpm, 200 rpm, 300 rpm, 400 rpm, 500 rpm, and 600 rpm) was performed in three different sized containers (5 ml, 100 ml, and 500 ml) and particle counts were determined using light obscuration. In parallel, stress simulations were performed using a computational fluid dynamic simulations software STAR-CCM+; CD Adapco, Nürnberg, Germany.

7.2 Experimental setup

Stress simulations were performed at 150 rpm, 200 rpm, 300 rpm, 400 rpm, 500 rpm, and 600 rpm using STAR-CCM+software (CD Adapco, Nürnberg, Germany) in 5 ml, 100 ml, 500 ml, and 5000 ml glass bottles. Container and stirrer bar dimensions, density and viscosity of IgG_1-formulation (table 1) are needed besides stirring speed to accomplish simulations. Computational fluid dynamic simulations were carried out in STAR-CCM+ software to gain knowledge of the dependence of the stress distributions in the liquid phase to the rational velocity. Minimal, maximal and averaged stress tensor magnitudes were extracted from simulations.

Table 1: Density and viscosity of liquid and gas phase

Liquid phase: IgG_1-formulation	
Density	1.0224 g/cm^3
Viscosity	1.2017 mPas
Gas phase: Air	
Density	$1.184 * 10^{-3}$ g/cm^3
Viscosity	0.01855 mPas

Stirring experiments were performed in different containers (5 ml, 100 ml, and 500 ml glass bottles) at 150 rpm, 200 rpm, 300 rpm, 400 rpm, 500 rpm, and 600 rpm (each n = 3). One experiment was performed in a 5000 ml glass bottle at 400 rpm (n = 1). Particle counts for different particle size classes (e.g. ≥1 µm and ≥10 µm) were determined using classical light obscuration (LO).

Filling volumes of glass bottles were as follows: 5 ml (filled with 5 ml protein solution), 100 ml (filled with 40 ml), 500 ml (filled with 200 ml), and 5000 ml (filled with 2000 ml). The magnitudes of the stress tensors from simulations and particle counts from laboratory experiments were plotted to find correlations between experimental and simulated values.

7.3 Results and discussion

7.3.1 Situation for particles ≥1 µm

In a first approach IgG_1-solution in histidine buffer (5 mg/ml) at pH 6.0 was stirred at different stirring speeds in 5 ml vials and particle counts were taken afterwards. In parallel, applied stress on the IgG_1-formulation during the stirring experiments was simulated by Computational Fluid Dynamics (CFD) and stress tensor magnitudes (minimal, maximal and averaged) were extracted. For this purpose, a virtual mesh is built and laid over vial dimensions and the stress tensor is calculated for each cuboid. The minimal and maximal stress tensors are easily extracted; the averaged stress tensor is calculated by the software relating to the total volume of the cuboids.

A quasi-linear correlation between averaged stress tensor and stirring speed could be detected (figure 1, continuous line). Additionally, particle counts for particles ≥1 µm correlated linearly with averaged stress tensors (figure 2, continuous line).

As no linear dependencies of particle formation and minimal or maximal stress tensor were found (data not shown), we concentrated on averaged stress tensor for further correlations.

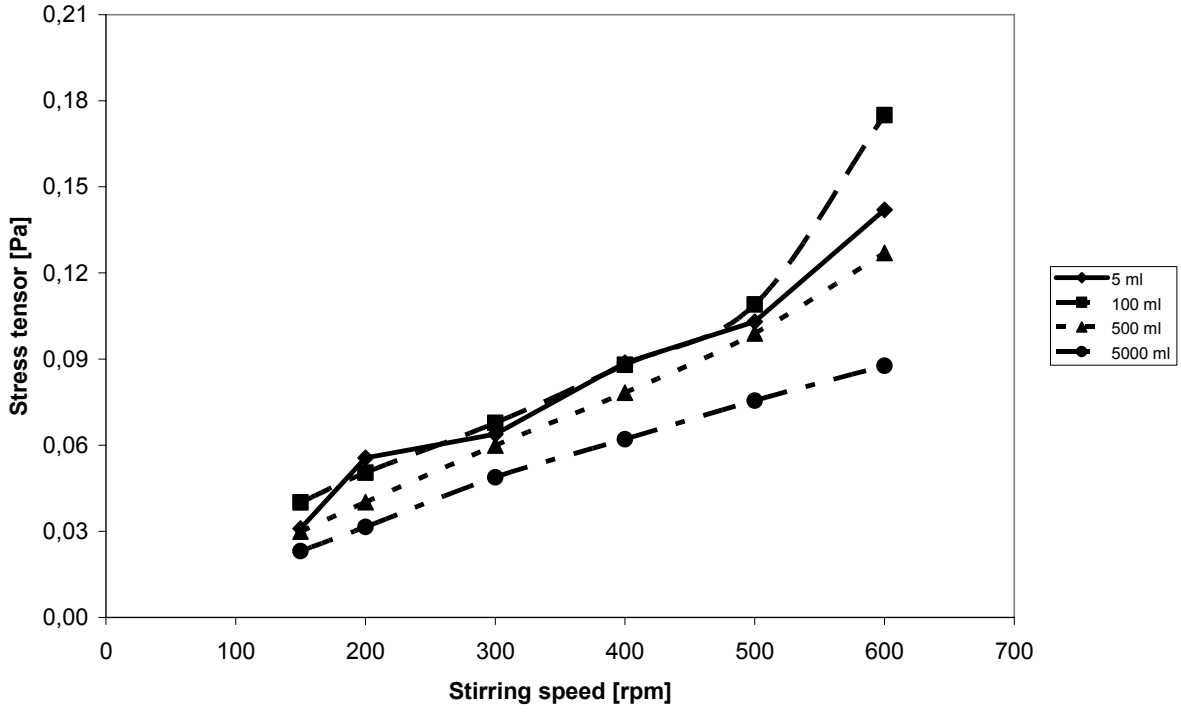

Fig. 1: Averaged stress tensor [Pa] extracted from stirring simulations in different containers over stirring speed

We were interested whether the averaged stress tensor during stirring would be predictable for upscaling. IgG_1-solution was stirred at different stirring speeds in 100 ml and 500 ml glass containers and applied stress during stirring on the IgG_1-solution was simulated using CFD; stress tensor magnitudes [Pa] were extracted. Linear correlations of averaged stress tensor and stirring speed were found (figure 1, dotted and dashed lines). The averaged stress tensor is linearly and almost congruently increasing over increasing stirring speed, independent of container size. This leads to the conclusion that the applied stress is similar at the same stirring speed in all tested containers.

To find out whether also particle formation during stirring would be predictable for upscaling, stirring experiments were performed; particle counts were taken and correlated with averaged stress tensor magnitude. Experiments resulted in linear increases of particle counts for particles ≥1 µm over averaged stress tensor in all container sizes (figure 2). However, the slopes are not parallel, the same stress tensor did not result in the same particle count. Particle numbers are larger in smaller containers and filling volumes after stirring.

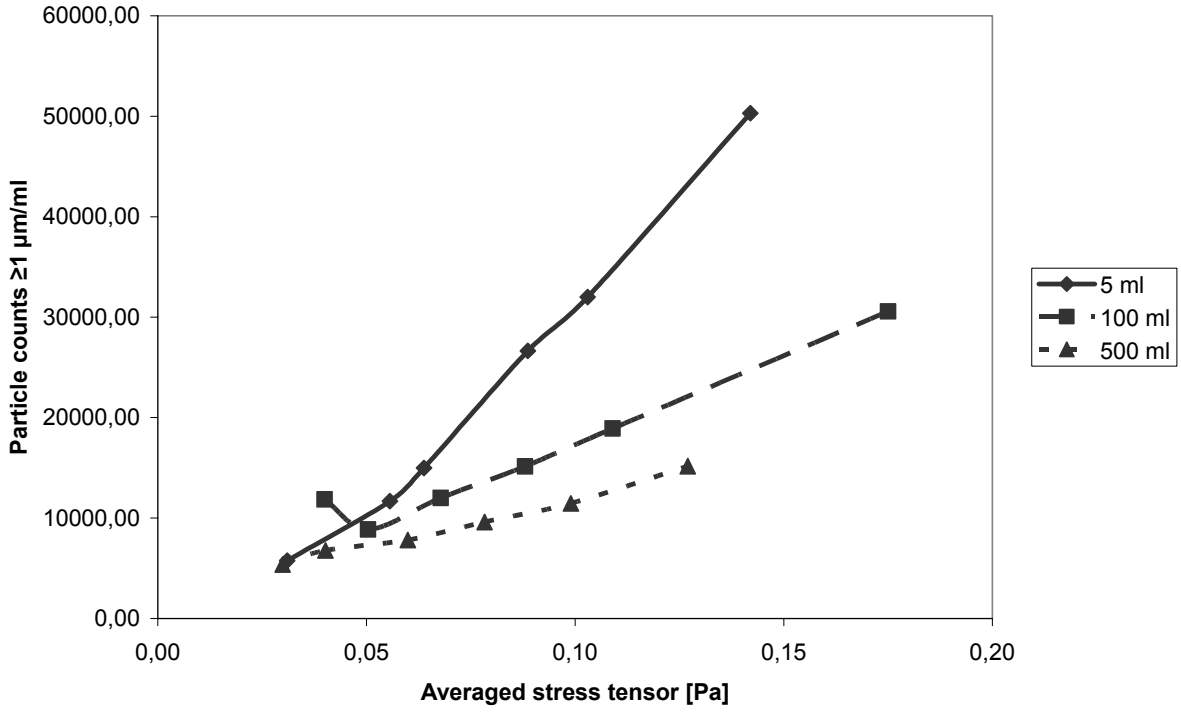

Fig. 2: Particles ≥1 µm found in different bottle sizes at different quantities of stress: linear increase of particle formation over increasing stir stress

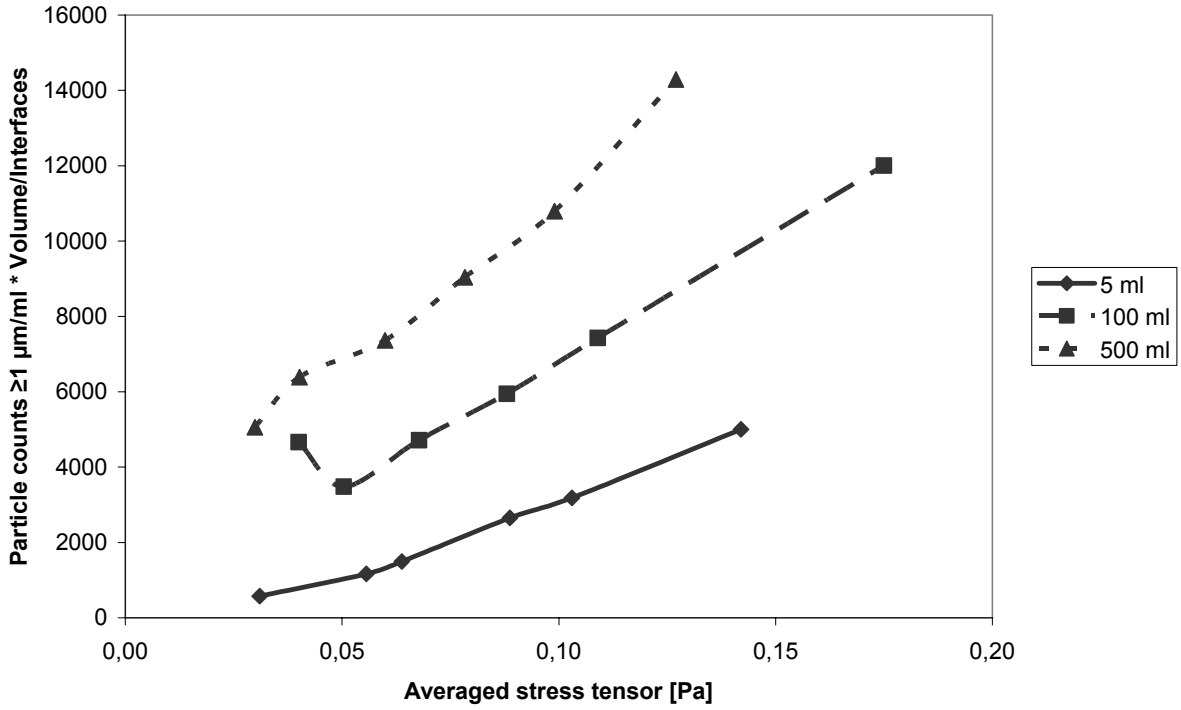

Fig. 3: Particle count found in different bottle sizes at different quantities of stress after including the factor of volumes and air-/ glass-interfaces with samples (equation 3): linearity and parallelism

The fact that fewer particles are formed in larger container sizes during stirring might be due to smaller surface exposure of IgG_1-molecules to container surfaces and water and air surfaces (equation 1) [Bee et al., 2009; Bee et al., 2010; Chang et al., 1996; Maa et al., 1997]. The larger the container, the smaller the surfaces compared to the containing volume.

$$surfaces = 2 * \pi * r(h + r) \quad \textbf{Equation 1}$$

$$volume = \pi * r^2 * h \quad \textbf{Equation 2}$$

$$f = \frac{\pi * r^2 * h}{2 * \pi * r(h + r)} * p \quad \textbf{Equation 3,}$$

whereas p = particle counts for particles >1 µm

It is plausible that a smaller container surface leads to less adsorption [Baszkin et al., 2001; Chang et al., 2005] and particle formation. Considering total filling volume and respective interfaces with container walls and air, particle generation and stress tensor correlate with the same slope for all three container sizes (figure 3 and equation 3).

When applying the STAR CCM+ software information about filling volume and vessel dimensions are requested. However, obviously STAR CCM+ is not adequately accounting for ratio of filling volume and interfaces. Particle counts are resulting from many factors, including ratio of filling volume and interfaces. And considering this factor, graphs are found to be nearly parallel (figure 3). The fact that the graphs are shifted parallel indicates that there is another factor influencing particle formation. On the one hand, the particle formation of particles ≥1 µm is controlled by the stirring speed, on the other hand the particle formation is influenced by the particle degradation of larger particles into smaller ones (see 7.3.2).

7.3.2 Situation for particles ≥10 µm

Interestingly, in contrast to the situation for smaller particles (≥1 µm), formation of particles ≥10 µm decreased with increasing stirring speed (figure 4).

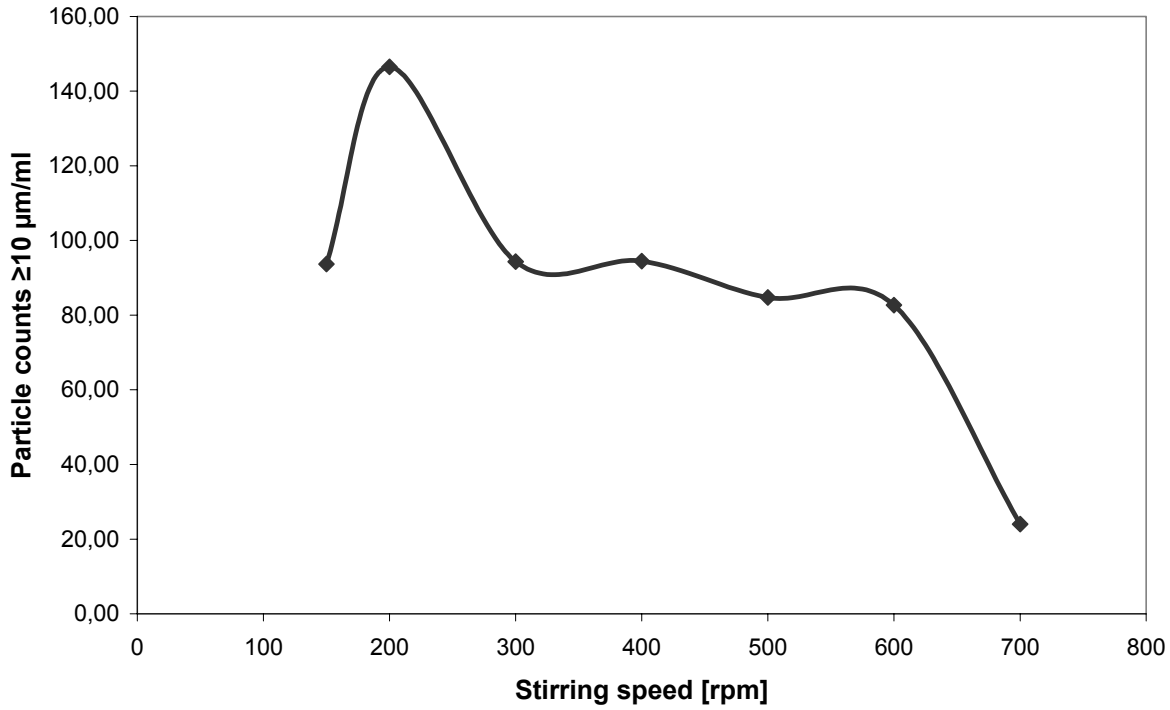

Fig. 4: Number of particles ≥10 µm decrease over increasing stirring speed; example 5 ml vials

To investigate if larger particles would be reduced in size by stirring with increasing speed, a different experimental approach was applied. Particles ≥10 µm were generated by applying freeze-thaw stress to the IgG_1-solution [Hawe et al., 2009]. Afterwards samples were stirred using different stirring speeds. The particle number after stirring was inversely correlated to stirring speed (figure 5).

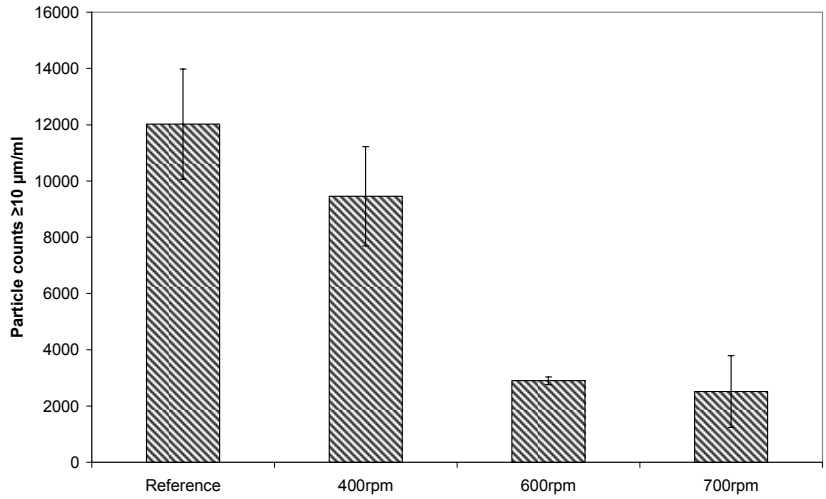

Fig. 5: IgG1 particles ≥10 µm were generated by freeze-thaw stress and reduced by stir stress

Obviously, stirring stress can reduce the number of larger particles when they were generated by freeze-thawing.

A model assuming a linear or exponential steady relation between particle number and stress tensor is valid for small particles (≥1 µm) but not for larger particles where the situation is more complex.

7.3.3 Upscaling experiment

Due to shortage of protein material only one further upscaling laboratory experiment in the 5000 ml bottle was performed at 400 rpm, whereas simulations of stir stress in the 5000 ml bottle were performed using CFD at all stirring speeds (150 rpm, 200 rpm, 300 rpm, 400 rpm, 500 rpm, and 600 rpm).

Simulating the stir stress in 5000 ml bottle with 2000 ml filling volume resulted in smaller stress tensor values as found for smaller containers at same stirring speeds (figure 1). Still, linear dependencies were found for stirring speed and averaged stress tensor. However, simulations showed that stress caused by stirring is less in 5000 ml bottle (figure 1, dashed-dotted line): Obviously, average Stress Tensor Magnitude is slightly decreasing over increasing bottle size.

The stir stress simulations revealed an average stress tensor of 0.0621 Pa during stirring 2000 ml IgG_1-solution at 400 rpm in a 5000 ml bottle (figure 1).

To prove the theory, that particle formation at same stirring speed is reduced in larger containers, not more than 8000 particles ≥1 µm/ml should be found for 0.0621 Pa stir stress in the laboratory experiment (compare figure 2). However, 15000 particles ≥1 µm/ml were found. With this experiment a correlation between stress tensor and

particle count could not be proven. However, we only performed one experiment (n = 1) at one stirring speed.

7.4 Conclusion

Simulations of stir stress in lab scale sized containers (5 ml, 100 ml, and 500 ml) provided almost same dependencies of averaged stress tensor and stirring speed (figure 3). Further, particle formation for particles ≥1 µm was found to increase linearly over increasing stirring speed/stress and decrease with increasing vessel size due to larger volume/surface ratios (figure 4).

Summarizing, particle formation of particles ≥1 µm is linearly dependent to stress tensor magnitudes, whereas for larger particles ≥10 µm the situation is more complex. Nucleation and particle generation and consecutive particle growth run in parallel with particle degradation of larger particles during stirring.

Prediction of particle formation for lab scale experiments is possible; however, relevant and interesting prediction of particle formation during upscaling into larger containers is not possible with the applied model software STAR CCM+. Vessel and stirrer bar sizes are requested when performing stir simulations, however, volume/surface ratios are not adequately taken into account and particle formation is definitely influenced by exposure to surfaces.

STAR CCM+ simulation software is not adapted for protein solutions as physicochemical properties of proteins are not considered [Caflisch, 2006].

7.5 Reference List

1. Baszkin,A., Boissonnade,M.M., Kamyshny,A., Magdassi,S., 2001. Native and Hydrophobically Modified Human Immunoglobulin G at the Air/Water Interface. J Colloid Interface Sci., 239, 1-9.

2. Bee,J.S., Chiu,D., Sawicki,S., Stevenson,J.L., Chatterjee,K., Freund,E., Carpenter,J.F., Randolph,T.W., 2009. Monoclonal antibody interactions with micro- and nanoparticles: adsorption, aggregation, and accelerated stress studies. J Pharm. Sci., 98, 3218-3238.

3. Bee,J.S., Davis,M., Freund,E., Carpenter,J.F., Randolph,T.W., 2010. Aggregation of a monoclonal antibody induced by adsorption to stainless steel. Biotechnol. Bioeng., 105, 121-129.

4. Caflisch,A., 2006. Computational models for the prediction of polypeptide aggregation propensity. Curr. Opin. Chem. Biol., 10, 437-444.

5. Carpenter,J.F., Randolph,T.W., Jiskoot,W., Crommelin,D.J., Middaugh,C.R., Winter,G., Fan,Y.X., Kirshner,S., Verthelyi,D., Kozlowski,S., Clouse,K.A., Swann,P.G., Rosenberg,A., Cherney,B., 2008. Overlooking subvisible particles in therapeutic protein products: Gaps that may compromise product quality. J Pharm. Sci., 98, 1-5.

6. Chang,B.S., Kendrick,B.S., Carpenter,J.F., 1996. Surface-induced denaturation of proteins during freezing and its inhibition by surfactants. J Pharm. Sci., 85, 1325-1330.

7. Chang,S.H., Chen,L.Y., Chen,W.Y., 2005. The effects of denaturants on protein conformation and behavior at air/solution interface. Colloids Surf. B Biointerfaces., 41, 1-6.

8. Hawe,A., Kasper,J.C., Friess,W., Jiskoot,W., 2009. Structural properties of monoclonal antibody aggregates induced by freeze-thawing and thermal stress. Eur. J Pharm. Sci., 38, 79-87.

9. Kiese,S., Papppenberger,A., Friess,W., Mahler,H.C., 2008. Shaken, not stirred: mechanical stress testing of an IgG1 antibody. J Pharm. Sci., 97, 4347-4366.

10. Maa,Y.F., Hsu,C.C., 1997. Protein denaturation by combined effect of shear and air-liquid interface. Biotechnol. Bioeng., 54, 503-512.

11. Patten,P.A., Schellekens,H., 2003. The immunogenicity of biopharmaceuticals. Lessons learned and consequences for protein drug development. Dev. Biol. (Basel), 112, 81-97.

12. Roberts,C.J., Darrington,R.T., Whitley,M.B., 2003. Irreversible aggregation of recombinant bovine granulocyte-colony stimulating factor (bG-CSF) and implications for predicting protein shelf life. J Pharm. Sci., 92, 1095-1111.

13. Rosenberg,A.S., 2006. Effects of protein aggregates: an immunologic perspective. AAPSJ, 8, E501-E507.

14. Schellekens,H., 2003. Immunogenicity of therapeutic proteins. Nephrol. , Dial. , Transplant., 18, 1257-1259.

15. Schellekens,H., 2005. Factors influencing the immunogenicity of therapeutic proteins. Nephrol. , Dial. , Transplant., 20, vi3-vi9.

16. Sundström,S., Ljungqvist,B., Reinmüller,B., Stallgard,M., 2010. The use of computational fluid dynamics for the study of particle dispersion routes in the filling area of a blow-fill-seal process. Eur. J. Par. Pharm. Sci, 15, 5-11.

17. Wang,W., 2005. Protein aggregation and its inhibition in biopharmaceutics. Int. J Pharm., 289, 1-30.

18. Weiss,W.F., Young,T.M., Roberts,C.J., 2009. Principles, approaches, and challenges for predicting protein aggregation rates and shelf life. J Pharm. Sci., 98, 1246-1277.

19. Youssef, A.M.K., 2010, Systematic studies to correlate microcalorimetry with stability studies on liquid formulations of various protein drugs. Department of Pharmacy, LMU Munich, [PhD].

8. Final Summary of the thesis

8.1.1 Relevance of submicron particle counting

The relevance of submicron particle counting in pharmaceutical protein solutions is discussed controversially within the scientific community. The presence of protein aggregates of all sizes jeopardizes the pharmaceutical quality and safety of parenteral products. Blood vessel occlusions and immune system reactions are the most critical adverse effects with regard to protein aggregates. Pharmacopoeias have set limits for the presence of subvisible particles in parenterals ≥10 µm and ≥25 µm to be counted with light obscuration or microscopic methods. However, there is reason to think that these size limitations are too insensitive, as proteins are usually not very stable and tend to form aggregates. Further, it is known that large protein aggregates can grow from smaller aggregates. There is a huge risk that a lot of particles < 10 µm or even <1 µm are overlooked whose effect is not finally known.

A new particle counter, the AccuSizer FY nano® marketed with a detection and counting limit of 150 nm to 10 µm was compared to classical methods. The AccuSizer would perfectly close the gap in particle detection in parenterals as particle counting is currently only possible for particles ≥1 µm. However, experiments showed that counting is only meaningful with the AccuSizer® for particles ≥750 nm. Indeed, the AccuSizer® is detecting particles <750 nm; however the background noise is too high to detect beginning aggregation or changes in particle count. The AccuSizer® has two detectors: a light scattering (LS) detector that captures the light intensities of particles from 150 –610 nm and a classical light obscuration (LO) for particles >610 nm. The results of our studies showed that the LS detector is not appropriate for counting protein particles, whereas the LO detector performs as reliable as classical LO instruments. Additionally, the AccuSizer® has an autodilution tool. Samples are diluted automatically until a given particle concentration is reached. However, dilution of aggregated protein samples can lead to artifacts. Aggregates can be redissolved and measurements can lead to false negative results or dilution with the wrong medium can even foster aggregation. All in all, the AccuSizer® did not close the gap in analytical methods.

To study the relevance of counting submicron particles, four proteins were stressed mechanically, thermally and by freeze-thawing. During stress, samples were taken and analyzed with the new AccuSizer® FY nano (AS) and classical methods (Light

Obscuration (LO), Dynamic Light Scattering (DLS), Size-exclusion Chromatography (SEC), Microflow Imaging (MFI) and optical density measurements at 550 nm (OD)). Analytical results (e.g. particle counts or monomer decrease) of each method were plotted over time and the "points of detection" were determined. The "point of detection" was defined as time point, where e.g. protein aggregates increases and/or protein monomer decreases significantly. The comparison of the "points of detection" of each method and protein were used to draw conclusions regarding the relevance of submicron particle counting.

Studying the relevance of submicron particle counting revealed that protein aggregates after mechanical stress and freeze-thawing can be detected well with particle counting methods, whereas protein aggregates formed during thermal stress are hardly detectable. Already very early SEC detects changes in thermally stressed samples, whereas aggregates formed during mechanical stress or freeze-thawing can not be detected chromatographically. Thermal stress leads to structural changes, whereas shaking or freeze-thawing leads to interfacial adsorption or unfolding and aggregation.

Furthermore, "points of detection" of particle size classes of particles ≥1 µm and ≥10 µm were compared regarding their sensitivity to detect changes. As protein aggregation is reported to start with small nuclei which grow into larger aggregates, a particle count increase during stress should be detected first with particle size class ≥1 µm, then particle size classes ≥10 µm should be increasing. Our studies confirmed this aggregation theory. Indeed, particles ≥1 µm increased earlier during stressing process than particles ≥10 µm in 6 of 12 cases. However, the difference was not always given, and in 2 of 12 cases even particles ≥10 µm increased before particles ≥1 µm.

Microflow Imaging™ (MFI) is also a particle counting instrument with a working range of 1-100 µm. MFI combines digital microscopy, micro-fluidics, and image processing. Besides particle count and size, MFI delivers information about form, translucency, or morphologic properties. For detection with MFI, a smaller refractive index difference between particles and fluid is required as e.g. for detection with LO, giving higher particle counts when aggregates were very translucent. We also assessed MFI with regards to ability of early and sensitive protein aggregate detection. Results showed that MFI indeed deliver slightly more information than classical LO: particles formed during mechanical or freeze-thaw stress are earlier detectable with MFI. Protein

particles that are not translucent but dense are detected as well as with LO. Polysorbate 80 (PS-80) can play a role regarding the appearance of particles. IgG_1 particles formed during mechanical or freeze-thaw stress under PS-80 protection are found to be consistently dark and detectable with LO, whereas protein particles generated in formulations without PS-80 protection can be translucent and only detectable with MFI.

For the time being, it is recommended to use SEC and LO for particles Nr.10 µm (as required in regulatory guidelines) to cover the particle formation after common stresses. Assessing a sample with SEC and LO allows a sensitive analytic . However, regulatory guidelines should be amended: Including particle counting of particles Nr.1 µm using MFI as a new particle counter is very helpful and informative regarding the assessment of protein particles and their appearance.

8.1.2 Particulate matter in serum solutions

Protein aggregation is discussed controversially, however only recently the discussions received a new impulse towards *in vivo* experiments. Many studies have been performed observing the protein particles *in vitro*. However, it is much more important to learn about the fate of accidently aggregated proteins *in vivo*. In our studies a first approach in this direction has been made. Protein particles are incubated in serum mimicking solution and particles were counted. We were interested, whether protein aggregates dissolve or rather grow fast due to further adsorption or aggregation.

In our studies, three different proteins (IgG_1, GCSF and rPA) were stressed mechanically or by freeze-thawing and diluted into serum solution, phosphate buffer and formulation buffers, particle counts were monitored directly after dilution and after 20 hours.

The results showed that protein particles of IgG_1 were stable in serum solution over tested time, whereas GCSF and rPA particles were becoming translucent and the particle count increased. Translucent particles were not detectable by LO, whereas MFI was perfectly able to detect the less dense particles. The fact that protein particle counts can increase and that protein particles can become translucent is alarming, as particle counts within parenteral solutions are currently monitored with LO.

8.1.3 Effects of dilution, pH and standing time on particulate matter

During experiments evaluating “particulate matter in serum solutions” (Chapter 8.1.2) decreasing particle counts were found after dilution of mechanically stressed IgG_1 into phosphate buffer. The effect of time, pH-shifts and standing time on stressed IgG_1-formulation was monitored within these studies, particle counts were taken with LO and MFI. IgG_1-formulation was mechanically stressed and diluted into phosphate buffers of different ionic strengths and pH values.

It was found that smaller particles grow into larger ones over time, more pronounced at alkaline pH close to the isoelectric point (IEP at pH 8.81) and at higher buffer molarities. These results prove the theory that protein aggregates can grow from small nuclei.

MFI-images of samples were compared regarding their intensity mean, which is described in illumination intensity levels. Our studies show that mean intensity decreases over increasing pH and also over time. Mean intensity gives information about the appearance of the detected particles. High intensity mean values are found for translucent particles at lower pH values. The more stable aggregates are, the denser they appear.

8.1.4 Comparison of TopLyo® vials (Schott) with standard glass type I vials

Primary packaging materials should be chosen carefully as they are in contact with protein solutions. The interactions of recently marketed hydrophobically coated TopLyo® vials with IgG_1 are studied with regard to particulate matter. The hydrophobic coating is intended to minimize adhesion and interaction of substances and prevent the cake from collapsing. However, the hydrophobic surface might also exhibit the risk of protein unfolding and accompanying aggregation or adsorption. A connection was found between protein adsorption to vial surfaces and particle formation during freeze-drying processes: If reference solutions of unstressed protein show a higher adsorption to glass vial surfaces than freeze-dried or freeze-thawed samples, protein is detached during processing and protein particles are formed.

Protein reference is IgG_1-α solution filled into the glass vials to be examined and stored in the refrigerator. IgG_1-α showed stronger adsorption to TopLyo® vials and corresponding high amounts of particles.

TopLyo® vials are not the first choice for freeze-drying or freeze-thawing of an IgG_1-α.

8.1.5 Stress simulations

Defining the most adequate stirring speed during upscaling processes is usually a critical factor in protein formulation development. Computational Fluid Dynamics (CFD) offers the possibility to simulate stresses during stir processes. We assessed the possibility to predict mechanical stress during upscaling with regard to particulate matter. Linear dependencies of particle counts for particles ≥1 µm and stirring speed were found for all tested volumes. Additionally, particle formation of particles ≥1 µm is linearly correlated to stress tensor magnitudes. For larger particles the situation was more complex as nucleation and degradation during stirring run in parallel. When larger particles are formed they may be dispersed into smaller particles by the stirrer. Further, CFD does not sufficiently account for the ratio of container volume and surface; only after recalculation parallel dependencies are found between particle counts ≥1 µm and stirring speed in different containers. In summary CFD is not adequate to predict protein particle formation during upscaling as physicochemical properties are not well enough included.

8.2 Conclusion

Protein particle formation is a complex issue within development and manufacture of protein drug products. Every step and equipment has to be carefully chosen to minimize protein aggregation as the aim of pharmaceutical development is quality by design. Accidently aggregated protein drug products can cause reactions of the immune system. The fact that aggregates may even be growing upon administration *in vivo* has to be considered.

The need of new pharmacopoeial methods is controversially discussed and our studies shall contribute to this field. On the one hand, the tested particle counters did not deliver reliable particle counts for the submicron range. Further, particle growths of particles ≥1 µm and ≥10 µm happened almost parallel. On the other hand, we showed that during stirring nucleation and degradation of larger particles run at the same time. This leads us to the proposal to monitor at least particles ≥1 µm. MFI proved to be an informative method to count and visualize protein particles. It is much more sensitive than classical LO and should be considered as a new pharmacopoeial method.

9. Appendix

To complete the data assessed in chapter 3 (Relevance of submicron particle counting for development and quality assurance of protein pharmaceuticals), following data sets are presented.

Four proteins were stressed using three different stressing methods. Each of those 12 experiments was attended using six instruments and methods: three particle counters, SEC, DLS and turbidity measurements. The particle counter data were sub classified into particle size classes (MFI and LO: particles ≥1.0 µm and ≥10.0 µm; AccuSizer: particles ≥250 nm, ≥500 nm, ≥750 nm, ≥1.0 µm, ≥2.5 µm, ≥5.0 µm and ≥7.5 µm) to get a better overview about particle formation in those different size classes. In total, 14 raw data sets were obtained for each single experiment. In order to outline the raw data, an overview about the time points of first detection is presented in this appendix. The time point of first detection, marked in dark grey, is the point at which stress results in e.g. formation of particle or an increase of turbidity.

9.1 Overview tables of time points of first detection after stressing IgG_1-α

Table 1: Heat stress of IgG_1-α; detection power of different methods (results of particle counters were distinguished in different size classes, n = 3)

	Reference	20 min	40 min	60 min	80 min	100 min	120 min	140 min	160 min	180 min
SEC										
DLS										
MFI ≥10.0 µm										
$OD_{550\ nm}$										
MFI ≥1.0 µm										
LO ≥1.0 µm										
LO ≥10.0 µm										
AS ≥1.0 µm										
AS ≥0.25 µm										
AS ≥0.75 µm										
AS ≥0.50 µm										
AS ≥2.5 µm										
AS ≥5.0 µm										
AS ≥7.5 µm										

Table 2: Mechanical stress of IgG_1-α; detection power of different methods (results of particle counters were distinguished in different size classes, n = 3)

	Reference	30 min	60 min	90 min	120 min	180 min	240 min	300 min	360 min
$OD_{550\ nm}$									
AS ≥0.75 µm									
LO ≥10.0 µm									
AS ≥1.0 µm									
MFI ≥1.0 µm									
MFI ≥10.0 µm									
LO ≥1.0 µm									
DLS									
AS ≥2.5 µm									
SEC									
AS ≥0.25 µm									
AS ≥0.50 µm									
AS ≥5.0 µm									
AS ≥7.5 µm									

Table 3: Freeze-thaw stress of IgG_1-α; detection power of different methods (results of particle counters were distinguished in different size classes, n = 3)

	Reference	1.cycle	2.cycle	3.cycle	4.cycle	5.cycle
MFI ≥10.0 µm						
MFI ≥1.0 µm						
LO ≥10.0 µm						
LO ≥1.0 µm						
AS ≥1.0 µm						
AS ≥2.5 µm						
AS ≥0.50 µm						
AS ≥0.75 µm						
DLS						
$OD_{550\ nm}$						
SEC						
AS ≥5.0 µm						
AS ≥7.5 µm						
AS ≥0.25 µm						

9.2 Overview tables of time points of detection after stressing IgG1-ß

Table 4: Heat stress of IgG_1-ß; detection power of different methods (results of particle counters were distinguished in different size classes, n = 3)

	Reference	20 min	40 min	60 min	80 min	100 min	120 min	140 min	160 min	180 min
SEC										
DLS										
$OD_{550\ nm}$										
AS ≥0.75 µm										
AS ≥1.0 µm										
LO ≥1.0 µm										
LO ≥10.0 µm										
MFI ≥1.0 µm										
MFI ≥10.0 µm										
AS ≥0.25 µm										
AS ≥0.50 µm										
AS ≥2.5 µm										
AS ≥5.0 µm										
AS ≥7.5 µm										

Table 5: Mechanical stress of IgG_1-ß; detection power of different methods (results of particle counters were distinguished in different size classes, n = 3)

	Reference	90 min	180 min	270 min	360 min	450 min	540 min
AS ≥1.0 µm							
AS ≥0.25 µm							
AS ≥0.5 µm							
LO ≥1.0 µm							
LO ≥10.0 µm							
AS ≥0.75 µm							
AS ≥2.5 µm							
MFI ≥1.0 µm							
MFI ≥10.0 µm							
AS ≥5.0 µm							
AS ≥7.5 µm							
SEC							
DLS							
$OD_{550\ nm}$							

Table 6: Freeze-thaw stress of IgG_1-ß; detection power of different methods (results of particle counters were distinguished in different size classes, n = 3)

	Reference	1.cycle	2.cycle	3.cycle	4.cycle	5.cycle
AS ≥0.25 µm						
AS ≥1.0 µm						
LO ≥1.0 µm						
LO ≥10.0 µm						
AS ≥0.5 µm						
AS ≥0.75 µm						
AS ≥2.5 µm						
AS ≥5.0 µm						
AS ≥7.5 µm						
MFI ≥1.0 µm						
MFI ≥10.0 µm						
SEC						
DLS						
$OD_{550\ nm}$						

9.3 Overview tables of time points of detection after stressing GCSF

Table 7: Heat stress of GCSF; detection power of different methods (results of particle counters were distinguished in different size classes, n = 3)

	Reference	15 min	30 min	45 min	60 min	75 min	90 min	105 min	120 min
SEC									
AS ≥1.0 µm									
LO ≥1.0 µm									
MFI ≥10.0 µm									
AS ≥0.75 µm									
AS ≥2.5 µm									
LO ≥10.0 µm									
AS ≥5.0 µm									
MFI ≥1.0 µm									
AS ≥0.25 µm									
AS ≥0.5 µm									
AS ≥7.5 µm									
DLS									
$OD_{550\ nm}$									

Table 8: Mechanical stress of GCSF; detection power of different methods (results of particle counters were distinguished in different size classes, n = 3)

	Reference	60 min	90 min	120 min	150 min	180 min	210 min
SEC							
LO ≥10.0 µm							
AS ≥0.75 µm							
AS ≥1.0 µm							
AS ≥2.5 µm							
AS ≥5.0 µm							
LO ≥1.0 µm							
AS ≥0.25 µm							
AS ≥0.50 µm							
MFI ≥10.0 µm							
MFI ≥1.0 µm							
AS ≥7.5 µm							
DLS							
$OD_{550\ nm}$							

Table 9: Freeze-thaw stress of GCSF; detection power of different methods (results of particle counters were distinguished in different size classes, n = 3)

	Reference	1.cycle	2.cycle	3.cycle	4.cycle	5.cycle
SEC						
AS ≥2.5 µm						
MFI ≥1.0 µm						
MFI ≥10.0 µm						
AS ≥1.0 µm						
LO ≥1.0 µm						
AS ≥0.75 µm						
LO ≥10.0 µm						
AS ≥5.0 µm						
AS ≥0.25 µm						
AS ≥0.5 µm						
AS ≥7.5 µm						
DLS						
$OD_{550\ nm}$						

9.4 Overview tables of time points of detection after stressing rPA

Table 10: Heat stress of rPA; detection power of different methods (results of particle counters were distinguished in different size classes, n = 3)

	Reference	15 min	30 min	45 min	60 min	75 min	90 min	105 min	120 min
SEC									
AS ≥2.5 µm									
AS ≥1.0 µm									
AS ≥0.75 µm									
MFI ≥1.0 µm									
LO ≥1.0µm									
DLS									
$OD_{550\ nm}$									
AS ≥5.0 µm									
AS ≥0.25 µm									
LO ≥10.0 µm									
MFI ≥10.0 µm									
AS ≥0.5 µm									
AS ≥7.5 µm									

Table 11: Mechanical stress of rPA; detection power of different methods (results of particle counters were distinguished in different size classes, n = 3)

	Reference	30 min	60 min	90 min	120 min	150 min	180 min
SEC							
LO ≥1.0 µm							
MFI ≥1.0 µm							
MFI ≥10.0 µm							
DLS							
LO ≥10.0 µm							
AS ≥0.75 µm							
$OD_{550\ nm}$							
AS ≥1.0 µm							
AS ≥0.25 µm							
AS ≥0.50 µm							
AS ≥2.5 µm							
AS ≥5.0 µm							
AS ≥7.5 µm							

Table 12: Freeze-thaw stress of rPA; detection power of different methods (results of particle counters were distinguished in different size classes, n = 3)

	Reference	1.cycle	2.cycle	3.cycle	4.cycle	5.cycle
AS ≥1.0 µm						
AS ≥0.5 µm						
AS ≥0.75 µm						
AS ≥2.5 µm						
$OD_{550\ nm}$						
MFI ≥1.0 µm						
MFI ≥10.0 µm						
AS ≥0.25 µm						
LO ≥1.0 µm						
LO ≥10.0 µm						
AS ≥5.0 µm						
SEC						
AS ≥7.5 µm						
DLS						

Presentations associated with this thesis:

July 11	Poster presentations at the Colorado Protein Stability Conference, Breckenridge, USA
October 10	Poster presentation at the DPHG Conference, Braunschweig, Germany
March 10	Poster presentation at the World Meeting on Pharmaceutics, Biopharmaceutics and Pharmaceutical Technology, Malta
October 09	Poster presentation and oral presentation at the Science to Market Conference, Hannover, Germany

Veronika Maria Spalthoff

Personal Data

Date of Birth	25.03.1980
Place of Birth	Meppen
Nationality	German

Professional Experience

01/2012 – present	Compliance Expert at Sanofi, Frankfurt
11/2006 – 09/2008	Bench Scientist at Sanofi, Frankfurt
12/2006 – 12/2007	Licensed pharmacist at Engel-Apotheke, Duisburg

University Education

10/2008 – 12/2011	PhD student at Department of Pharmacy, Pharmaceutical Technology and Biopharmaceutics, Ludwigs-Maximilians-University, Munich Supervisor: Prof. Dr. Gerhard Winter
02/2006 – 07/2006	Research scholar at University of Florida, Gainesville
06/2005 – 11/2005	2nd half of preregistration year at Engel-Apotheke, Duisburg
12/2004 – 05/2005	1st half of preregistration year at Sanofi, Frankfurt
10/2000 – 11/2004	Study of Pharmacy at Technical University Carolo-Wilhelmina, Braunschweig

Secondary Education

1992 – 1999	Gymnasium Marianum, Meppen